Optimisation fiabiliste des structures : méthodes et applications au contrôle des vibrations

Hang Yu

Numéro d'ordre: 2011-38 Anée 2011

Reliability-Based Design Optimization of Structures: Methodologies and Applications to Vibration Control

Thèse de doctorat

Ecole Doctorale MEGA
(Mécanique, Energétique, Génie civil, Acoustique)

Présentée et soutenue publiquement
le 15 novembre 2011
à l'Ecole Centrale de Lyon

Par
Hang Yu

Devant le jury ci-dessous :

G. Scorletti	Président	Ecole Centrale de Lyon
A. El Hami	Rapporteur	INSA de Rouen
M. Collet	Rapporteur	FEMTO ST Univ. de Franche-Comté
F. Gillot	Examinateur	Ecole Centrale de Lyon
O. Bareille	Examinateur	Ecole Centrale de Lyon
M. Ichchou	Directeur de thèse	Ecole Centrale de Lyon

Laboratoire de Tribologie et Dynamique des Systèmes (LTDS) UMR-CNRS 5513,
Ecole Centrale de Lyon, 36 Avenue Guy de Collongue, 69134 Ecully Cedex, France

ÉCOLE CENTRALE LYON **Direction de la recherche**

Liste des personnes Habilitées à Diriger des Recherches en poste à l'Ecole Centrale de Lyon

Nom-Prénom	*Corps grade*	Laboratoire ou à défaut département ECL	Etablissement
BEROUAL Abderrahmane	*professeur*	AMPERE	ECL
BURET François	*professeur*	AMPERE	ECL
JAFFREZIC-RENAULT Nicole	*directeur de recherche*	AMPERE	CNRS/ECL
KRÄHENBÜHL Laurent	*directeur de recherche*	AMPERE	CNRS/ECL
NICOLAS Alain	*professeur*	AMPERE	ECL
NICOLAS Laurent	*directeur de recherche*	AMPERE	CNRS/ECL
SCORLETTI Gérard	*professeur*	AMPERE	ECL
SIMONET Pascal	*directeur de recherche*	AMPERE	CNRS/ECL
VOLLAIRE Christian	*professeur*	AMPERE	ECL

Nbre Ampère 9

HELLOUIN Yves	*maître de conférences*	DER EEA	ECL

Nbre DER EEA 1

GUIRALDENQ Pierre	*professeur émérite*	DER STMS	ECL
VINCENT Léo	*professeur*	DER STMS	ECL

Nbre DER STMS 2

LOHEAC Jean-Pierre	*maître de conférences*	ICJ	ECL
MAITRE Jean-François	*professeur émérite*	ICJ	ECL
MARION Martine	*professeur*	ICJ	ECL
MIRONESCU Elisabeth	*professeur*	ICJ	ECL
MOUSSAOUI Mohand	*professeur*	ICJ	ECL
MUSY François	*maître de conférences*	ICJ	ECL
ZINE Abdel-Malek	*maître de conférences*	ICJ	ECL

Nbre ICJ 7

DAVID Bertrand	*professeur*	ICTT	ECL

Nbre ICTT 1

CALLARD Anne-Ségolène	*professeur*	INL	ECL
CLOAREC Jean-Pierre	*maître de conférences*	INL	ECL
GAFFIOT Frédéric	*professeur*	INL	ECL
GAGNAIRE Alain	*maître de conférences*	INL	ECL
GARRIGUES Michel	*directeur de recherche*	INL	CNRS/ECL
GENDRY Michel	*directeur de recherche*	INL	CNRS/ECL
GRENET Geneviève	*directeur de recherche*	INL	CNRS/ECL
HOLLINGER Guy	*directeur de recherche*	INL	CNRS/ECL
KRAWCZYK Stanislas	*directeur de recherche*	INL	CNRS/ECL
LETARTRE Xavier	*chargé de recherche*	INL	CNRS/ECL
O'CONNOR Ian	*professeur*	INL	ECL
PHANER-GOUTORBE Magali	*professeur*	INL	ECL

ROBACH Yves	*professeur*	INL	ECL
SAINT-GIRONS Guillaume	*chargé de recherche*	INL	CNRS/ECL
SEASSAL Christian	*directeur de recherche*	INL	CNRS/ECL
SOUTEYRAND Eliane	*directeur de recherche*	INL	CNRS/ECL
TARDY Jacques	*directeur de recherche*	INL	CNRS/ECL
VIKTOROVITCH Pierre	*directeur de recherche*	INL	CNRS/ECL

Nbre INL 18

CHEN Liming	*professeur*	LIRIS	ECL

Nbre LIRIS 1

BAILLY Christophe	*professeur*	LMFA	ECL
BERTOGLIO Jean-Pierre	*directeur de recherche*	LMFA	CNRS/ECL
BLANC-BENON Philippe	*directeur de recherche*	LMFA	CNRS/ECL
BOGEY Christophe	*chargé de recherche*	LMFA	CNRS/ECL
CAMBON Claude	*directeur de recherche*	LMFA	CNRS/ECL
CARRIERE Philippe	*directeur de recherche*	LMFA	CNRS/ECL
CHAMPOUSSIN J-Claude	*professeur émérite*	LMFA	ECL
COMTE-BELLOT geneviève	*professeur émérite*	LMFA	ECL
FERRAND Pascal	*directeur de recherche*	LMFA	CNRS/ECL
GALLAND Marie-Annick	*professeur*	LMFA	ECL
GODEFERD Fabien	*directeur de recherche*	LMFA	CNRS/ECL
GOROKHOVSKI Mikhail	*professeur*	LMFA	ECL
HENRY Daniel	*directeur de recherche*	LMFA	CNRS/ECL
JEANDEL Denis	*professeur*	LMFA	ECL
JUVE Daniel	*professeur*	LMFA	ECL
LE RIBAULT Catherine	*chargée de recherche*	LMFA	CNRS/ECL
LEBOEUF Francis	*professeur*	LMFA	ECL
PERKINS Richard	*professeur*	LMFA	ECL
ROGER Michel	*professeur*	LMFA	ECL
SCOTT Julian	*professeur*	LMFA	ECL
SHAO Liang	*directeur de recherche*	LMFA	CNRS/ECL
SIMOENS Serge	*chargé de recherche*	LMFA	CNRS/ECL
TREBINJAC Isabelle	*maître de conférences*	LMFA	ECL

Nbre LMFA 23

BENAYOUN Stéphane	*professeur*	LTDS	ECL
CAMBOU Bernard	*professeur*	LTDS	ECL
COQUILLET Bernard	*maître de conférences*	LTDS	ECL
DANESCU Alexandre	*maître de conférences*	LTDS	ECL
FOUVRY Siegfrid	*chargé de recherche*	LTDS	CNRS/ECL
GEORGES Jean-Marie	*professeur émérite*	LTDS	ECL
GUERRET Chrystelle	*chargé de recherche*	LTDS	CNRS/ECL
HERTZ Dominique	*past*	LTDS	ECL
ICHCHOU Mohamed	*professeur*	LTDS	ECL
JEZEQUEL Louis	*professeur*	LTDS	ECL
JUVE Denyse	*ingénieur de recherche*	LTDS	ECL
KAPSA Philippe	*directeur de recherche*	LTDS	CNRS/ECL
LE BOT Alain	*directeur de recherche*	LTDS	CNRS/ECL
LOUBET Jean-Luc	*directeur de recherche*	LTDS	CNRS/ECL
MARTIN Jean-Michel	*professeur*	LTDS	ECL
MATHIA Thomas	*directeur de recherche*	LTDS	CNRS/ECL
MAZUYER Denis	*professeur*	LTDS	ECL
PERRET-LIAUDET Joël	*maître de conférences*	LTDS	ECL
SALVIA Michelle	*maître de conférences*	LTDS	ECL

SIDOROFF François	*professeur*	LTDS	ECL
SINOU Jean-Jacques	*professeur*	LTDS	ECL
STREMSDOERFER Guy	*professeur*	LTDS	ECL
THOUVEREZ Fabrice	*professeur*	LTDS	ECL
TREHEUX Daniel	*professeur*	LTDS	ECL
VINCENS Eric	*maître de conférences*	LTDS	ECL
		Nbre LTDS 25	
	Total HdR ECL	91	

Declaration of Authorship

I, Hang YU, declare that this thesis titled, "Reliability-Based Design Optimization of Structures: Methodologies and Applications to Vibration Control" and the work presented in it are my own. I confirm that:

- This work was done wholly or mainly while in candidature for a research degree at this grand school.
- Where I have consulted the published work of others, this is always clearly attributed.
- Where I have quoted from the work of others, the source is always given. With the exception of such quotations, this thesis is entirely my own work.
- I have acknowledged all main sources of help.
- Where the thesis is based on work done by myself jointly with others, I have made clear exactly what was done by others and what I have contributed myself.

Signed:

Date:

Remerciements

Cette thèse a été réalisée au sein de l'équipe Dynamique des Structures et des Systèmes de l'École Centrale de Lyon, au Laboratoire de Tribologie et Dynamique des Systèmes. Je remercie chaleureusement mon directeur de recherche, M. Mohamed Ichchou, qui m'a proposé ce sujet et qui m'a, outre consacré une partie de son temps durant ces trois années, témoigné de sa confiance dans les moments difficiles.

Mes remereciments vont également à M. Frédéric Gillot pour son aide scientifique, son constant soutien moral tout au long de ces trois années, et son gentillesse qu'il a manifestées à mon égard durant les revues et cette thèse.

Je remercie M. Scorletti pour l'honneur qu'il m'a fait de bien vouloir présider mon jury de thèse. Je remercie très sincèrement Messieurs El Hami et Collet qui ont accepté d'être rapporteurs de mon travail. Le présent manuscrit se trouve sensiblement amélioré grâce aux corrections qu'ils ont suggérés. D'une manière générale, je remercie l'ensemble des personnes qui m'ont fait l'honneur d'être membres du jury.

En ce qui concerne la partie financière de ce travail, je remercie le conseil des boures d'études de la Chine (China Scholarship Council, CSC) et le service de l'éducation de l'ambassade de Chine en France pour l'occasion qui me permet de faire mes études en France et de découvrir la culture française et européene.

Je terminerai en profitant de l'occasion pour adresser tous mes remerciments à mes aimes et à ma famille. Je leur dois beaucoup; ces dernières années ont été difficiles, et je ne m'en serais pas sorti sans eux.

Résumé

En conception de produits ou de systèmes, les approches d'optimisation déterministe sont de nos jours largement utilisées. Toutefois, ces approches ne tiennent pas compte des incertitudes inhérentes aux modèles utilisés, ce qui peut parfois aboutir à des solutions non fiables. Il convient alors de s'intéresser aux approches d'optimisation stochastiques. Les approches de conception robuste à base d'optimisation stochastique (Reliablity Based Robust Design Optimization, RBRDO) tiennent compte des incertitudes lors de l'optimisation au travers d'une boucle supplémentaire d'analyse des incertitudes (Uncertainty Anlysis, UA). Pour la plupart des applications pratiques, l'UA est réalisée par une simulation de type Monte Carlo (Monte Carlo Simulation, MCS) combinée avec l'analyse structurale. L'inconvénient majeur de ce type d'approche réside dans le coût de calcul qui se révèle être prohibitif. Par conséquent, nous nous sommes intéressés dans nos travaux aux développements de méthodologies efficaces pour la mise en place de RBRDO s'appuyant sur une analyse MCS.

Nous présentons une méthode d'UA s'appuyant sur une analyse MCS dans laquelle la réponse aléatoire est approximée sur une base du chaos polynomial (Polynomial Chaos Expansion, PCE). Ainsi, l'efficacité de l'UA est grandement améliorée en évitant une trop grande répétition des analyses structurales. Malheureusement, cette approche n'est pas pertinente dans le cadre de problèmes en grande dimension, par exemple pour des applications en dynamique. Nous proposons ainsi d'approximer la réponse dynamique en ne tenant compte que de la résolution aux valeurs propres aléatoires. De cette façon, seuls les paramètres structuraux aléatoires apparaissent dans le PCE. Pour traiter le problème du mélange des modes dans notre approche, nous nous sommes appuyés sur le facteur MAC qui permet de le quantifier. Nous avons développé une méthode univariable permettant de vérifier quelle variable générait un mélange de modes de manière à le réduire ou le supprimer.

Par la suite, nous présentons une approche de RBRDO séquentielle pour améliorer l'efficacité et éviter les problèmes de non-convergence présents dans les approches de RBRDO. Dans notre approche, nous avons étendu la stratégie séquentielle classique, visant principalement à découpler l'analyse de fiabilité de la procédure d'optimisation,

en séparant l'évaluation des moments de la boucle d'opimisation. Nous avons utilisé une approximation exponentielle locale autour du point de conception courant pour construire des objectifs déterministes équivalents ainsi que des contraintes stochastiques. De manière à obtenir les différents coefficients pour notre approximation, nous avons développé une analyse de sensibilité de la robustesse basée sur une distribution auxiliaire ainsi qu'une analyse de sensibilité des moments basée sur l'approche PCE.

Nous montrons la pertinence ainsi que l'efficacité des approches proposées au travers de différents exemples numériques. Nous appliquons ensuite notre approche de RBRDO pour la conception d'un amortisseur dans le domaine du contrôle passif vibratoire d'une structure présentant des grandeurs aléatoires. Les résultats obtenus par notre approche permettent non seulement de réduire la variabilité de la réponse, mais aussi de mieux contrôler l'amplitude de la réponse au travers d'un seuil choisi par avance.

Mots clés: fiabilité, robustesse, optimisation, chaos polynomial, Monte Carlo, formulation séquentielle, contrôe des vibrations.

Abstract

Deterministic design optimization is widely used to design products or systems. However, due to the inherent uncertainties involved in different model parameters or operation processes, deterministic design optimization without considering uncertainties may result in unreliable designs. In this case, it is necessary to develop and implement optimization under uncertainties. One way to deal with this problem is reliability-based robust design optimization (RBRDO), in which additional uncertainty analysis (UA, including both of reliability analysis and moment evaluations) is required. For most practical applications however, UA is realized by Monte Carlo Simulation (MCS) combined with structural analyses that renders RBRDO computationally prohibitive. Therefore, this work focuses on development of efficient and robust methodologies for RBRDO in the context of MCS.

We presented a polynomial chaos expansion (PCE) based MCS method for UA, in which the random response is approximated with the PCE. The efficiency is mainly improved by avoiding repeated structural analyses. Unfortunately, this method is not well suited for high dimensional problems, such as dynamic problems. To tackle this issue, we applied the convolution form to compute the dynamic response, in which the PCE is used to approximate the modal properties (i.e. to solve random eigenvalue problem) so that the dimension of uncertainties is reduced since only structural random parameters are considered in the PCE model. Moreover, to avoid the modal intermixing problem when using MCS to solve the random eigenvalue problem, we adopted the MAC factor to quantify the intermixing, and developed a univariable method to check which variable results in such a problem and thereafter to remove or reduce this issue.

We proposed a sequential RBRDO to improve efficiency and to overcome the non-convergence problem encountered in the framework of nested MCS based RBRDO. In this sequential RBRDO, we extended the conventional sequential strategy, which mainly aims to decouple the reliability analysis from the optimization procedure, to make the moment evaluations independent from the optimization procedure. Locally "first-order" exponential approximation around the current design was utilized to construct

the equivalently deterministic objective functions and probabilistic constraints. In order to efficiently calculate the coefficients, we developed the auxiliary distribution based reliability sensitivity analysis and the PCE based moment sensitivity analysis.

We investigated and demonstrated the effectiveness of the proposed methods for UA as well as RBRDO by several numerical examples. At last, RBRDO was applied to design the tuned mass damper (TMD) in the context of passive vibration control, for both deterministic and uncertain structures. The associated optimal designs obtained by RBRDO cannot only reduce the variability of the response, but also control the amplitude by the prescribed threshold.

Keywords: reliability, robustness, optimization, polynomial chaos, Monte Carlo, sequential formulation, vibration control.

Contents

List of Figures

List of Tables

Abbreviations

AMV	Advanced Mean Value
CDF	Cumulative Distribution Function
CMV	Conjugate Mean Value
CRP	Cost Optimization with Reliability Constraints
CSDO	Conventional Stochastic Design Optimization
COV	Coefficient of Variance
DDO	Deterministic Design Optimization
FEA	Finite Element Analysis
FORM	First-Order Reliability Method
HMV	Hybrid Mean Value
HPCE	Hermite Polynomial Chaos Expansion
LSF	Least Square Method
MAC	Modal Assurance Criterion
MCS	Monte Carlo Simulation
MPP	Most Probable Point of Failure
PCE	Polynomial Chaos Expansion
PDF	Probability Density Function
PMA	Performance Measure Approach
RBDO	Reliability-Based Design Optimization
RBRDO	Reliability-Based Robust Design Optimization
RCP	Reliability Optimization with Cost Constraints
RDO	Robust Design Optimization
RIA	Reliability Index Approach
RSM	Response Surface Method
SDO	Stochastic Design Optimization
SFEM	Stochastic Finite Element Method
SORA	Sequential Optimization and Reliability Assessment
SORM	Second-Order Reliability Method
SQP	Sequential Quadratic Programming
TMD	Tuned Mass Damper
UA	Uncertainty Analysis

Chapter 1

Introduction

1.1 Motivation, objective and scope

1.1.1 Uncertainties in design optimization

Nowadays, increasingly competitive markets drive engineers to design products or systems characterized by low cost, high quality and high reliability, which cover a variety of fields ranging from children's toys to passenger cars and space systems such as satellites or space stations [1]. To fulfill such requirements, the modern design process is usually in conjunction with optimization techniques. The process of obtaining optimal designs is known as design optimization which relies largely on simulation methods. In this sense, advanced simulation techniques are required to allow for reproduction of the complexity of real systems with high fidelity. Thanks to the significant developments of computer science during the last 50 years, large-scale simulation tools (e.g. finite element codes and computational fluid codes) have been well developed for simulations and analyses of practical engineering systems.

Traditional approaches for design optimization coupled with the aforementioned advanced simulation techniques are usually based on the assumption of deterministic models and parameters in most engineering applications. This is the so-called deterministic design optimization (**DDO**) which has been successfully applied to reduce the cost and to improve the performances. However, the deterministic models are only the simplifications of practical systems since observations and measurements of physical processes clearly show variability and randomness in different model parameters. In this case, the optimal design will not be located at the design A provided by DDO (see Fig. 1.1) but tends to occur in an area around A. More often such area falls outside the safe region. This implies DDO leads to a failed design.

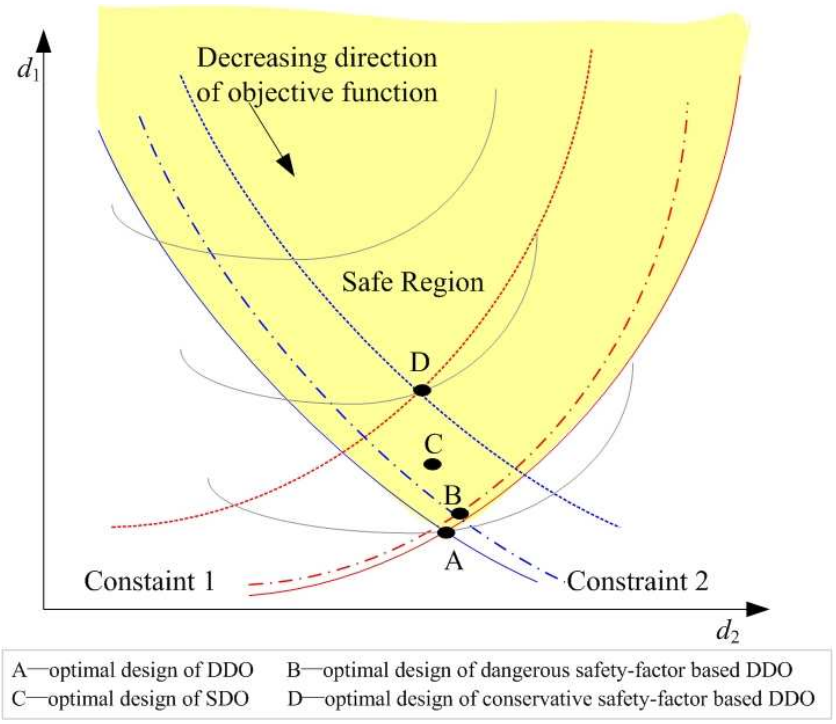

FIGURE 1.1: Development of design optimization [2, 3]. d_1 and d_2 are the two design variables, and the safe region is confined in the shadow area.

In DDO, despite of the fact that the propagation of uncertainties is usually hidden behind the use of the well-known "safety factors", the associated designs are calibrated for average situation but the extreme cases [2, 4] which might cause severe failures. From Fig. 1.1, the point B represents such a design compared with the optimal design C obtained by the design under uncertainties (e.g. reliability-based design optimization). There is also a possibility that the final design is too conservative when the "safety factors" are overestimated (shown by D in Fig. 1.1). On the other hand, due to an increasingly global competitive market, optimal designs are pushed to limits of system failure boundaries using DDO, leaving very little or no room for tolerances in modeling and simulating uncertainties [5]. Accordingly, final designs obtained by DDO may result in unreliable designs without taking the uncertainties into account. Consequently, uncertainties must be involved in design optimization and such problems are named by stochastic design optimization (**SDO**) in this study.

It is remarkable that although design optimization is widely used in various fields, the focus is confined to structural systems since the wide applications can be found in engineering. One can refer to the literatures on DDO [6] or on SDO [7, 8]. Furthermore, the linear structural systems are the research objective in respect that they are the most

frequently concerned in engineering practice.

1.1.2 Categories of uncertainty

For a real structural system, uncertainties might be involved in the design stage, in the manufacturing progress, during the service/operation and throughout the entire life time. In the design stage, uncertainties are derived from mathematical-mechanical modeling process or incomplete knowledge about the system. Variabilities related to the manufacturing progress are reflected by the manufacturing tolerance, material scatter on account of the limited precision in tools and processes or the lack of advanced technologies. During the service, uncertainties in the excitations (such as seismic loads, waves, temperature changes and any other kind of environmental loads) and boundary conditions as well as human factors are the major concerns. In respect that any structure owns limited age, randomness is usually introduced because of the deterioration of material properties. Accordingly, uncertainties may be imposed upon, but not all included, geometry tolerances, material properties, excitations, etc. These uncertainties can influence the performances all through the life time of the systems.

One significant issue that must be considered is how to quantify uncertainties in design optimization. To this end, it is indispensable to introduce the associated basic theories. Over the last decades, much attention to uncertainties has been brought by engineers, scientists and decision makers. There exist various representations and theories for uncertainties. Each of them is characterized by distinct mathematical model according to the information available. By far, uncertainties can be categorized as aleatory uncertainty, epistemic uncertainty and error. The classification [9–12] as well as the associated theories [11–14] are illustrated in Fig. 1.2.

As shown in Fig. 1.2, aleatory uncertainty is such a kind of uncertainty that the statistical properties are priori known. Accordingly, the probability theory, such as the classical theory [16], Bayesian networks [17, 18] and the random matrix theory [19, 20], can be applied. In contrast, epistemic uncertainty results from a lack of knowledge about the system or is derived from some ignorance. The associated uncertainty quantification (**UQ**) or uncertainty analysis (**UA**) depends mainly on the non-probabilistic theories, including fuzzy set theory, evidence theory, convex model, etc. As is the common case, the error should be avoided by careful examination or advanced methods.

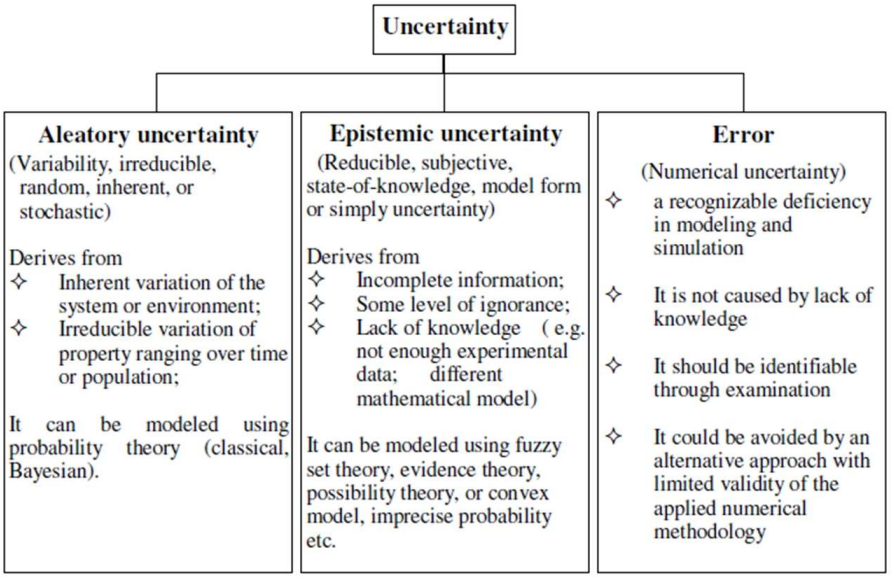

FIGURE 1.2: A well-known classification of uncertainty [15]

To carry out UA hence, the type of uncertainties must be figured out first since there is no generally mathematical model for all uncertainties. With respect to multiple types of uncertainties, hybrid models might be utilized. In this work, we assume all the required information is available, which means the aleatory type quantified by the probability theory is mainly concerned.

1.1.3 RBDO and RDO

In the context of the design optimization under aleatory uncertainties, one may refer to reliability-based design optimization (**RBDO**) or robust design optimization (**RDO**). However, they seek for the optimum by different criteria. RBDO aims to find the optimal designs with low probabilities of failure corresponding some critical failure mechanisms. While RDO concentrates on the optimal ones that make the performance (mainly as to the objective function) less sensitivity to uncertainties. Namely, the main target of RDO is to reduce the variability of the system performance, which is characterized most often by its standard deviation [21].

The differences between RBDO and RDO can be also interpreted by the distinguished definition of the objective function [22]: the objective function in RBDO is always with respect in the mean (or deterministic) sense, whereas the one connected with RDO is usually uncertain. For this reason, the correspondingly applicable scope may be quite

different and one could complement the other. Therefore, it is natural to take both RBDO and RDO as the research targets to fulfill various requirements in engineering (e.g. vibration control). More general, both of robustness and reliability are desired characteristics for the design optimization under uncertainties [23], i.e. design objective robustness and design feasibility robustness [24]. Therefore, the integrated framework, reliability-based robust design optimization (**RBRDO**) will be the final concentration of this work, in which the robust design is obtained under uncertain constraints quantified by the associated probability of failure. For convenience and clarity, we narrow the scope of SDO onto RBDO, RDO and RBRDO in this dissertation.

In the context of vibration control, supplemental passive, active, hybrid, and semiactive damping strategies offer attractive means to protect structures, including base isolation systems, viscoelastic dampers and the tuned mass dampers, are well understood and are widely accepted by the engineering community as a means for mitigating the effects of dynamic loadings on structures [25]. However, the passive methods are unable to adapt to structural changes and loading conditions. Then robust control methods in the domain of active control were proposed so that the optimal controller can provide robust performance and stability for a set of possible models of the systems. Nonetheless, if passive devices are designed under uncertainties, i.e. in the framework RBDO, RDO or RBRDO, the obtained optimal devices are somehow adaptive. Especially, the concept of robustness in RDO or RBRDO is to reduce the variability of the performance, i.e. to adapt a set of possible models of the systems, the goal of which is similar to the robust control. Moreover, RBDO and RBRDO can also provide optimal passive devices to make the protected systems with low probabilities of failure. Consequently, RBDO, RDO and RBRDO can be applied to design passive controllers.

Unfortunately, practical applications of RBDO and RDO are usually restricted or even prohibitive owing to their low efficiency. Two reasons are included. One is the UA or UQ. The associated UA in RBDO is reliability analysis, whereas the mean and standard deviation of the random response are essential in RDO. For convenience, reliability analysis or moment (the mean and standard deviation) evaluations are termed by UA indistinguishably. Generally, the target of UA is to determine the statistical properties related to the random response. The latter can be specified explicitly just for simple cases. In most practical structures however, the random response is only available in numerical way, i.e. finite element analysis (**FEA**). Accurate results can be obtained by

calculating large quantities of random responses in the context of Monte Carlo simulation (**MCS**). Moreover, a single transient response analysis may need a lot of CPU time. In this sense, UA is a time consuming task.

The other one is the formulation of RBDO or RDO, the interpretation of which is how UA is involved into the optimization process. Traditionally, UA involved in the probabilistic constraints and the objective function is nested into the design optimization. As is well known, the optimization algorithm is usually realized by the iteration process. During each iterative step, one or more function evaluations are needed to be carried out, i.e. the same number of UA is required. When the convergence rate is slow, the number of iterative steps is large, which implies the number of UA is large. Then, it is not difficult to imagine that RBDO or RDO is practically intractable due to its high computational effort.

Hence, this study also attempts to develop advanced approaches for RBDO and RDO that are computationally efficient and mathematically robust. Especially, these approaches are capable to establish connections among DDO, UA and deterministic FEA. Two aspects ought to be considered to achieve this target, i.e. efficient methods for UA and advanced formulations for RBDO or RDO.

Since either reliability analysis or moment evaluations (or the both) associated with the random response are required in RBDO or RDO (or the both in RBRDO), it would be better to develop an approach which can compute the both, fast and effectively. Considering that estimating the random response takes up the most computational effort in UA since the random response is practically obtained by repeated FEA, it is reasonable to reduce the number of FEA to improve efficiency. In the framework of the polynomial chaos expansion (**PCE**), the random response can be approximated with an acceptable accuracy. In this sense, UA can be carried out efficiently and easily.

If the efficient method for UA aims to reduce the time for a single reliability analysis or moment evaluation procedure, the advanced formulation is to reduce the number of UA. The main concern to achieve the latter target is to establish an explicit relation between the probability of failure/moments and the design variables. This is the so-called sequential formulation. In this occasion, there is no need to execute UA for each function evaluation. Then the efficiency is improved.

1.1.4 Failure mechanisms

In both RBDO and RDO, the corresponding constraints are always defined by some failure mechanisms of interest, which are very important to perform an optimization procedure. According to [26, 27], the mechanisms of failure can be divided into two broad categories: over-stress mechanisms (such as large elastic deformation, yield, buckling, fracture) and wear-out mechanisms (such as fatigue crack initiation and growth as well as creep).

In the former case, an failure event occurs only if the stress to which the structure is subjected exceeds the allowable strength. If the stress is below the strength, the stress has no permanent effect on the structure. In the latter case, however, the stress causes damage that usually accumulates irreversibly. The accumulated damage does not disappear when the stress is removed, although sometimes annealing is possible. The cumulative damage does not cause any performance degradation until is it below the endurance limit. Once this limit is reached, the structure fails.

As to random vibration, similar failure mechanisms can also be found in [28]: (1) Failure can occur at the first time that the random response reaches a certain level; (2) Failure can be due to the issue that the accumulation of small damages reaches a fixed sum. The estimation of the first passage (or first excursion) probability of failure is usually in conjunction with the former case; while the aging engineering belongs to the latter one. In this work, we concentrate on the over-stress or the first passage failure mechanism. Simply, when the structure is subjected to static loads, the over-stress mechanism is considered; when the structure is under dynamic loads, the first passage problem is regarded.

1.2 Organization of the dissertation

This dissertation is composed of six chapters, the organization of which will be described as follows:

- In Chapter 1, the motivation, objective and scope have been underlined that are the core of the rest of this dissertation. Namely, RBDO and RDO (or RBRDO)

for linear structural systems are mainly regarded in the context of the probability theory, following the over-stress or first passage failure mechanism. For the sake of practical applications, advanced methods for RBDO and RDO, which are computationally efficient and mathematically robust, are also concentrated on.

- In Chapter 2, the basic considerations of SDO for structural systems are introduced, including the fundamentals (DDO and UA) as well as the formulations for RBDO and RDO. In this chapter, we begin with DDO which provides the basic knowledge of design optimization. UA is sequently followed, in which the basic probability theories are introduced and the associated methods are reviewed. As to SDO, the various formulations and methods corresponding to RBDO and RDO are also reviewed. Based on the review, it is found that it is valuable to integrate RDO and RBDO, i.e. the RBRDO problem. For comprehension, comparative studies are shown between RBDO and DDO, as well as between RBDO and RBRDO. All the work in this dissertation depends on this chapter.

- In Chapter 3, we propose a PCE based MCS method for UA. The efficiency is mainly improved by avoiding repeated structural analyses. To overcome the curse of high dimensionality in dynamic problems induced by the stochastic excitations, the convolution form is used to compute the dynamic response, in which the PCE is raised to approximate the modal properties so that the dimension of uncertainties is reduced since only structural random parameters are considered. To correctly capture the uncertainties in the modal content, it is indispensable to avoid modal intermixing problem which is always encountered when using MCS to solve the random eigenvalue problem. Since the proposed method relies on MCS and modal analysis, this problem is also regarded. The MAC factor is applied to quantify the intermixing, and we develop a unvariable method to check which variable results in such a problem and thereafter to remove or reduce this issue.

- In Chapter 4, the sequential formulation of RBRDO is considered. The main advantages of this formulation are to improve efficiency and to overcome the non-convergence problem encountered in nested MCS based RBRDO. Different from conventional sequential strategy that mainly aims to decouple the reliability analysis from the optimization procedure, we also concentrate on making the moment evaluations independent from the optimization procedure. To realize the sequential RBRDO, locally "first-order" exponential approximation around the current

design is implemented to construct the equivalently deterministic objective functions and probabilistic constraints. We develop the auxiliary distribution based reliability sensitivity analysis and the PCE based moment sensitivity analysis to calculate the associated coefficients within one reliability analysis or one moment evaluation procedure respectively, such that the number of UA is reduced.

- In Chapter 5, main contribution is to apply RBRDO on passive vibration control, i.e. the design optimization of the TMD. Unlike CSDO, this framework is capable to consider uncertainties in both parameters and excitations. Minimization of the mean square of the response is retained in objective function, which aims to reduce the variability of the random response. Reliability analysis is involved in the probability constraint not only to obtain high reliability but also to control the amplitude of the random response within some prescribed threshold. Numerical simulations demonstrate that RBRDO is a powerful tool to optimally design the TMD.

- In Chapter 6, we present the conclusion of this dissertation and provide some perspectives of the future work.

Chapter 2

Stochastic design optimization for structural systems

2.1 Introduction

In this chapter, the main concerns of SDO for structural systems are regarded. To execute a SDO procedure, two aspects must be considered, i.e. DDO and UA. DDO plays a very important role in SDO since it provides the basic optimization theories and methods for SDO. If the values in DDO are uncertain, one needs UA to give the associated statistical measures, such as the mean, standard deviation and probability of failure. Therefore, three parts will be introduced in sequence:

1. We begin with the concerns related to DDO, including the terms, definitions, formulations and methodologies that are very closely associated with this dissertation.

2. To quantify uncertainties, the relevance of UA is introduced next. Not only the basic theories containing probability theory and probabilistic transformation are regarded, but also the methods are briefly reviewed that will be combined into DDO to construct SDO. Roughly speaking, these methods may give us a global perspective of UA. Their applicable scopes will be specified respectively, from which we can have an insight into which method is potential to give not only the probability of failure but also the moments.

3. The formulations and methods of SDO are finally discussed. Considering different criteria, RBDO, RDO and the integration of the two – RBRDO are all regarded. For comprehension, comparative studies are shown between RBDO and DDO, as well as between RBDO and RBRDO.

2.2 Deterministic design optimization

2.2.1 Terms and definitions

As underlined before, designers can search for optimal designs by applying a deterministic model in the framework of DDO. Typically, some variables and functions are very significant:

- *Design variables* denoted by the design vector $\mathbf{d} = [d_1, d_2, \ldots, d_{N_d}]^{\mathrm{T}},\ \mathbf{d} \in \mathbb{R}^{N_d}$, are the parameters that need to be determined to obtain the desired structural performance under some constraints. In structural optimization, they can be geometry parameters like beam length, plate thickness and cross section, as well as material properties including reinforcement distribution, etc.

- *State variables* denoted by the vector $\mathbf{x}(\mathbf{d}) = [x_1(\mathbf{d}), x_2(\mathbf{d}), \ldots x_n(\mathbf{d})]^{\mathrm{T}},\ \ \mathbf{x} \in \mathbb{R}^n$, are the parameters representing responses of the structure. A typical response refers to displacement, velocity, acceleration, stress, strain and so on. In practical applications, the state variables are mostly implicit functions of design variables and available in numerical way, e.g FEA. That leads to the implicit objective function or constraints.

- *Objective function* denoted by the function $f(\mathbf{d})$ or $f(\mathbf{d}, \mathbf{x}(\mathbf{d}))$, is the function to evaluate the merit of a design. Frequently, one objective function can measure weight, stiffness, displacement in a given direction, or simple costs. Thus, the objective function is usually termed by the cost function. Without generality, the objective function is commonly formulated by a minimization problem. In cases where only one objective function is considered, the optimization is termed as single-objective optimization; while for two or more objective functions, multi-objective optimization is regarded.

- *Deterministic constraint* denoted by the function $h(\mathbf{d})$ or $h(\mathbf{d}, \mathbf{x}(\mathbf{d}))$, is the restriction that must be satisfied in a structural design optimization corresponding some critical failure mechanism. Such a constraint divides the design space into the failure domain $h(\mathbf{d}) < 0$, the safety domain $h(\mathbf{d}) > 0$ and the limit state $h(\mathbf{d}) = 0$.

- Side constraints denoted by $\mathbf{d}^{\mathrm{L}} \leq \mathbf{d} \leq \mathbf{d}^{\mathrm{U}}$, provide the the lower bound $\mathbf{d}^{\mathrm{L}}$ and upper bound $\mathbf{d}^{\mathrm{U}}$ of the design variables $\mathbf{d}$.

The terms defined above characterize optimization problems. According to the types of design variables, three categories [6] of optimization tasks are distinguished within the structural design optimization community: sizing, shape and topology. Simply, design variables associated with geometry dimensions like cross section of a beam belong to sizing optimization; the ones with respect to geometry parameters like the height of a shell are attached to shape optimization; the ones regarding to structural configuration such as adding a new or removing an existing truss member of a truss is involved in topology optimization.

2.2.2 Formulations and methodologies

2.2.2.1 Single-objective optimization

The classical formulation of DDO for structures is mathematically expressed by:

$$\begin{aligned} \text{find} \quad & \mathbf{d} \\ \text{minimize} \quad & f(\mathbf{d}) \\ \text{subject to} \quad & -h_i(\mathbf{d}) \leq 0,\ i = 1, 2, \ldots, N_h \\ & \mathbf{d}^{\mathrm{L}} \leq \mathbf{d} \leq \mathbf{d}^{\mathrm{U}}, \end{aligned} \tag{2.1}$$

where $h_i(\mathbf{d})$ is the ith deterministic constraint and N_h is the total number. Generally, the optimum is located in the feasible design space $\mathbf{D}$, which is defined as the set $\mathbf{D} = \{\mathbf{d} | -h_i(\mathbf{d}) \leq 0,\ i = 1, 2, \ldots, N_h;\ \text{and}\ \mathbf{d}^{\mathrm{L}} \leq \mathbf{d} \leq \mathbf{d}^{\mathrm{U}}\}$. Note that in this expression, there is only one objective function which implies only one design target is focused on. To solve the above optimization problem, much attention has been drawn to develop more efficient and more powerful methods.

Particularly, the sequential quadratic programming (**SQP**) [29] method is one of the most used methods. SQP is a standard mathematical programming algorithm for solving non-linear programming optimization problems. It makes use of derivatives of the function with respect to the design variables to construct an approximate model of the initial problem. A new design point producing a decrease of the objective function can be found by a line search along the searching direction according to the information of the derivatives. This method can assure a local optimum but not a global one. This

shortcoming may be avoided by multiple initial designs. In this dissertation, we will use SQP to perform the optimization procedure.

Apart from SQP (also called the conventional methods), some innovative approaches employing analogies of physics and biology, such as simulated annealing method[30], genetic algorithm [31] and evolutionary algorithm [32], are applied for the solution of global optimization problems. Generally, in these approaches no gradient information is needed, whereas a large number of function evaluations are required.

2.2.2.2 Multi-objective optimization

When more than one objective functions, i.e. $\mathbf{f}(\mathbf{d}) = [f_1(\mathbf{d}), f_2(\mathbf{d}), \ldots, f_{N_f}(\mathbf{d})]^{\mathrm{T}}$ are needed to be optimized, multi-objective optimization is regarded. The principles of multi-objective optimization, also known as multi-criteria or vector optimization, are very different from those of a single-objective one. If all the objective functions are compatible, only one function is active and the others are redundant. More often, the objective functions are conflicting. In this case, a multi-objective optimization gives rise to a set of optimal solutions rather than one general optimal solution. Each possible solution cannot be considered to be better than the others. The relevant problem is known as Pareto optimality [33], which is defined as follows:

Definition 1. Pareto Optimal: A point, $\mathbf{d}^* \in \mathbf{D}$, is Pareto optimal if there does not exist another point, $\mathbf{d} \in \mathbf{D}$, such that $\mathbf{f}(\mathbf{d}) \leq \mathbf{f}(\mathbf{d}^*)$, and $f_i(\mathbf{d}) < f_i(\mathbf{d}^*)$ for at least one function.

A point is Pareto optimal if there is no other point that improves *at least one* objective function without detriment to another function. For practical applications, algorithms also provide solutions satisfying other criteria but Pareto optimal, such as weakly Pareto, the definition of which is described as:

Definition 2. Weakly Pareto Optimal: A point, $\mathbf{d}^* \in \mathbf{D}$, is weakly Pareto optimal if there does not exist another point, $\mathbf{d} \in \mathbf{D}$, such that $\mathbf{f}(\mathbf{d}) \leq \mathbf{f}(\mathbf{d}^*)$.

Obviously, a point is weakly Pareto optimal if there is no other point that improves *all* of the objective functions simultaneously [34]. Pareto optimal points are weakly Pareto optimal, but weakly Pareto optimal points are not Pareto optimal.

Many contributions have been made to solve the multi-objective optimization. The usual way is to convert the multiple objective functions into one objective function, which is also termed as the utility function. Before stating the "**utility function**" method, some common function transformation methods will be introduced first. Such transformations that make the objective functions dimensionless are advantageous when the objective functions have different units.

One way to construct non-dimensional objective function is given as follows [35]:

$$f_i^{\text{trans}}(\mathbf{d}) = \frac{f_i(\mathbf{d}) - f_i^*}{f_i^*}, \tag{2.2}$$

where f_i^* is the minimum of $f_i(\mathbf{d})$ for each $i = 1, \ldots, N_f$. This approach provides a dimensionless objective function with zero lower bound and unbounded upper value. In this formulation, computational difficulties can arise by the zero denominator or the negative value.

A variation on Eq. (2.2) is also developed [36]:

$$f_i^{\text{trans}}(\mathbf{d}) = \frac{f_i(\mathbf{d})}{f_i^*}, \qquad f_i^* > 0. \tag{2.3}$$

This approach overcomes the both difficulties of Eq. (2.2). Although it is impossible to guarantee $f_i^* > 0$ for all problems, this transformation is advantageous in some practical applications since the quantities of interest are usually positive, e.g. in the context of RDO. Note that it may be prohibitively expensive to compute f_i^* used in the foregoing approaches or f_i^* is not attainable; therefore, one may use alternatives, such as initial values [37]. Other analogical formulations can also be seen in relative works [38, 39].

In the following, combined with the transformed objective function, the "utility function" method is introduced in the presence of articulation of different objectives or the associated importance order. Regarding to the former, one of the most general utility functions is expressed in its simplest form as the **weighted exponential sum** [40, 41]:

$$f(\mathbf{d}) = U = \sum_{i=1}^{N_f} w_i (f_i(\mathbf{d}))^p, \qquad f_i(\mathbf{d}) > 0 \forall i, \tag{2.4}$$

$$f(\mathbf{d}) = U = \sum_{i=1}^{N_f} (w_i f_i(\mathbf{d}))^p, \qquad f_i(\mathbf{d}) > 0 \forall i, \tag{2.5}$$

where U represents the utility function, p is the exponent, w_i denotes the weights typically set by the design makers such that $\sum_{i=1}^{N_f} w_i = 1$ and $w_i > 0$, and $f_i(\mathbf{d})$ can be replaced by Eq. (2.3). Extensions of the above two expressions can be found in works [42–44], described as

$$f(\mathbf{d}) = U = \left[\sum_{i=1}^{N_f} w_i (f_i(\mathbf{d}) - f_i^*)^p \right]^{\frac{1}{p}}, \tag{2.6}$$

$$f(\mathbf{d}) = U = \left[\sum_{i=1}^{N_f} w_i^p (f_i(\mathbf{d}) - f_i^*)^p \right]^{\frac{1}{p}}. \tag{2.7}$$

Here, $f_i(\mathbf{d}) - f_i^*$ can be taken place by Eq. (2.2). In the weighted exponential sum family, the most common approach is the weighted sum method,

$$f(\mathbf{d}) = \sum_{i=1}^{N_f} w_i f_i(\mathbf{d}), \tag{2.8}$$

which can be treated as a special form of Eq. (2.4) or Eq. (2.5) with $p = 1$. $f_i(\mathbf{d})$ here can also be replaced by Eq.(2.3).

To check if or not these formulations (not confined to the weighted exponential sum formulations) can provide Pareto optimal sets, a necessary and/or a sufficient condition is central:

- If a formulation provides a necessary condition, then for a point to be Pareto optimal, it must be a solution to that formulation. However, some solutions obtained by this formulation may not be Pareto optimal.
- If a formulation provides a sufficient condition, then its solution is always Pareto optimal. However, this formulation may not produce all the points of the associated Pareto optimal sets.

Generally, formulations that provide both necessary and sufficient conditions for Pareto optimality are preferable [34]. When one is interested in determining a single solution belonging to Pareto optimal sets, methods giving a sufficient condition are applicable. This situation may be more attractable for some practical applications. Accordingly, the effectiveness for the formulations in Eq.(2.5)-Eq.(2.8) are listed as follows:

- Eq. (2.5) is sufficient and necessary for Pareto optimality according to the work [41]. The property $f_i(\mathbf{d}) > 0 \ \forall i$ is very valuable for RDO since the associated dimensionless mean and standard deviation are both positive. Therefore, a RDO problem can be formulated like this. A relatively large value of p may be helpful to capture certain Pareto optimal points for non-convex Pareto optimal sets. However, as p trends to infinity, this formulation is only weakly sufficient.

- Eq. (2.6) is sufficient [44] as long as $w_i > 0, i = 1, \ldots, N_f$, which can be applied when one single solution is required. Analogically, Eq. (2.7) is also proved to be sufficient by Zeleny [43].

- Eq. (2.8) is sufficient for Pareto optimality but necessary [45]. This formulation is impossible to deal with non-convex Pareto optimal sets, but non-convex phenomenon is rare. Moreover involved in a local optimal problem, the non-convex issue may be ignored.

In the weighted exponential family, varying only p can yield part of Pareto optimal points. Typically, p and w_i are not changed simultaneously. Design makers usually fix p and change w_i to produce a set of Pareto points. In this vein, a set of Pareto optimal points might be obtained by varying the weights.

On the other hand, the bounded objective function methods have been developed in the sense of importance order. Essentially, the most significant objective function is extracted and the others are used to form additional constraints. Among these methods, Haimes *et al.* [46] introduced the $\varepsilon-$constraint approach (also termed as the $\varepsilon-$constraint or trade-off approach), which is described as

$$\begin{aligned} & f(\mathbf{d}) = f_j(\mathbf{d}) \\ & f_i(\mathbf{d}) \leq \varepsilon_i, \quad i = 1, 2, \ldots, j-1, j+1, \ldots, N_f. \end{aligned} \tag{2.9}$$

It is apparent that the upper bound ε_i must be specified to construct the additional constraints. In this sense, a systematic variation of ε_i yields a set of Pareto optimal points. However, improper choice can lead to infeasible solutions.

Apart from the "unity function" method which converts the original multi-objective optimization into a single-objective optimization, there exists approaches that can solve the

multi-objective problems directly, such as the genetic algorithm NSGA-II [47]. Genetic algorithms for multi-objective optimization provide a set of Pareto optimal solutions by one running rather than solve a sequence of single-objective problems as the "unity function" method does. In this dissertation, the main task is not to develop advanced optimization algorithms, so only the close relevance is regarded in this brief review. For more multi-objective optimization methods, one may refer to the survey [34].

2.3 Uncertainty analysis

So far, the fundamentals and formulations of DDO have been known. To consider uncertainties, one needs to add them in the framework of DDO. In this sense, it is indispensable to state the way to quantify uncertainties before introducing SDO. For the aleatory uncertainty is focused on, we therefore in this part begin with the probability theory. The transformation techniques are sequentially specified which are essential in some UA methodologies. At last various methods for the UA that are frequently used are reviewed.

2.3.1 Basic probability theory

In the context of the probability theory, the uncertainties are modeled by random variables, stochastic processes or random fields that can be either continuous or discrete. They are characterized by the moments and correlation. Let y be a realization of continuous random variable Y, the randomness of which is represented by the probability density function (**PDF**), $q_Y(y)$. The probability of Y in the interval $[a, b]$ is calculated by the integral

$$P(a \leq Y \leq b) = \int_a^b q_Y(y)dy, \tag{2.10}$$

where $P(\cdot)$ is the probability operator. The cumulative distribution function (**CDF**) denoted as $Q_Y(y)$ can be obtained by

$$Q_Y(y) = \int_{-\infty}^{y} q_Y(y)dy, \tag{2.11}$$

where $q_Y(y) = dQ_Y(y)/dy$. The mean of Y, denoted as μ, the standard deviation of Y, denoted as σ, and the correlation of two random variables Y_1 and Y_2 denoted as ρ_{12} are

respectively given by

$$\mu = \int_{-\infty}^{\infty} y q_Y(y) dy, \tag{2.12}$$

$$\sigma^2 = \int_{-\infty}^{\infty} (y-\mu)^2 q_Y(y) dy, \tag{2.13}$$

$$\rho_{12} = \frac{1}{\sigma_1 \sigma_2} \int_{-\infty}^{\infty} \int_{-\infty}^{\infty} (y_1-\mu_1)(y_2-\mu_2) q_{Y_1,Y_2}(y_1,y_2) dy_1 y_2, \tag{2.14}$$

where $q_{Y_1,Y_2}(y_1,y_2)$ is the joint probability density function of Y_1 and Y_2. In cases where Y_1 and Y_2 are independent, the joint PDF can be rewritten as

$$q_{Y_1,Y_2}(y_1,y_2) = q_{Y_1}(y_1) q_{Y_2}(y_2). \tag{2.15}$$

Eq. (2.10)– Eq. (2.15) can be extended to multi-dimensional situations. This will be shown later.

2.3.2 Probabilistic transformation

Let $\mathbf{Y} = [Y_1, \ldots, Y_n]^{\mathrm{T}}$ and $\mathbf{U} = [U_1, \ldots, U_n]^{\mathrm{T}}$ denote an arbitrary random vector and a standard normal vector respectively. $\mathbf{y} = [y_1, \ldots, y_n]^{\mathrm{T}}$ and $\mathbf{u} = [u_1, \ldots, u_n]^{\mathrm{T}}$ are the associated realizations. Consider a transformation of these two:

$$\mathbf{U} = \mathrm{Tr}(\mathbf{Y}). \tag{2.16}$$

The probabilistic transformation in the last equation depends on the joint PDF $q_{\mathbf{Y}}(\mathbf{y})$ of $\mathbf{Y}$. Three types of practical considerations are possible:

- $\mathbf{Y}$ is a random vector with independent variables. The joint PDF can be given

$$q_{\mathbf{Y}}(\mathbf{y}) = q_{Y_1}(y_1) q_{Y_2}(y_2) \cdots q_{Y_n}(y_n). \tag{2.17}$$

  The probabilistic transformation in this case is directly obtained by the one to one mapping

$$u_i = \Phi^{-1}(Q_{Y_i}(y_i)), \tag{2.18}$$

  where $\Phi^{-1}(\cdot)$ is the inverse CDF of standard normal variable and $Q_{Y_i}(\cdot)$ is the CDF corresponding to the ith random variable Y_i.

- $\mathbf{Y}$ is a normal random vector with dependent variables, the PDF of which is in the form of

$$q_{\mathbf{Y}}(\mathbf{y}) = \frac{1}{\sqrt{(2\pi)^n \det\mathbf{C}}} \exp(-\frac{1}{2}\bar{\mathbf{y}}^T \mathbf{C}^{-1} \bar{\mathbf{y}}), \tag{2.19}$$

where $\bar{\mathbf{y}} = \mathbf{y} - \boldsymbol{\mu} = [y_1 - \mu_1, \ldots, y_n - \mu_n]^{\mathrm{T}}$ and $\det\mathbf{C}$ is the determinant of the covariance matrix $\mathbf{C}$, which is defined by

$$\mathbf{C} = \begin{bmatrix} \sigma_1^2 & \rho_{12}\sigma_1\sigma_2 & \cdots & \rho_{1n}\sigma_1\sigma_n \\ \rho_{21}\sigma_2\sigma_1 & \sigma_2^2 & \cdots & \rho_{2n}\sigma_2\sigma_n \\ \vdots & \vdots & \ddots & \vdots \\ \rho_{n1}\sigma_n\sigma_1 & \cdots & \cdots & \sigma_n^2 \end{bmatrix}, \qquad \rho_{ij} = \rho_{ji}. \tag{2.20}$$

The probabilistic transformation is then calculated by

$$\mathbf{u} = \mathrm{Tr}(\mathbf{y}) = \mathbf{A}^{-1}\bar{\mathbf{y}}, \tag{2.21}$$

where $\mathbf{A}$ is obtained by the Cholesky decomposition of covariance matrix

$$\mathbf{C} = \mathbf{A}\mathbf{A}^{\mathrm{T}}. \tag{2.22}$$

- $\mathbf{Y}$ is a non-normal random vector with dependent variables. The joint PDF of these random variables is not known. Two kinds of transformations may be regarded according to the information known priori: Nataf model [48] and Rosenblatt transformation [49]. If the marginal distributions and correlation matrix are available, the Nataf model is applied, i.e.

$$u_i = \Phi^{-1}(Q_{Y_i}(y_i)), \tag{2.23}$$

where $Q_{Y_i}(y_i)$ is referred particularly to the marginal CDF of ith random variable Y_i, and the associated marginal PDF is represented by $q_{Y_i}(y_i)$. The joint PDF by Nataf model is expressed as

$$q_{\mathbf{Y}}(\mathbf{y}) = \phi_n(\mathbf{u}, \mathbf{C}_0) \frac{q_{Y_1}(y_1) \ldots q_{Y_n}(y_n)}{\phi(u_1) \ldots \phi(u_n)}, \tag{2.24}$$

where $\phi(\cdot)$ is the PDF of standard normal variable, $\phi_n(\mathbf{u}, \mathbf{C}_0)$ is expressed similar to the Eq. (2.19) and the $\mathbf{C}_0 = \mathbf{A}_0\mathbf{A}_0^{\mathrm{T}}$ has the same formulation with Eq. (2.20)

with $\sigma_i = 1$. Then the probabilistic transformation to the standard normal space is

$$\mathbf{u} = \mathrm{Tr}(\mathbf{y}) = \mathbf{A}_0^{-1}\mathbf{u} = \mathbf{A}_0^{-1}[\Phi^{-1}(Q_{Y_1}(y_1)), \ldots, \Phi^{-1}(Q_{Y_n}(y_n))]^{\mathrm{T}}, \tag{2.25}$$

If the conditional PDF is known, the Rosenblatt transformation is applied. It permits the mapping of jointly distributed, continuous valued random variables from the physical space into the space of uncorrelated, standard normal random variables. The associated definition is as follows:

$$\begin{cases} u_1 &= \Phi^{-1}(Q_{Y_1}(y_1)) \\ u_2 &= \Phi^{-1}(Q_{Y_2}(y_2|y_1)) \\ \ldots & \\ u_n &= \Phi^{-1}(Q_{Y_n}(y_n|y_1, \ldots, y_{n-1})), \end{cases} \tag{2.26}$$

where $Q_{Y_1}(y_1), Q_{Y_2}(y_2|y_1), \ldots, Q_{Y_n}(y_n|y_1, \ldots, y_{n-1})$ are known as the conditional CDFs.

TABLE 2.1: Analytical transformation

Distribution Type	Parameters	Transformation
Uniform	a, b	$a + (b-a)(\frac{1}{2} + \frac{1}{2}\mathrm{erf}(u/\sqrt{2}))$
Normal	μ, σ	$\mu + \sigma u$
Lognormal	μ, σ	$\exp(\mu + \sigma u)$
Gamma	a, b	$ab(u\sqrt{\frac{1}{9a}} + 1 - \frac{1}{9a})^3$
Exponential	λ	$-\frac{1}{\lambda} log(\frac{1}{2} + \frac{1}{2}\mathrm{erf}(u/\sqrt{2}))$
Weibull	a, b	$a(-ln(\Phi(-u))^{\frac{1}{b}}$

[1] $\mathrm{erf}(x) = \frac{2}{\sqrt{\pi}} \int_0^x e^{-t^2} dt$, error function; $\Phi(x) = \frac{1}{\sqrt{2\pi}} \int_0^x e^{\frac{-t^2}{2}} dt$, CDF of standard normal variable

Some analytical transformations mentioned in [50, 51] between random variables of common univariate distributions and standard normal variables have been list in Table 2.1. These linear or nonlinear relations offer convenient transformations in UA.

2.3.3 Methodologies and applications

In this section, the relevant methods for UA are reviewed. Basically, the statistics of the random response can be completed by a variety of approaches, among which the perturbation method, polynomial chaos expansion (**PCE**) method, first- or second-order

reliability method (**FORM/SORM**), response surface method (**RSM**), direct Monte Carlo Simulation (**MCS**) and advanced MCS are frequently used.

Some of them are special for reliability analysis, whereas some of them dominate in moment evaluations. Roughly speaking, the aforementioned methods may give us a global perspective of UA. Their applicable scopes will be specified respectively, from which we can have an insight into which method is potential to give the probability of failure and the moments at the same time.

In the framework of mechanical engineering, let the random vector $\boldsymbol{\theta} = [\theta_1, \ldots, \theta_{N_s}]^{\mathrm{T}},\ \boldsymbol{\theta} \in \mathbb{R}^{N_s}$ denote the N_s-dimensional random structural parameters (e.g. material property and geometry tolerance) and the random vector $\mathbf{Z} = [Z_1, \ldots, Z_{N_l}]^{\mathrm{T}},\ \mathbf{Z} \in \mathbb{R}^{N_l}$ represent the N_l-dimensional random inputs (e.g. excitations). All the uncertainties of interest can be described as the union of the random structural parameters and random inputs, say $\boldsymbol{\Theta} = \{\boldsymbol{\theta}, \mathbf{Z}\},\ \boldsymbol{\Theta} \in \mathbb{R}^N, N = N_s + N_l$.

Generally, the probability of failure, the complement of reliability, is determined by a multi-dimensional integral over the failure region:

$$P_F = P(F) = \int_F q(\boldsymbol{\Theta}) d\boldsymbol{\Theta}, \tag{2.27}$$

where F is associated with the failure region defined by $g(\boldsymbol{\Theta}) < 0$, while $g(\boldsymbol{\Theta}) = 0$ is the limit state function and $g(\boldsymbol{\Theta}) > 0$ denotes the safe region, $q(\boldsymbol{\Theta})$ denotes the joint PDF and $P(\cdot)$ is the failure probability operator. Note that $g(\boldsymbol{\Theta})$ represents the uncertain constraint, which is the function of the random response. Let $x_i(\boldsymbol{\Theta}),\ i = 1, \ldots, n$ represent any one of n random responses (or state variables). The associated mean μ_i, standard deviation σ_i and correlation coefficients ρ_{ij} are formed as

$$\mu_i = \int_{\mathbb{R}^N} x_i(\boldsymbol{\Theta}) q(\boldsymbol{\Theta}) d\boldsymbol{\Theta}. \tag{2.28}$$

$$\sigma_i^2 = \int_{\mathbb{R}^N} (x_i(\boldsymbol{\Theta}) - \mu_i)^2 q(\boldsymbol{\Theta}) d\boldsymbol{\Theta}. \tag{2.29}$$

$$\rho_{ij} = \frac{1}{\sigma_i \sigma_j} \int_{\mathbb{R}^N} (x_i(\boldsymbol{\Theta}) - \mu_i)(x_j(\boldsymbol{\Theta}) - \mu_j) q(\boldsymbol{\Theta}) d\boldsymbol{\Theta}. \tag{2.30}$$

2.3.3.1 Perturbation method

The perturbation method, introduced in the late 1970's in the context of the stochastic finite element method (**SFEM**) [52], has been successfully employed for random eigenvalue problems [53, 54], for geotechnical problems [55, 56], for dynamic problems [21, 57, 58] and for static problems [21, 59], thanks to its attractive efficiency. This method is based on Taylor series expansion in terms of a set of zero mean random variables. It can be used advantageously in cases where the random fluctuations are small [60] compared with the nominal structure, such that terms of order two or higher are negligible. The recommended coefficients of variance of the uncertainties in structures should be $< 5\%$ [61]. Hence, the perturbation method has the capability to determine the uncertainties without large dispersion, especially for moment evaluations of the random response. Additionally, according to the knowledge of the author, there is less applications of such method to reliability analysis.

2.3.3.2 Polynomial chaos expansion

The original PCE, also termed as the homogenous chaos and Hermite polynomial chaos expansion (**HPCE**), was developed by Wiener [62]. Over the last decades, the application of PCE within the SFEM [63] has drawn significant attention. The application of PCE, especially HPCE, may refer to modeling uncertain input parameters [64, 65], representing non-Gaussian stochastic processes [66, 67], evaluating second order statistics of the stochastic response [68–72], carrying out reliability analysis [73–75] and sensitivity analysis [76–78].

As to representation of random inputs, the K-L expansion [79] has been widely used and shown the almost sure convergence for Gaussian processes or fields. However, the covariance structure of the random field is required which is always not available due to the lack of available experimental data. The main advantage of the PCE compared to the K-L expansion is that the covariance structure is not required.

In most applications mentioned above, HPCE is utilized to represent the random response within SFEM or independent from the SFEM [80]. Yet, the implementations apart from the structural analysis, such as the fluid analysis [81–84], transport transformation modeling [51], are still called much attention. Since HPCE has the capability to

approximate the random response, it is not difficult to deduce that HPCE in conjunction with direct MCS can be involved in UA, including both moment evaluations and reliability analysis.

In cases where the random inputs are not normal, HPCE may be applied by transforming the non-normal random variables to the standard normal variables. The associated transformation techniques have been introduced in Section 2.3.2. However, the convergence rate may be substantially slow when representing the random response by HPCE due to the random inputs are not normal. To this end, extensions to other orthogonal polynomials in terms of non-Gaussian random variables, named Wiener-Askey or general PCE, could be used according to the work of Xiu and Karniadakis [85].

Generally, PCE is, from the efficiency point of view, more applicable for problems with small number of random inputs. This situation is more involved with static problems rather than dynamic ones since the stochastic excitation is discretized by a uncertainty sequence with high dimension [86]. Hence, it is not surprising to find that most applications are related to the static analysis according to the survey [87]. Regarding to the dynamic problem, the associated analysis is mainly concentrated on the modal properties, in which the uncertainties of the excitation are not included. Nonetheless, it is possible to extend the PCE to approximate the dynamic response for a quite important class of structures – linear random structures, thanks to its linear relation between outputs and inputs. This study will be introduced in Chapter 3.

2.3.3.3 First- or second-order reliability method

FORM are the most probable point of failure (**MPP**) based reliability analysis method. They are always realized in an independent and standard normal random space. Namely, an arbitrary random vector $\boldsymbol{\Theta} = [\Theta_1, \Theta_2, \ldots, \Theta_N]^{\mathrm{T}}$ is mapped as $\boldsymbol{\xi} = [\xi_1, \xi_2, \ldots, \xi_N]^{\mathrm{T}}$, an independent standard normal vector. The limit state function is then transformed into standard normal space is $g(\boldsymbol{\Theta}) = G(\boldsymbol{\xi})$. Two formulations [50, 88, 89] of FORM have been developed: the reliability index approach (**RIA**) and the performance measure approach (**PMA**).

Pioneered by the work of Cornell [90], the reliability index was brought into the researchers' horizon. However, Cornell reliability index is not invariant to the selection of

the failure surface [91]. To overcome this weakness, FORM was developed due to the contributions by Hasofer and Lind [92], Rackwitz and Fiessler [93] as well as Hoenbichler and Rackwitz [94]. Such studies have provided a foundation for the RIA, in which the reliability index β is obtained by the following optimization problem in the standard normal space

$$\begin{aligned} \min \quad & \|\boldsymbol{\xi}\| \\ \text{s.t.} \quad & G(\boldsymbol{\xi}) = 0. \end{aligned} \tag{2.31}$$

The solution associated with the minimum distance from the limit state surface $G(\boldsymbol{\xi}) = 0$ to the origin is the MPP denoted as $\boldsymbol{\xi}^*$. Then the reliability index is obtained by $\beta = \|\boldsymbol{\xi}^*\|$.

An alternative FORM, the advanced mean value (**AMV**) method has been proposed by Wu et al. [95]. This research defines an inverse reliability analysis compared to RIA for FORM, termed by the PMA. However, the AMV is well suited for problems with convex performance functions, while for concave ones the conjugate mean value (**CMV**) [96] is more appropriate. The hybrid mean value (**HMV**) is an adaptive method also proposed in [96] associated with either convex or concave type. Mathematically, the PMA formulation is in the form of

$$\begin{aligned} \min \quad & G(\boldsymbol{\xi}) \\ \text{s.t.} \quad & \|\boldsymbol{\xi}\| = \beta_t, \end{aligned} \tag{2.32}$$

where β_t is the target reliability index required in RBDO. The solution of the last optimization problem is concerned with the MPP $\boldsymbol{\xi}^*$ where the performance $G(\boldsymbol{\xi}^*)$ is minimized. It has been reported that PMA is inherently robust and far more effective when the probabilistic constraint is either very feasible or very infeasible [50].

FORM has been widely used in engineering [97] for many years. However, its applications are restricted for some aspects. Since FORM is a point estimation method (MPP search) with linear approximation, it encounters difficulties when dealing with problems with strongly non-linear limit state functions or with high dimension, criticized for its inaccuracy and inefficiency. Moreover, the effort to compute the MPP grows proportionally with the dimension [98].

To enhance the results by FORM, SORM has been proposed. The basic idea is to approximate the limit state function by a quadratic surface at the MPP. Examples can be found in the studies [99, 100]. In SORM, besides the evaluation of the MPP, some curvatures are needed to be calculated compared with FORM. From this view, the computational burden is aggravated. Analogically, with the dimension increasing, the results may be questionable. Note that both methods are seldom applied in moment evaluations. From the view of comprehension, a simple $2-$D example for FORM and SORM is depicted by Fig. 2.1.

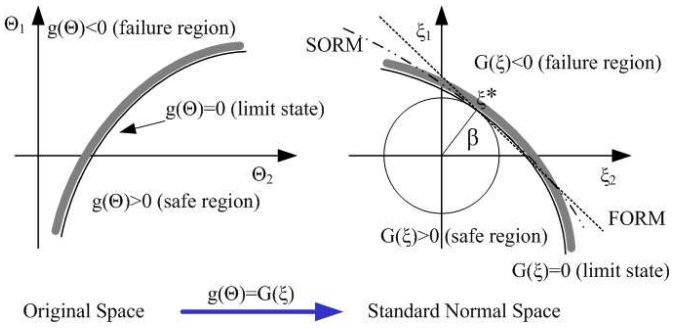

FIGURE 2.1: FORM/SORM [1]

2.3.3.4 Response surface method

Most often, it is hard to find the close-form limit state functions for practical considerations, which can be commonly available by numerical way. In this case, applications of FORM/SORM are confined. Direct and advanced MCS are "fit candidates", but MCS is cumbersome due to its high computational expense. To incur excessive computational costs, researchers have adopted the RSM [101–104] that permits FEA to be combined with FORM/SORM. Profited from this procedure, a polynomial response function up to second order is generally evaluated by performing Taylor series expansion around the MPP. The reason of abandoning higher order polynomials is because of their possibly instable solutions [105]. To evaluate the associated coefficients, the least square method (**LSF**) is usually utilized, where the experimental data are prepared either by physical experiment or by numerical analysis.

The RSM has been used in researches and it works well when the number of input variables is small. However, analogical to FORM/SORM, it may be criticized for its inaccuracy and inefficiency with a large number of input variables. To that end, one can turn to other approaches for sound solutions, e.g. advanced MCS.

2.3.3.5 Direct Monte Carlo simulation

Direct MCS is the most generally applicable procedure to simulate and quantify uncertainties. The word "direct" here is associated with the original MCS to distinguish the advanced one. Both the moments and probabilities of failure can be evaluated by this procedure. It was proposed by physicists [106] for the Manhattan Project of Los Alamos Labs. And now, it is extended to the fields ranging from finance, social science, chemistry, medicine, biology and mathematics [107–111]. Several advantages have been shown with the application of direct MCS. The following discussions are limited in the context of mechanical engineering.

1. It provides the possibility to deal with any mechanical models. That implies the structural properties, i.e. linear or nonlinear, static or dynamic, continuous or discrete, are inessential.

2. There is no need to modify the numerical code when applying direct MCS, which ensures that direct MCS can deal with very complex structural systems. Furthermore, with such an advantage, it can also be coupled with parallel processes to improve efficiency.

3. It is insensitive to the number of the uncertainties. It happens that the large number of uncertainties are more frequent situations encountered in engineering.

In mechanical engineering, direct MCS is implemented to generate samples from the given PDF, and to provide the information of the random responses in the presence of the moments and probabilities of failure. Mathematically, the multi-dimension integral in Eq. (2.27) can be rewritten as

$$P_F = P(F) = \int_F f(\boldsymbol{\Theta}) d\boldsymbol{\Theta} = \int_{\mathbb{R}^N} I_F(\boldsymbol{\Theta}) f(\boldsymbol{\Theta}) d\boldsymbol{\Theta} = E(I_F(\boldsymbol{\Theta})), \tag{2.33}$$

where $E(\cdot)$ denotes the mean or mathematical expectation, and $I_F(\boldsymbol{\Theta})$ is the indicator function. The interpretation is $I_F(\boldsymbol{\Theta}) = 1,\ \boldsymbol{\Theta} \in F$; otherwise, $I_F(\boldsymbol{\Theta}) = 0$. The Monte-Carlo estimator of P_F is then formulated as

$$\hat{P}_F = \frac{1}{N_{\text{mc}}} \sum_{k=1}^{N_{\text{mc}}} I_F(\boldsymbol{\Theta}^{(k)}), \tag{2.34}$$

where $\boldsymbol{\Theta}^{(k)}$ is the kth set of random variables and N_{mc} is the number of samples used by direct MCS. Its convergence is measured by the coefficient of variation of $\hat{P}_F$

$$\delta_{\text{mc}} = \frac{\sqrt{\text{Var}(\hat{P}_F)}}{P_F} = \sqrt{\frac{1 - P_F}{N_{\text{mc}} P_F}}, \tag{2.35}$$

where the variance of $\hat{P}_F$ is calculated by

$$\text{Var}(\hat{P}_F) = \frac{(1 - \hat{P}_F)\hat{P}_F}{N_{\text{mc}}}. \tag{2.36}$$

Similarly, the Monte-Carlo estimator for the mean and standard deviation of the random response $x_i(\boldsymbol{\Theta})$ can be respectively expressed by

$$\hat{\mu}_i = \frac{1}{N_{\text{mc}}} \sum_{k=1}^{N_{\text{mc}}} x_i(\boldsymbol{\Theta}^{(k)}). \tag{2.37}$$

$$\hat{\sigma}_i^2 = \frac{1}{N_{\text{mc}} - 1} \sum_{k=1}^{N_{\text{mc}}} (x_i(\boldsymbol{\Theta}^{(k)}) - \hat{\mu}_i)^2. \tag{2.38}$$

$$\hat{\rho}_{ij} = \frac{1}{N_{\text{mc}} \hat{\sigma}_i \hat{\sigma}_j} \sum_{k=1}^{N_{\text{mc}}} (x_i(\boldsymbol{\Theta}^{(k)}) - \hat{\mu}_i)(x_j(\boldsymbol{\Theta}^{(k)}) - \hat{\mu}_j). \tag{2.39}$$

Consideration of requirements of high accuracy however, direct MCS is computational intensive because a lot of samples, more general structural analyses, are required. As a consequence, its implementation is practically prohibitive especially for large-scale structural systems whose responses are only available in numerical way, i.e. FEA. This is aggravated to estimate small probability of failure. For example, in civil engineering, it is common to use an admissible probability of failure of $P_F = 10^{-4}$ for the ultimate limit state. That implies at least 10^4 structural analyses are required. More refined target values can be found in the Eurocodes.

2.3.3.6 Advanced Monte Carlo simulation

To overcome the main disadvantages mentioned in Section 2.3.3.5 and to make use of the advantages of direct MCS, advanced MCS has been raised. The word "advanced" emphasized here is with respect to high efficiency compared to direct MCS.

The most significant concern for reliability analysis is the variance reduction technique, among which the important sampling theory [108, 112] is widely used. The basic idea

is to generate more samples from the failure regions and thereafter the total number of samples is reduced. The critical issue of importance sampling is to recognize the failure region and to formulate the importance sampling density.

Importance sampling methods [113–115] based on design points or pre-samples are well suited for static problems. These methods have difficulties to deal with problems with high dimension of uncertainties, e.g. structures with stochastic excitations. Hence, for dynamic structures alternatives are needed. One can refer to a very efficient method [116] which is appropriate for the linear dynamic systems with deterministic structural parameters. As to more general cases, subset simulation family [117–119] have shown their advantages especially involved in problems with high dimension of uncertainties. This has been demonstrated by a benchmark study [120].

Apart from the importance sampling, other methods such as line sampling methods [121] and an approximate method by selecting the reference point of the random structural parameters [122] have the advantages in estimating the first-passage probability of failure for random linear dynamic systems.

Note that the methods mentioned above are mainly regarding reliability analysis, the efficiency of which is improved by reducing the number of samples. The contributions of this methodology should be paid pretty much respect. This methodology dominates without doubt in reliability analysis, whereas it may not obtain the moments of the associated response accurately. We can deduce that the moments may be overestimated by the importance sampling since most of samples are located in the failure region which may be very relevant to the tails of the PDF.

If the improvement of efficiency is realized by fast calculation of the random response rather than reducing the number of samples, as is done by PCE, direct MCS becomes computational manageable. It is not difficult to expect that with the help of this strategy, the associated probability of failure, the mean, and the standard deviation of the random response are readily obtained by Eq. (2.34), Eq. (2.37) and Eq. (2.38) respectively. In this sense, the PCE based MCS belongs to advanced MCS since its efficiency is improved. This method is proposed in this work that will be specified in Chapter 3.

Until now, two basic parts (i.e. DDO and UA) of SDO are well known. In the following, the issues related to SDO are introduced.

2.4 Stochastic design optimization

As stated in DDO, an optimal design is searched under deterministic merit functions and constraints. While in SDO, these functions are either deterministic or uncertain, which are usually shown by their statistical measurements, i.e. the mean, standard deviation and probability of failure. In the framework of structural optimization, most of practical applications pursue at least three conflicting aims [123]: low structural cost, high reliability and good structural performance.

1. **Low structural cost**. Generally, the cost refers to the total cost C_{T} all through the life cycle, which consists of the initial cost C_{I} (including design, manufacturing, transport and construction costs), the failure cost C_{F} (function of P_F), the preventive maintenance cost C_{M}, the inspection cost C_{S}, the repair cost C_{P}, the use cost C_{U} and the recycling cost C_{R} and destruction cost C_{D} [124], leading to the cost function

$$C_{\mathrm{T}} = C_{\mathrm{I}} + C_{\mathrm{F}} + C_{\mathrm{M}} + C_{\mathrm{S}} + C_{\mathrm{P}} + C_{\mathrm{U}} + C_{\mathrm{R}} + C_{\mathrm{D}}. \tag{2.40}$$

   Consideration of human factors and economy levels with respect to different countries, except the initial cost the total cost is very complicated to estimate, for example, the failure cost. Hence, the above equation is not tractable to utilize and only the initial cost is involved, say $C_{\mathrm{T}} = C_{\mathrm{I}}$ [2]. Accordingly, to reduce the cost, design makers at least try to minimize the initial cost C_{I}.

2. **High reliability**. In essence, high reliability is equivalent to small probability of failure, which gives the probability that one performance index exceeds the prescribed value, e.g. the probability of the stress greater than the allowable strength. To achieve this kind of design, reliability analysis is a powerful tool.

3. **Good structural performance**. This implies the serviceability and good quality are insured during the life time. A reasonable way to achieve these goals is connected with the dispersion reduction of the performance. This requires a robust design where the structural performance is less sensitive to the variation of parameters.

To achieve such aims, RBDO, RDO and the integration of the both RBRDO have been developed and implemented corresponding to specified requirements. In the following, the formulations and methodologies are reviewed respectively.

2.4.1 Reliability-based design optimization

2.4.1.1 General formulations

RBDO is a methodology for finding optimized designs that are characterized with a low probability of failure. Primarily, RBDO consists of optimizing a merit function by satisfying probabilistic and deterministic constraints. Mathematically, a basic formulation is described as

$$\begin{aligned} \text{find} \quad & \mathbf{d} \\ \text{minimize} \quad & f(\mathbf{d}) \\ \text{subject to} \quad & P(g_i(\mathbf{d}, \boldsymbol{\Theta}) \leq 0) - P_{F_{t,i}} \leq 0,\ i = 1, 2, \ldots, N_g \\ & - h_j(\mathbf{d}) \leq 0,\ j = 1, 2, \ldots, N_h \\ & \mathbf{d}^{\mathrm{L}} \leq \mathbf{d} \leq \mathbf{d}^{\mathrm{U}}. \end{aligned} \tag{2.41}$$

This formulation is similar to DDO, except that the probabilistic constraints $P(g_i(\mathbf{d}, \boldsymbol{\Theta}) \leq 0) - P_{F_{t,i}} \leq 0,\ i = 1, 2, \ldots, N_g$ are involved, where $g_i(\mathbf{d}, \boldsymbol{\Theta}) < 0$ defines the failure region, $g_i(\mathbf{d}, \boldsymbol{\Theta}) = 0$ is the limit state function and $g_i(\mathbf{d}, \boldsymbol{\Theta}) > 0$ refers to safe region; $P_{F_{t,i}}$ is the associated target probability of failure; N_g represents the total number of the probabilistic constraints. Note that $g_i(\mathbf{d}, \boldsymbol{\Theta})$ is equivalent to $g_i(\boldsymbol{\Theta})$. The later replaced by the former is to stress the concept of design. For convenience of the notation, we also denote $P_{F,i}(\mathbf{d}, \boldsymbol{\Theta}) = P(g_i(\mathbf{d}, \boldsymbol{\Theta}) \leq 0)$.

Design vector $\mathbf{d}$ in this case, may comprise deterministic parameters, e.g. geometry dimensions, or distribution parameters, i.e. the means of random variables $\boldsymbol{\mu}_{\boldsymbol{\Theta}}$. The variance design is seldom used as an independent design parameter due to the practically uncontrollably manufacturing process [5]. In this case, the variance is always assumed according to the manufacturing criteria and the practical requirements. Generally, the coefficient of variance (**COV**, the ratio between the mean μ and standard deviation σ of a random variable, i.e. μ/σ) is not very large.

In RBDO, deterministic objective function at the mean values of random variables are often used [23]. When the objective function is also uncertain, i.e. $f(\mathbf{d}, \boldsymbol{\Theta})$, a more rigorous mathematical notation is in writing $E(f(\mathbf{d}, \boldsymbol{\Theta}))$ instead of $f(\mathbf{d})$, which is pursuing the nominal design. For simplicity, the notation $f(\mathbf{d})$ is maintained. As to the associated standard deviation that represents the quality control and dispersion reduction aspects will be referred to the concept of the robust design and not involved in the context of RBDO. We will talk about it later.

Generally, the objective function is also termed as the cost function, i.e. $f(\mathbf{d}) = C_I(\mathbf{d})$. In this sense, the formulation in Eq. (2.42) is called the cost optimization with reliability constraints (**CRP**) [123] since the cost is minimized subject to a given minimum reliability, say

$$\begin{aligned} \text{find} \quad & \mathbf{d} \\ \text{minimize} \quad & C_{\mathrm{I}}(\mathbf{d}) \\ \text{subject to} \quad & P(g_i(\mathbf{d}, \boldsymbol{\Theta}) \leq 0) - P_{F_{t,i}} \leq 0, \ i = 1, 2, \ldots, N_g \\ & - h_j(\mathbf{d}) \leq 0, \ j = 1, 2, \ldots, N_h \\ & \mathbf{d}^{\mathrm{L}} \leq \mathbf{d} \leq \mathbf{d}^{\mathrm{U}}. \end{aligned} \tag{2.42}$$

The optimal design can also be obtained by minimizing the probability of failure subject to a given maximum cost, which is known as the reliability optimization with cost constraints (**RCP**) [123]. Then RCP formulation is written as

$$\begin{aligned} \text{find} \quad & \mathbf{d} \\ \text{minimize} \quad & P_F(\mathbf{d}, \boldsymbol{\Theta}) \\ \text{subject to} \quad & C_{\mathrm{I}}(\mathbf{d}) - C_{\mathrm{I},t} \leq 0 \\ & - h_j(\mathbf{d}) \leq 0, \ j = 1, 2, \ldots, N_h \\ & \mathbf{d}^{\mathrm{L}} \leq \mathbf{d} \leq \mathbf{d}^{\mathrm{U}}, \end{aligned} \tag{2.43}$$

where $C_{\mathrm{I},t}$ is the target cost. Note that in the above formulation, only one probability of failure is treated as merit function. This is a simplified expression. When concerning two or more probabilities of failure need to be minimized, one may construct a multi-objective optimization problem (see Section 2.2.2.2) for solutions. In cases where the minimum cost is priori unknown, a variant [2] of CRP is particularly useful. It is realized

by maximizing the reliability per unit cost under other constraints:

$$\begin{aligned} \text{find} \quad & \mathbf{d} \\ \text{maximize} \quad & \frac{1}{P_F(\mathbf{d}, \boldsymbol{\Theta}) C_{\mathrm{I}}(\mathbf{d})} \\ \text{subject to} \quad & -h_j(\mathbf{d}) \leq 0, \ j = 1, 2, \ldots, N_h \\ & \mathbf{d}^{\mathrm{L}} \leq \mathbf{d} \leq \mathbf{d}^{\mathrm{U}}. \end{aligned} \tag{2.44}$$

Among these three, the first formulation, i.e. CRP (see Eq. (2.41) or (2.42)), is the most frequently used. One probable reason is because the RCP problem requires considerably more numerical effort than CRP, which was shown in the case study of the work [123]. Nonetheless, applications of RCP can be found in some fields, such as design optimization for the tuned mass damper [125, 126].

Over the last couple of decades, a variety of approaches have been proposed to perform RBDO (mainly concerning CRP). Because reliability analysis is a computationally expensive task in engineering, in order to reduce the computational burden of RBDO, two kinds of approaches are mainly applied. One is through improving the efficiency of reliability analysis as shown in Section 2.3.3. The other is the way that reliability analysis is involved in the optimization procedure, based on which these approaches can be divided into three broad categories.

2.4.1.2 Nested double loop

The traditional way to perform RBDO is the so-called nested double loop algorithm, as shown in Fig. 2.2. This formulation is basic but the most expensive. It is evident that reliability analyses are included in the outer optimization loop. Often, reliability analysis is realized by an MPP-based iterative numerical analysis procedure, such as FORM. This is the reason why the traditional RBDO is called as nested double loop.

When applying FORM, the probability of failure has a non-linear relation with the corresponding reliability index, $P_F = \Phi(-\beta)$ or $\beta = -\Phi^{-1}(P_F)$, where $\Phi(\cdot)$ and $\Phi^{-1}(\cdot)$ are the Gaussian CDF and inverse Gaussian CDF respectively.

Combined with the algorithm of RIA (see Section 2.3.3.3), where the probabilistic constraints in Eq. (2.41) is taken place by the reliability index constraints, then the **RIA**

based RBDO is expressed as

$$\begin{aligned} \text{find} \quad & \mathbf{d} \\ \text{minimize} \quad & f(\mathbf{d}) \\ \text{subject to} \quad & -\beta_i(\mathbf{d}, \boldsymbol{\Theta}) + \beta_{t,i} \leq 0, \ i = 1, 2, \ldots, N_g \\ & -h_j(\mathbf{d}) \leq 0, \ j = 1, 2, \ldots, N_h \\ & \mathbf{d}^{\mathrm{L}} \leq \mathbf{d} \leq \mathbf{d}^{\mathrm{U}}, \end{aligned} \tag{2.45}$$

where the reliability index $\beta_i(\mathbf{d}, \boldsymbol{\Theta})$ related to the ith limit state function $g_i(\mathbf{d}, \boldsymbol{\Theta})$ is the solution of RIA optimization procedure solved in the standard normal space (shown in Eq. (2.31)), and $\beta_{t,i}$ is the associated target reliability index.

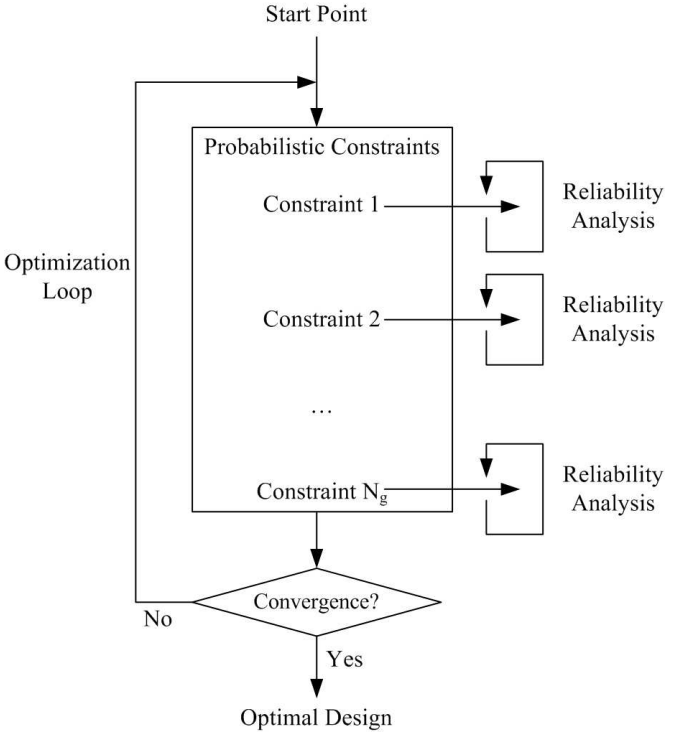

FIGURE 2.2: Generalized nested double loop of RBDO

The statistical description of the failure of the limit state function $g_i(\mathbf{d}, \boldsymbol{\Theta})$ can be characterized by its CDF $F_{g_i}(0)$ as

$$P(g_i(\mathbf{d}, \boldsymbol{\Theta}) \leq 0) = F_{g_i}(0) \leq \Phi(-\beta_{t,i}), \tag{2.46}$$

i.e.

$$g_i(\mathbf{d}, \boldsymbol{\Theta}) = F_{g_i}^{-1}(\Phi(-\beta_{t,i})) \geq 0, \tag{2.47}$$

and therefore an alternative constraint is brought in, based on which the **PMA based RBDO** is constructed in the form of

$$\begin{aligned} \text{find} \quad & \mathbf{d} \\ \text{minimize} \quad & f(\mathbf{d}) \\ \text{subject to} \quad & -g_i(\mathbf{d}, \boldsymbol{\Theta}) \leq 0, \ i = 1, 2, \ldots, N_g \\ & -h_j(\mathbf{d}) \leq 0, \ j = 1, 2, \ldots, N_h \\ & \mathbf{d}^{\mathrm{L}} \leq \mathbf{d} \leq \mathbf{d}^{\mathrm{U}}, \end{aligned} \tag{2.48}$$

where $g_i(\mathbf{d}, \boldsymbol{\Theta})$ is evaluated by PMA (see Section 2.3.3.3) mentioned in Eq. (2.32) in the standard normal space. Solving RBDO by the PMA formulation is usually more efficient and robust than the RIA one where the reliability analysis is executed directly. The efficiency lies in the fact that the search for the MPP of an inverse reliability problem (PMA) is easier to realize than the search for the MPP corresponding to an actual reliability [89]. Moreover, the RIA based RBDO fails to converge for distributions with bound (e.g., uniform) and extreme type distributions (e.g., Gumbel) [127]. Hence, the PMA based RBDO is more frequently used than the RIA based RBDO.

It is found that the PMA based RBDO is not that efficient for large-scale applications. To this end, a PMA+ [128] based RBDO is proposed to make RBDO computationally affordable. When there is not sensitivity information available or no closed form limit state function, the PMA family may not be efficient enough. To attain this objective, a new RBDO methodology [102] is developed to integrate the PMA method with a new RSM, in which a moving least square method is implemented.

Apart from the integration of FORM into RBDO framework, one can also utilize M-CS, especially for the situation when there are a large number of random variables, when no closed-form limit state function exists or when the limit state function is high-nonlinear. In the context of MCS, advanced MCS is more attractive thanks to its high efficiency. A reliability-based structural optimization, combination of neural networks and importance sampling into the evolution strategy optimization, is proposed [129]. In this method, the neural networks are applied to construct implicit deterministic or probabilistic constraints and thereafter importance sampling is employed to carry out the associated reliability analysis.

Recall that all aforementioned RBDO is in the nested double loop content, the improved efficiency of which is mainly achieved by advanced reliability analysis. The nested double loop is computationally intensive for problems where the function evaluations are expensive. This problem will be aggravated as the number of probabilistic constraints increase. To alleviate the computational expense, sequential RBDO have been developed and widely applied.

2.4.1.3 Sequential double loop

The basic idea behind sequential double loop of RBDO is to decouple the reliability analysis from the optimization loop, which provides the designer with the option of using existing optimizers and the probabilistic software without code modifications. In sequential RBDO, the optimization loop and the reliability analysis are performed sequentially and the entire procedure is repeated until the desired convergence is achieved. For convenience, a sub-sequential-procedure comprising one or more reliability analyses (or several reliability analyses) and an equivalently deterministic optimization loop is defined. By repeating several these sub-procedures, it is possible to find the local or global optimum. A generalized procedure is illustrated in Fig. 2.3. The task of the reliability analysis here is used to providing the information required by the optimization.

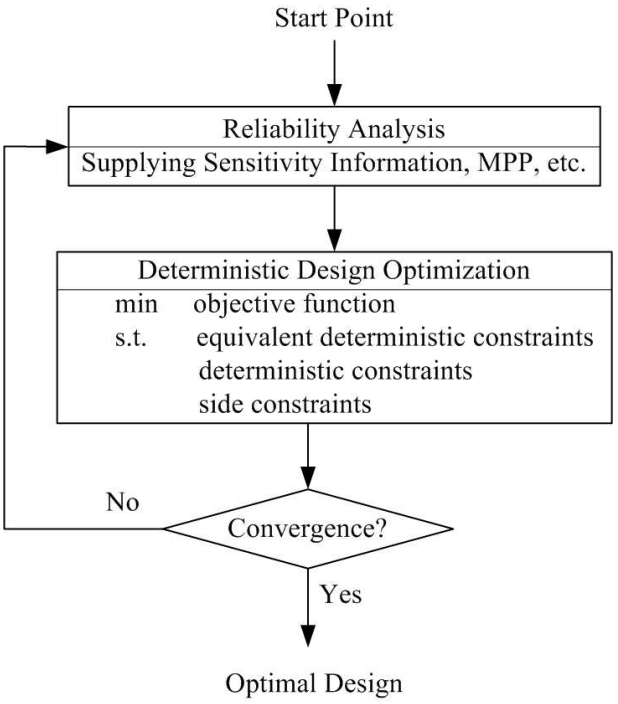

FIGURE 2.3: Generalized sequential double loop of RBDO

In most sequential RBDO, a design is obtained by performing an equivalent DDO by converting probabilistic constraints into equivalent deterministic ones and is updated based on the information supplied by the reliability analysis, such as the sensitivity with respect to the design variables, the MPP when FORM is utilized, and other relevance. Consequently, the most critical issue is how to construct the equivalent deterministic constraints. Several techniques have been developed to achieve this target:

- Sequential optimization and reliability assessment (**SORA**)[130]. In SORA, the key concept is to shift the boundaries of violated deterministic constraints (with low reliability) to the feasible direction. PMA is used to do reliability analysis, which supplies the MPP and the associated shifted factors. Then the equivalent deterministic constraints are functions of the design variables and shifted factors.

- Safety-factor based RBDO [131]. This approach merges the safety-factor concept into the MPP concept to replace probabilistic constraints by deterministic constraints. The basic idea is to replace random variables by the safety-factor based values. After each reliability analysis, the MPP and design shift are given. With these value, a deterministic limit state function is formulated. Then DDO is performed and a new design is found. The whole process is repeated until the MPP procedure and DDO converge.

- Alternative way to construct the equivalent deterministic constraints is proposed by Agarwal [1]. In this method, the sensitivities of the MPP with respect to the decision variables are introduced to update the MPP during DDO of the sequential procedure. This method not only finds the optimal solution but also locates the exact MPP, which is important to ensure the target reliability index. The MPP update is based on the first order Taylor series expansion around the design point from the last sub-sequential-procedure. The inverse reliability analysis or PMA is used to search the MPP.

- When FORM is inaccurate for situations with higher nonlinearity or with large number of random variables, simulation techniques are necessary, e.g. MCS. To this end, the sequential RBDO with conjunction of MCS [132] is also raised. The equivalent deterministic constraints are approximated by a first order Taylor series expansion around the current design points. Apart from the usage of the sequential strategy, the importance sampling is implemented to improve efficiency of MCS.

2.4.1.4 Single loop

Besides the sequential RBDO, there is also an alternatively advanced formulation, the so-called single loop, which can reduce the computational expense. In the single loop, the reliability constraints are replaced by their corresponding first-order Karush-Kuhn-Tuchker (KKT) necessary optimality conditions in the optimization loop, as the works [123, 133, 134] did. Accordingly, there is no need to execute reliability analysis and the nested double loop is converted into a single optimization loop. Such a single loop is equivalent to the originally nested one as long as the optimization is solved by numerically satisfying the KKT conditions.

It should be noted that the dimension of the design space is usually increased. The reason is that the random variables entering the optimization are also seen as design variables [133, 134]. Additionally, the converged solutions are the desired MPPs according to the work [133], in which the Lagrange multipliers are also treated as design variables and needed to be optimized.

2.4.1.5 Comparative study between DDO and RBDO

This simple case study aims at showing that to get a more security design, uncertainties must be taken into account in practical engineering. Consider a mathematical model [50] of RBDO with the distribution type of design variables $\mathbf{d} = [\mu_{\Theta_1}, \mu_{\Theta_2}]^{\mathrm{T}}$. The RBDO problem is described as follows

$$\begin{aligned} \text{find} \quad & \mathbf{d} \\ \text{minimize} \quad & f(\mathbf{d}) = d_1 + d_2 \\ \text{subject to} \quad & P(g_i(\mathbf{d}, \boldsymbol{\Theta}) \leq 0) \leq \Phi(-\beta_{t,i}),\ i = 1, 2, 3 \\ & 0 \leq d_j \leq 10,\ j = 1, 2, \end{aligned} \tag{2.49}$$

where

$$\begin{aligned} g_1(\boldsymbol{\Theta}) &= \Theta_1^2 \Theta_2 / 20 - 1, \\ g_2(\boldsymbol{\Theta}) &= (\Theta_1 + \Theta_2 - 5)^2 / 30 - (\Theta_1 - \Theta_2 - 12)^2 / 120 - 1, \\ g_3(\boldsymbol{\Theta}) &= 80 / (\Theta_1^2 + 8\Theta_2 + 5) - 1, \end{aligned} \tag{2.50}$$

and $\beta_{t,i} = 3$, the standard deviation $\sigma_i = 0.3$, $i = 1, 2, 3$ and $\boldsymbol{\Theta}$ follow normal distribution. To investigate the difference between DDO and RBDO, $\boldsymbol{\Theta}$ are treated as deterministic variables in DDO, i.e. $\mathbf{d} = [\Theta_1, \Theta_2]^{\mathrm{T}}$.

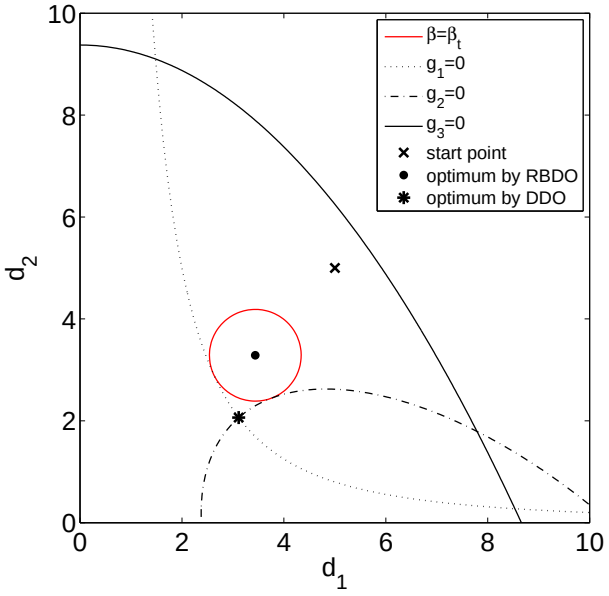

FIGURE 2.4: Comparison of DDO and RBDO. d_1 and d_2 are two design variables. In RBDO, $d_1 = \mu_{\Theta_1}$ and $d_2 = \mu_{\Theta_2}$; In DDO, $d_1 = \Theta_1$ and $d_2 = \Theta_2$.

Both optimization processes begin with the same start point $\mathbf{d}^0 = [5, 5]^{\mathrm{T}}$ shown by "x" in Fig. 2.4. The optimal designs obtained by RBDO and DDO are $\mathbf{d}^{\mathrm{RBDO}} = [3.4391, 3.2866]^{\mathrm{T}}$ and $\mathbf{d}^{\mathrm{DDO}} = [3.1139, 2.0626]^{\mathrm{T}}$, respectively.

From Fig. 2.4, it is evident that no matter what optimization problem is considered, only two constraints (g_1 and g_2) are active. When uncertainties are involved, consideration of a deterministic model to take place of the random model brings sever failure, since the optimum (depicted by "$*$") provided by DDO is located at the crossing of the active limit states whereas the RBDO optimum falls in the safe region (shown by "$\bullet$").

2.4.2 Robust design optimization

2.4.2.1 Concept of robust design

As outlined before, RBDO is a methodology for finding optimized designs that are characterized with a low probability of failure. However, RDO is a very different paradigm.

Robust design is an engineering methodology for optimal design of products and process conditions that are less sensitive to system variations [21]. The aim of RDO is to improve the quality of a product through minimizing the effect of variation without eliminating the causes [135]. Consequently, RDO is to reduce the variability of the system performances.

Fig. 2.5 compares a DDO with a RDO for a one-dimensional performance function to give a conceptual comprehension of RDO. With the same variability of a design variable, the robust optimum shows less variation of the performance function $f(d)$ than the deterministic optimum.

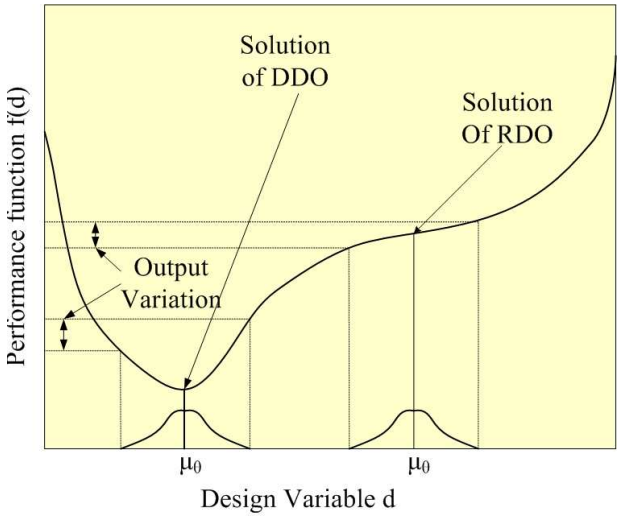

FIGURE 2.5: Comparison of RDO and DDO [37]. In DDO, the design variable d is deterministic, while in RDO the design variable d is random, e.g. the associated mean value $d = \mu_\theta$. The objective function $f(d)$ is related to the performance.

RDO always emphasizes on achieving the robustness of the performance (usually for design objective, seen from Fig. 2.5). In this context, the associated objective function is usually uncertain which might not be dealt with the mean sense as is done in RBDO. This problem will be concerned later.

Basically, robust design addresses both the design objective robustness and the design feasibility robustness. The former is realized by minimizing the variability of the objective function, whereas the latter is guaranteed by satisfying the uncertain constraints, such as in manner of reliability analysis. To achieve these targets, unlike RBDO, there is not a unified mathematical formulation in the literatures. The distinctions among all are mainly shown by the way to quantify the design objective robustness and the design feasibility robustness.

To discuss various developed formulation of RDO, a typical design model under uncertainties is given first, i.e.

$$\begin{aligned} \text{find} \quad & \mathbf{d} \\ \text{minimize} \quad & f(\mathbf{d}, \boldsymbol{\Theta}) \\ \text{subject to} \quad & -g_i(\mathbf{d}, \boldsymbol{\Theta}) \leq 0,\ i = 1, 2, \ldots, N_g \\ & \mathbf{d}^{\mathrm{L}} \leq \mathbf{d} \leq \mathbf{d}^{\mathrm{U}}, \end{aligned} \tag{2.51}$$

where $f(\mathbf{d}, \boldsymbol{\Theta})$ is the uncertain objective function which is distinguished from $f(\mathbf{d})$ by entering the uncertainties $\boldsymbol{\Theta}$, $\mathbf{d}$ is the design vector which can be deterministic variables or distribution parameters of random design variables, and $g_i(\mathbf{d}, \boldsymbol{\Theta})$ is the uncertain constraint. For simplicity, the deterministic constraint $h_j(\mathbf{d})$ is not listed here. If the random response $x(\mathbf{d}, \boldsymbol{\Theta})$ is involved in the objective function, the notation $f(\mathbf{d}, \boldsymbol{\Theta})$ is equivalent to $f(\mathbf{d}, \boldsymbol{\Theta}, x(\mathbf{d}, \boldsymbol{\Theta}))$. For convenience, we use $f(\mathbf{d}, \boldsymbol{\Theta})$ to represent the both.

2.4.2.2 Design objective robustness

It has been recognized that the robustness of a design objective can be achieved by simultaneously minimizing the mean performance and the performance variance [21, 22, 24]. In this case, the objective function can be expressed as

$$\text{minimize} \quad \mathbf{f}(\mathbf{d}, \boldsymbol{\Theta}) = [\mu_f(\mathbf{d}, \boldsymbol{\Theta}), \sigma_f(\mathbf{d}, \boldsymbol{\Theta})]^{\mathrm{T}}. \tag{2.52}$$

Within this formulation, RDO is solved in the framework of multi-objective optimization. As introduced in Section 2.2.2.2, one can adds a weight factor before each entry to transform the vector objective type to a scalar type. More often, a normalized formulation is used, i.e.

$$\text{minimize} \quad f(\mathbf{d}, \boldsymbol{\Theta}) = w_1 \frac{\mu_f(\mathbf{d}, \boldsymbol{\Theta})}{\mu^*} + w_2 \frac{\sigma_f(\mathbf{d}, \boldsymbol{\Theta})}{\sigma^*}, \tag{2.53}$$

where $\mu_f(\mathbf{d}, \boldsymbol{\Theta})$, $\sigma_f(\mathbf{d}, \boldsymbol{\Theta})$ are the mean and standard deviation of the objective function $f(\mathbf{d}, \boldsymbol{\Theta})$ respectively; $w_1,\ 0 < w_1 < 1$ and $w_2,\ 0 < w_2 < 1$ are the positive wight factors, the relation of which is $w_1 + w_2 = 1$; μ^* is the normalized factor obtained by $w_1 = 1$ and $w_2 = 0$, and σ^* is analogically evaluated by $w_1 = 0$ and $w_2 = 1$. This formulation

in Eq. (2.53) is actually following the principle shown in Eq. (2.8) in which the original objective function is transformed as Eq. (2.3).

Alternative formulations based on Eq. (2.4) have also been developed [37]. Three typical formulations are stated as follows:

- Nominal-the-best type.

$$\text{minimize} \quad f(\mathbf{d},\boldsymbol{\Theta}) = w_1(\frac{\mu_f(\mathbf{d},\boldsymbol{\Theta}) - f_t}{\mu^0 - f^0})^2 + w_2(\frac{\sigma_f(\mathbf{d},\boldsymbol{\Theta})}{\sigma^0})^2, \tag{2.54}$$

  where f_t and f^0 are the target nominal value and the initial nominal value of the objective function $f(\mathbf{d},\boldsymbol{\Theta})$, μ^0 and σ^0 are the values at the start point. This selection of normalized parameters can save CPU time when the convergence rate is slow.

- Smaller-the-better type.

$$\text{minimize} \quad f(\mathbf{d},\boldsymbol{\Theta}) = w_1 \cdot \text{sgn}(\mu_f(\mathbf{d},\boldsymbol{\Theta})) \cdot (\frac{\mu_f(\mathbf{d},\boldsymbol{\Theta})}{\mu^0})^2 + w_2(\frac{\sigma_f(\mathbf{d},\boldsymbol{\Theta})}{\sigma^0})^2. \tag{2.55}$$

- Larger-the-better type.

$$\text{minimize} \quad f(\mathbf{d},\boldsymbol{\Theta}) = w_1 \cdot \text{sgn}(\mu_f(\mathbf{d},\boldsymbol{\Theta})) \cdot (\frac{\mu^0}{\mu_f(\mathbf{d},\boldsymbol{\Theta})})^2 + w_2(\frac{\sigma_f(\mathbf{d},\boldsymbol{\Theta})}{\sigma^0})^2. \tag{2.56}$$

Since the weighted sum approach is utilized to solve the multi-objective optimization problem, it is natural to raise a problem: how to choose the weight factors. The most simple way is to fix different wight factors at each optimization process so that the associated solutions provide a possibility of generating a set of Pareto optima. Note that the final decision should be made by the designer based on the practical requirements and subjective judgement.

Apart from reducing the variance of the objective function to control the variability, alternative measure is also developed. In the original Taguchi's robust design [136], the "compound noise" is implemented to assess high or low quality performances. The associated typical value of $\pm\sqrt{3/2}\sigma$ for noise level does not always generate the highest and lowest quality performance. To overcome this drawbacks but maintain the basic idea of the "compound noise", recently a percentile performance difference method [23] has

been proposed to represent the variation of a performance, taking place of the frequently used standard deviation method (see Eq. 2.53). The percentile performance difference is given by

$$\Delta f_{\alpha_1}^{\alpha_2}(\mathbf{d}, \mathbf{\Theta}) = f^{\alpha_2}(\mathbf{d}, \mathbf{\Theta}) - f^{\alpha_1}(\mathbf{d}, \mathbf{\Theta}), \tag{2.57}$$

in which α_1 and α_2 are probabilities of failure or the CDFs of $f(\mathbf{d}, \mathbf{\Theta})$, i.e.

$$P(f(\mathbf{d}, \mathbf{\Theta}) \leq f^{\alpha_i}(\mathbf{d}, \mathbf{\Theta})) = \alpha_i, \ i = 1, 2, \tag{2.58}$$

where α_1 is a left-tail CDF, e.g. 0.05 or 0.01 that presents the performance at the left tail of its distribution and α_2 is a right-tail CDF, e.g. 0.95 or 0.99. Percentile performances $f^{\alpha_1}(\mathbf{d}, \mathbf{\Theta})$ and $f^{\alpha_2}(\mathbf{d}, \mathbf{\Theta})$ represent the low and high quantity levels respectively, as is depicted in Fig 2.6, from which we can see that the percentile performance difference is the distance between $f^{\alpha_2}(\mathbf{d}, \mathbf{\Theta})$ and $f^{\alpha_1}(\mathbf{d}, \mathbf{\Theta})$ corresponding α_1 and α_2 respectively. Minimizing the percentile performance difference helps to shrink the range of the distribution.

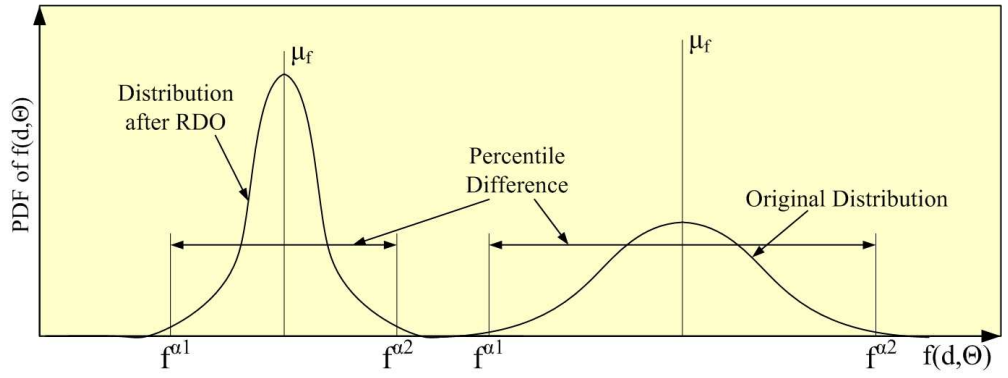

FIGURE 2.6: Concept of percentile difference method for RDO [23]

In the percentile performance difference method, the critical issue is to evaluate $f^{\alpha_1}(\mathbf{d}, \mathbf{\Theta})$ and $f^{\alpha_2}(\mathbf{d}, \mathbf{\Theta})$ that are obtained by the inverse reliability analysis (e.g. PMA), as is described in Section 2.3.3.3. In summary, the normalized formulation of the objective function is constructed as

$$\text{minimize} \quad f(\mathbf{d}, \mathbf{\Theta}) = w_1 \frac{\mu_f(\mathbf{d}, \mathbf{\Theta})}{\mu^*} + w_2 \frac{\Delta f_{\alpha_1}^{\alpha_2}(\mathbf{d}, \mathbf{\Theta})}{\Delta^*}, \tag{2.59}$$

where $w_i, \ i = 1, 2$, μ^* and Δ^* have the same definition with Eq. (2.53). Indicated also by Du et al. [23], this formulation is not suited for the non-unimodal distribution of the

performance function (or objective function) since the percentile performance difference at two tails may not decrease the variance of such performance distribution.

2.4.2.3 Design feasibility robustness

No matter what formulation of the objective function we use to achieve the robustness of product performance, it is critical to maintain the design feasibility under uncertainties [24]. This in fact, leads to a problem: the measure of uncertainties in uncertain constraints to ensure the requirements.

The probabilistic measure, i.e. probability of failure or reliability, is usually used as is done in RBDO. Considering the high computational burden, several alternatives with low computational expense have been developed:

- **The moment approach** [21]. In this approach, the first and second moments of g_i are used. According to Kang [21], the uncertain constraint is equivalent to

$$\mu_{g_i}(\mathbf{d}, \boldsymbol{\Theta}) - \beta_{t,i}\sigma_{g_i}(\mathbf{d}, \boldsymbol{\Theta}) \geq 0, \ i = 1, 2, \ldots, N_g, \tag{2.60}$$

  where $\mu_{g_i}(\mathbf{d}, \boldsymbol{\Theta})$ and $\sigma_{g_i}(\mathbf{d}, \boldsymbol{\Theta})$ are the mean and standard deviation of uncertain constraint g_i respectively, $\gamma_i = \mu_{g_i}(\mathbf{d}, \boldsymbol{\Theta})/\sigma_{g_i}(\mathbf{d}, \boldsymbol{\Theta})$ can be interpreted as the reliability index which is identical with the Cornell reliability index and $\beta_{t,i}$ can be seen as the target reliability index. Accordingly, the last expression is written as

$$\gamma_i \geq \beta_{t,i}. \tag{2.61}$$

  The mean and standard deviation can be evaluate efficiently by approximate method, such as the perturbation method and the first order Taylor's series. This formulation is not a real reliability measure unless the uncertain constraint g_i follows normal distribution. With this assumption, the moment matching formulation [137] was proposed. The associated uncertain constraint is replaced by the probabilistic constraint, say

$$P(g_i(\mathbf{d}, \boldsymbol{\Theta}) \leq 0) = \Phi(-\gamma_i) \leq \Phi(-\beta_{t,i}). \tag{2.62}$$

When the constraint g_i is not normal, the last expression is not an exact reliability formulation. As stressed, this method is attractive in cases where the the calculation cost is more concerned by the designers.

- **The worst case approach** [137]. It is another simplistic approach to evaluate the feasibility robustness. It is applicable to general robust design problems including those in which the distributions of random variables are not given. As the name defined, the worst case assumes that all fluctuations may occur simultaneously in the worst possible combinations. The variability of a uncertain constraint is estimated by a first Taylor's series.

  In most cases, the worst case approach is almost conservative because it is impossible that the worst cases of variable will simultaneously occur. On the contrary, the Taylor expansion may lead to inaccuracy for extreme conditions such as minimum and maximum. However, due to its low computational cost, its applications are widely accepted.

- **The corner space evaluation approach** [138]. Based on the basic idea of the worst case approach, the corner space evaluation method is developed, in which the descriptions of the distributions of random variables are not required. In this method, there is no need to propagate the uncertainties to the constraints and the "worst case" is determined in the tolerance space (T).

  Assume that a random design variable θ has a nominal value μ_θ and a tolerance $\Delta\theta$. A selection of points close to the target design point θ_t where each point represents a possible design variable construct the tolerance space, as

$$T(\theta_t) = \{\theta_t : |\theta_t - \theta| \leq \Delta\theta\}, \tag{2.63}$$

  according to which, the corner space (W) consists only of the corner vertices of the corresponding tolerance space, say

$$W(\theta_t) = \{\theta_t : |\theta_t - \theta| = \Delta\theta\}. \tag{2.64}$$

  Note that to maintain the design feasibility, the nominal value μ_θ should be inside the feasible region. This can be achieved by keeping the corner space always touching the original constraint boundary.

Comparative studies have been shown in the work [24], depending on which the applicable scope can be concluded as follows:

- Consideration of the accuracy to represent the uncertainties and to assure the design feasibility robustness, the probabilistic measure is an ideal method, while it is the most expensive, especially for cases where the approximate method, e.g. FORM, is not available and MCS is employed.
- If both the calculation cost and the accuracy are needed, the moment approach can be used. It provides an accurate estimation of the probability when the constraint normally distributed. The moment approach is much more computationally efficient than the probabilistic one. Unfortunately, such reliability index is not invariant depending on the formulation of the uncertain constraint [91].
- The worst case approach is usually a conservative method that provides safer designs. The obtained results are more accurate than those obtained by the moment approach, and meanwhile the efficiency is also attractive. However, the cost is not the minimum and it may not very competitive in the market. Furthermore, there is the possibility that the design points violate the constraint satisfactions. Consequently, we should use it with caution.
- When the economy is the most concerned, one can use the corner space evaluation approach since this approach avoids the statistical analysis. The accuracy of this method depends on whether the constraint function is monotonic with respect to all design variables in the tolerance space. One limitation is that it does not provide the information on the probability of failure of the constraint.

2.4.3 Reliability-based robust design optimization

With the development of computer science and algorithms of reliability analysis, reducing the computational burden will not be a tough task. Therefore, as to RDO both design objective robustness and the reliability analysis to the uncertain constraints are desired characteristics. Then we come to a hybrid paradigm, RBRDO. A typical formulation of

RBRDO is formulated as

$$\begin{aligned} \text{find} \quad & \mathbf{d} \\ \text{minimize} \quad & f(\mathbf{d}, \boldsymbol{\Theta}) = w_1 \frac{\mu_f(\mathbf{d}, \boldsymbol{\Theta})}{\mu^*} + w_2 \frac{\sigma_f(\mathbf{d}, \boldsymbol{\Theta})}{\sigma^*} \\ \text{subject to} \quad & P(g_i(\mathbf{d}, \boldsymbol{\Theta}) \leq 0) - P_{F_{t,i}} \leq 0, \ i = 1, 2, \ldots, N_g \\ & \mathbf{d}^{\mathrm{L}} \leq \mathbf{d} \leq \mathbf{d}^{\mathrm{U}}. \end{aligned} \tag{2.65}$$

Until now, the quantities of the weight factors are $0 < w_1 < 1$ and $0 < w_2 < 1$ to specify the applicable scope of RBBDO or RDO.

2.4.3.1 Relation between RDO, RBDO and RBRDO

Generally, the design feasibility robustness in RDO can be quantified by probabilistic method, the moment method, the worst case approach and so on. While in the context of RBRDO, the design feasibility robustness is guaranteed only by probabilistic method, which renders RBRDO a special case within RDO.

On the other hand, RBDO considers the cases where the objective function is deterministic or in the mean sense. From this view, RBDO and RBRDO are mutually complemented, with the design feasibility robustness guaranteed by the probabilistic measure. If we extend the scope of RDO and RBRDO onto $0 \leq w_1 \leq 1$ and $0 \leq w_2 \leq 1$, then RBDO can be seen as a part of RBRDO. Mathematically, that means $w_1 = 1, w_2 = 0$ in Eq. (2.65). In this occasion, a rough relation between RBDO, RDO and RBDRO is shown in Fig. 2.7.

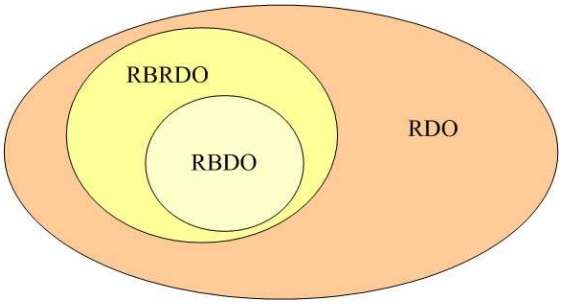

FIGURE 2.7: Relation between RBDO, RDO and RBDRO

In conclusion, RDO refers to the most wide considerations and applications since it contains both deterministic or uncertain objective function and various approaches to

ensure the design feasibility robustness. Based on the category of the objective function and the way to ensure the design feasibility robustness, RBRDO is a branch of RDO and RBDO is a subset of RBRDO. **In the following work, we will see RBDO involved in RBRDO.**

2.4.3.2 Comparative study between RBDO and RBRDO

The difference between RBDO and RBRDO is also illustrated by the mathematical example in Section 2.4.1.5 with the same constraints but different minimized objective $f(\mathbf{d}, \mathbf{\Theta}) = \Theta_1^2 + \Theta_1\Theta_2$, in which $\mathbf{d} = [\mu_{\Theta_1}, \mu_{\Theta_2}]^{\mathrm{T}}$ are the design variables, i.e. mean values of the random design variables $\mathbf{\Theta} = [\Theta_1, \Theta_2]^{\mathrm{T}}$. The RBRDO problem is formulated as

$$\begin{aligned} \text{minimize} \quad & f(\mathbf{d}, \mathbf{\Theta}) = w_1 \frac{\mu_f(\mathbf{d}, \mathbf{\Theta})}{\mu^*} + w_2 \frac{\sigma_f(\mathbf{d}, \mathbf{\Theta})}{\sigma^*}, \\ \text{subject to} \quad & P(g_i(\mathbf{d}, \mathbf{\Theta}) \leq 0) \leq \Phi(-\beta_{i,t}), \\ & 0 \leq d_j \leq 10, \ j = 1, 2. \end{aligned} \tag{2.66}$$

Since this problem is a multi-objective optimization, different set of weight factors can lead to different optimum which might comprise the Pareto optima. Under different selection of weight factor, we chose 11 sets of weight factors, i.e. $w_1 = 1 : -0.1 : 0$ corresponding to $w_2 = 0 : 0.1 : 1$.

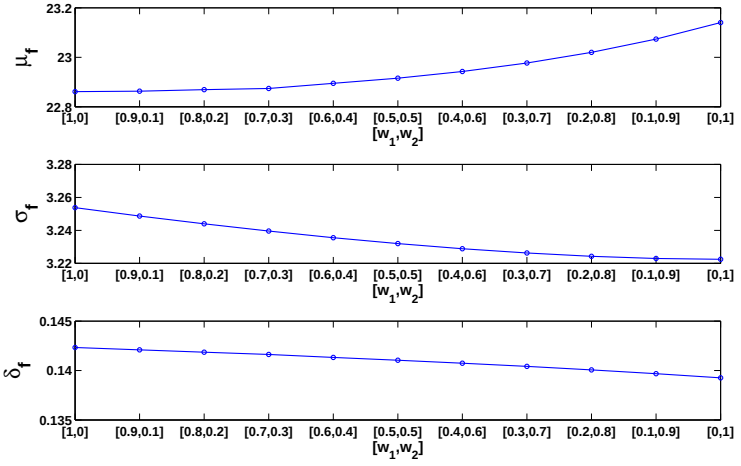

FIGURE 2.8: Mean (μ_f), standard deviation (σ_f) and coefficient of variance (δ_f) of objective function with different set of weight factors

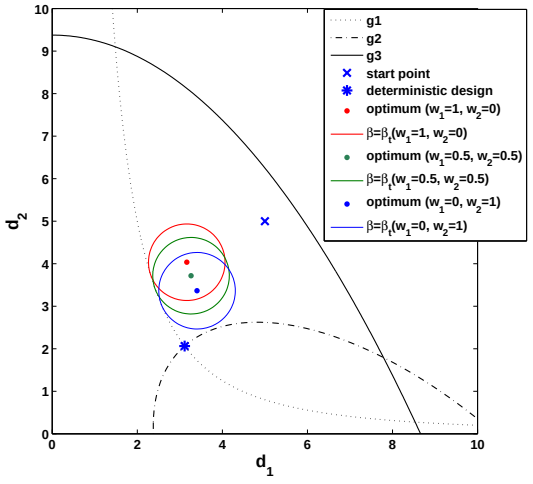

FIGURE 2.9: Comparison between RBDO and RBRDO. d_1 and d_2 are the two design variables, which are also the mean value of Θ_1 and Θ_2, i.e. $d_1 = \mu_{\Theta_1}$ and $d_2 = \mu_{\Theta_2}$.

Fig. 2.8 depicts the mean values (μ_f), standard deviation (σ_f) and coefficient of variance ($\delta_f = \sigma_f/\mu_f$) of the objective function under different sets of weight factors. It is evident that with increase of the weight factor w_1, the mean value of the objective function is monotone decreasing, while with increase of the weight factor w_2, the opposite results are observed. The corresponding standard deviation is decreased with increase of w_2, which signifies that the larger weight of the standard deviation, the less sensitive to the uncertainties the results are. More direct observation for variability reduction can be seen from the change of δ_f.

When $w_1 = 1$ and $w_2 = 0$, RBRDO is equivalent to RBDO. The results indicate that RBDO can provide the minimum mean value, whereas the maximum standard deviation is meanwhile obtained by RBDO. In robust design, designers care about the robustness more. Small standard deviation of objective function can help to achieve this target. In this sense, in RBRDO the objective in the mean sense cannot fulfill such a requirement, which implies RBDO is not adequate to solve the robust optimization problem.

Fig. 2.9 depicts the optimal designs obtained by RBDO ($\mathbf{d}^{\mathrm{RBDO}} = [3.1637, 4.0340]^{\mathrm{T}}$ under $w_1 = 1,\ w_2 = 0$) and RBRDO ($\mathbf{d}^{\mathrm{RBRDO}} = [3.2639, 3.7169]^{\mathrm{T}}$ under $w_1 = 0.5,\ w_2 = 0.5$, and $\mathbf{d}^{\mathrm{RBRDO}} = [3.4053, 3.3637]^{\mathrm{T}}$ under $w_1 = 0,\ w_2 = 1$). Apparently, when the weight w_2 increases, the associated optimum gets closed to the ones at $w_2 = 1$. Moreover, only the constraint g_1 is active for both RBDO and RBRDO.

2.5 Summary

In this chapter, the fundamentals and formulations of SDO are introduced, including the issues of DDO that are closely associated with the design optimization, the methods of UA which give us an almost global perspective of uncertainty quantification needed in SDO, and the formulations as well as methodologies for RBDO, RDO and RBRDO. All the concerns can be found in Figure 2.10.

In engineering, designers care about not only the design objective robustness but also the design feasibility robustness which is satisfied by reliability analysis (an ideal measure). Consequently, in the following work, RBRDO will take place of RDO as the research target and RBDO is included as a special case of RBRDO. Keeping in mind, RBDO is only related to RBRDO when the objective function is deterministic or in the mean sense, while RBRDO is also with respect to the rest situations that the dispersion in the objective cannot be neglectable.

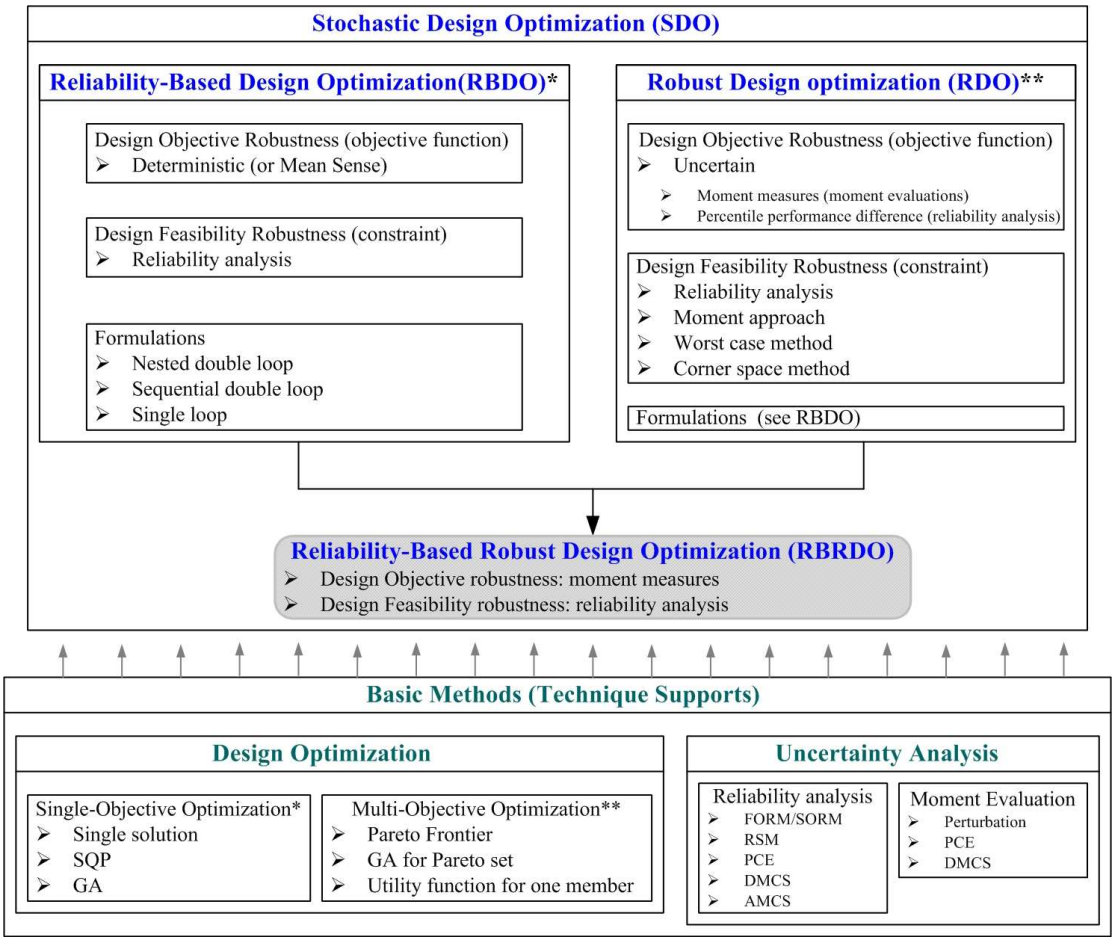

FIGURE 2.10: Concerns of stochastic design optimization (the shadow area is the main research formulation of this work)

Chapter 3

PCE based MCS method for uncertainty analysis

3.1 Introduction

This work aims to obtain the optimal design for random structures by means of RBRDO (RBDO is included). One of the most critical issues in RBRDO is UA, i.e. reliability analysis associated with the design feasibility robustness and moment evaluations related to the design objective robustness.

In the last chapter, the associated methodologies have been reviewed. It is found that the most effective approach usually corresponds to the procedure of FEA in conjunction with MCS within the framework of mechanical engineering. Unfortunately, this procedure is computationally intensive. To get over this, the importance sampling is implemented to improve efficiency of reliability analysis.

However, when the objective function is implicitly uncertain, e.g. usually in the presence of the random response, the associated moment evaluations also need high computational expense and may not be obtained by importance sampling accurately. From this sense, it would be better to develop a method which is capable to estimate not only the moments but also the probabilities of failure. Hence, this chapter is contributed to developing efficient methods for UA.

Note that the time used for UA (assuming that the associated samples are priori known) is much less than the one used for performing a large quantity of FEA (the process to calculate the random response). It is not difficult to imagine that if the relation between uncertainties and the random response is known, a large number of repeated FEA are avoided. From this view, we can expect that direct MCS is computationally manageable. Therefore, we propose a PCE based MCS method to carry out UA for

linear random structures, in which the time consuming repeated FEA is avoided in manner of approximating the random response by PCE.

However, applications of PCE are always restricted for the dynamic response approximation due to the curse of high dimensionality caused by the large dimension of stochastic excitations. To overcome this, we use the convolution form to compute the dynamic response, in which PCE is utilized to approximate the modal properties (natural frequency, modal damping ratio, mode shape or the functions of these values) so that the dimension of uncertainties is reduced since only structural random parameters are considered in the PCE approximation. As a matter of fact, the PCE here is applied to deal with the random eigenvalue problem.

Since the proposed method is based on MCS and modal analysis, there exists a problem named modal intermixing [139] or modal interaction [53, 140] always encountered when using Monte Carlo sampling to solve the random eigenvalue problem. To correctly capture the uncertainties in the modal content by analyzing the modal scatter observed in MCS, it is indispensable to avoid modal intermixing [139]. Therefore, this problem is also regarded.

It is found that the modal intermixing is caused by large dispersion of the random parameters. Immediate attempts to avoid this problem are to model uncertainties with small variances. Although the variances are difficult to control, based on some engineering criteria (such as the geometry tolerances), the variance is somehow controllable and is usually not large. Moreover, the similar issue has been pointed out in the work [141], which denoted that large variances (e.g. COV= 30%) of random parameters may lead to negative quantities and thereafter physically meaningless results. From above, application of relatively small variance (or COV) is practically reasonable.

Accordingly, to correctly obtain the uncertainties in the modal content, first the Modal Assurance Criterion (**MAC**) factor is implemented to quantify the intermixing. Then a unvariable method is raised to check which variable results in such a problem, according to which relatively smaller variance will be selected to remove or reduce the intermixing issue as far as possible.

3.2 PCE of second-order random variables

3.2.1 Basic theory and validity

The original PCE, also termed as HPCE, was developed by Wiener [62]. With this expansion, any second-order random variable or stochastic process, i.e. the quantities with finite variance, may be expanded as follows:

$$\begin{aligned} u = & \hat{u}_0 H_0 \\ & + \sum_{i_1=1}^{\infty} \hat{u}_{i_1} H_1(\xi_{i_1}) \\ & + \sum_{i_1=1}^{\infty} \sum_{i_2=1}^{i_1} \hat{u}_{i_1 i_2} H_2(\xi_{i_1}, \xi_{i_2}) \\ & + \sum_{i_1=1}^{\infty} \sum_{i_2=1}^{i_1} \sum_{i_3=1}^{i_2} \hat{u}_{i_1 i_2 i_3} H_3(\xi_{i_1}, \xi_{i_2}, \xi_{i_3}) + \cdots , \end{aligned} \tag{3.1}$$

where $H_p(\xi_{i_1}, \ldots, \xi_{i_p})$ denotes the multivariate Hermite polynomial chaos of order p in terms of standard normal vector $\boldsymbol{\xi} = [\xi_{i_1}, \ldots, \xi_{i_p}]^{\mathrm{T}}$ and $\hat{u}_{i_1 \ldots i_p}$ is the associated coefficient. For notational convenience, Eq. (3.1) can be rewritten as

$$u = \sum_{i=0}^{\infty} u_i \Psi_i(\boldsymbol{\xi}). \tag{3.2}$$

In this expression, there is a one-to-one correspondence between the polynomial basis functions $\Psi_i(\boldsymbol{\xi})$ and $H_p(\xi_{i_1}, \ldots, \xi_{i_p})$, and also the deterministic coefficients u_i and $\hat{u}_{i_1 \ldots i_p}$. The union of the former polynomials $\{\Psi_i\}$ forms a complete orthogonal basis, i.e.,

$$\Psi_0 \equiv 1, \qquad \langle \Psi_i = 0 \rangle , \qquad i > 0, \qquad \langle \Psi_i \Psi_j \rangle = \delta_{ij} \left\langle \Psi_i^2 \right\rangle , \tag{3.3}$$

where δ_{ij} is the Kronecker delta and $\langle \cdot, \cdot \rangle$ denotes the ensemble average. This is the inner product in the Hilbert space of Gaussian random variables defined by

$$\langle f(\boldsymbol{\xi}) g(\boldsymbol{\xi}) \rangle = \int f(\boldsymbol{\xi}) g(\boldsymbol{\xi}) q(\boldsymbol{\xi}) d\boldsymbol{\xi}, \tag{3.4}$$

where $q(\boldsymbol{\xi})$ is the multidimensional Gaussian joint PDF. Based on the theorem of Cameron-Martin [142], the expression in Eq. (3.2) converges in the L_2 sense. From

this point of view, most physical processes can be represented by HPCE since they are supposed to have finite variance.

According to Soize et al. [64], the chaos representation of the random response S may be written as

$$S = \sum_{i=0}^{\infty} \hat{S}_i \Gamma_i(\boldsymbol{\Theta}), \qquad \boldsymbol{\Theta} \in \mathbb{R}^N, \tag{3.5}$$

where $\{\Gamma_i\}$ is a Hilbertian basis of the suitable Hilbert space containing the response. Here the response S can be seen as a function of random inputs, i.e. N-dimensional uncertainties $\boldsymbol{\Theta}$. When the random inputs are standard normal, a possible Hilbertian basis is the multivariate Hermite polynomial chaos basis.

Pay attention that the HPCE is in the presence of standard normal variables $\boldsymbol{\xi}$; on the contrary, the response S is the function of $\boldsymbol{\Theta}$. Generally, $\boldsymbol{\Theta}$ and $\boldsymbol{\xi}$ are usually not the same. Nonetheless, implementation of transformation techniques mentioned in Section 2.3.2 can make HPCE available. Then Eq. (3.5) is rewritten in the form of HPCE

$$S = \sum_{i=0}^{\infty} S_i \Psi_i(\boldsymbol{\xi}), \qquad \boldsymbol{\xi} \in \mathbb{R}^N. \tag{3.6}$$

However, the convergence rate may be substantially slow when representing the random response by Eq. (3.6) rather than Eq. (3.5). In this case, extensions to other orthogonal polynomials in terms of non-Gaussian random variables, named Wiener-Askey or general PCE, could be used according to the work of Xiu and Karniadakis [85]. **In this study, we focus on the application of HPCE due to its wide applications**. If there is no other notification, PCE means HPCE.

Practically, the infinite summation will be truncated for computational purposes. Consideration of N-dimensional PCE up to order p, the approximate response is obtained as follows:

$$S \approx \sum_{i=0}^{P-1} S_i \Psi_i(\boldsymbol{\xi}), \qquad \boldsymbol{\xi} \in \mathbb{R}^N, \tag{3.7}$$

in which the total number of the PCE terms is P, and it is determined by

$$P = \begin{pmatrix} N+p \\ p \end{pmatrix} = \frac{(N+p)!}{N!p!}. \tag{3.8}$$

3.2.2 Coefficients determination

When applying PCE, one critical issue is to estimate the coefficients. A variety of methods have been developed. According to [77], two categories of methods are distinguished to determine the coefficients: the intrusive and non-intrusive methods.

Intrusive methods provide a weak solution in manner of Galerkin projection [63] of the equilibrium equation on the Hermite polynomial basis by minimizing the residual. However, it requires additional modification of the deterministic numerical code, i.e. finite element code. Considering the high-dimensional systems, this method could computationally expensive. Alternatively, non-intrusive methods termed by the projection and regression method were developed.

Projection method makes use of the orthogonality of the polynomial chaos basis. Taking the inner product in Eq. (3.4) with Ψ_j, we have

$$\langle S\Psi_j \rangle = \langle \sum_{i=0}^{P-1} S_i \Psi_i \Psi_j \rangle. \tag{3.9}$$

Based on the orthogonality of the basis, $\langle \Psi_i \Psi_j \rangle = 0,\ i \neq j$. Thus,

$$S_i = \frac{\langle S\Psi_i \rangle}{\langle \Psi_i^2 \rangle}. \tag{3.10}$$

The denominator in the above expression is known analytically and listed in [63]. In contrast, the numerator is only available in numerical way. Although direct MCS can deal with such a problem, large quantities of realizations of S are needed to achieve a reasonable accuracy at the cost of efficiency. Recall that the numerator follows the principle of the inner product defined in Eq. (3.4). This integral may be obtained by the full tensorization of one-dimensional Gaussian quadrature [143], Smolyak's cubature [77], the main shortage of which is that they will suffer low efficiency as the number of random inputs N and the order p increase. To reduce the total number of the terms $\{\Psi_i\}$, an adaptive-sparse scheme [80] to minimize the number of bivariate terms was developed. Yet, it may miss the information in the tails.

Regression method is in the sense of the least square measure. The estimator $\hat{\mathscr{S}} = [\hat{S}_1, \ldots, \hat{S}_P]^{\mathrm{T}}$ of $\mathscr{S} = [S_1, \ldots, S_P]^{\mathrm{T}}$ is estimated by solving the least square problem,

$$\hat{\mathscr{S}} = \arg\min \sum_{k=1}^{M} (S^{(k)} - \sum_{i=0}^{P-1} S_i \Psi_i(\boldsymbol{\xi}^{(k)}))^2, \tag{3.11}$$

where k represents the kth set of experimental points and M is the corresponding total number. Let us denote $\mathbf{S} = [S^{(1)}, \ldots, S^{(M)}]^{\mathrm{T}}$ the random output vector. The famous solution of the last equation is

$$\hat{\mathscr{S}} = (\boldsymbol{\Psi}^{\mathrm{T}}\boldsymbol{\Psi})^{-1}\boldsymbol{\Psi}^{T}\mathbf{S}, \tag{3.12}$$

where

$$\boldsymbol{\Psi} = \begin{bmatrix} \Psi_0(\boldsymbol{\xi}^{(1)}) & \Psi_1(\boldsymbol{\xi}^{(1)}) & \cdots & \Psi_P(\boldsymbol{\xi}^{(1)}) \\ \Psi_0(\boldsymbol{\xi}^{(2)}) & \Psi_1(\boldsymbol{\xi}^{(2)}) & \cdots & \Psi_P(\boldsymbol{\xi}^{(2)}) \\ \vdots & \vdots & \ddots & \vdots \\ \Psi_0(\boldsymbol{\xi}^{(M)}) & \Psi_1(\boldsymbol{\xi}^{(M)}) & \cdots & \Psi_P(\boldsymbol{\xi}^{(M)}) \end{bmatrix}. \tag{3.13}$$

The very important consideration of the least square method (**LSM**) is the choice of the experimental points $\boldsymbol{\xi}^{(k)}$. Collocation based method [51] allows to select the points corresponding to the roots of the Hermite polynomial of one degree higher than the maximum order of the current PCE. The total number of the collocation points is equal to $n_c = (p+1)^N$, which also has the curse of dimensionality as the approaches of Gaussian quadrature and Smolyak's cubature are challenged. This leads to the idea of selecting a subset N_c points out of n_c-dimensional ensemble. Its principle is to choose the points closest to the origin. However, different combination of collocation points may result in different coefficients. This imposes the instability of the collocation method. Furthermore, investigations by Berveiller [144] showed that selection like $N_c = 2P$ [51] does not yield accurate estimations in most applications. They proposed an empirical rule on the optimal number of regression points: $n_e = (N-1)P$.

In conclusion, the aforementioned approaches are dedicated to improving efficiency compared with direct MCS. Nonetheless, the improvement is still limited to the problems with high dimensionality. **In this context, we use the regression method**. The difference from the one stated above is that the experimental points are chosen arbitrarily but the collocation points so that the instability is inherently avoided. Moreover,

we utilize $N_{\mathrm{LSF}} = 3P$ experimental points according to the simulations, which is more competitive than the empirical rule when $N \geq 4$.

3.3 PCE based MCS method for UA

3.3.1 Random response approximated by PCE for linear systems

For static problems in which the number of random variables is relatively small, the random response such as the displacement, strain and stress can be approximated with Eq. (3.7) directly. However, in cases where the dimension of random variables $\boldsymbol{\Theta}$, $\boldsymbol{\Theta} \in \mathbb{R}^N$ is high, e.g. $N \geq 100$, the application of PCE is usually cumbersome since a large quantity of structural analyses are required to evaluate the coefficients. This is always the situation in dynamic problems because the excitations $\mathbf{Z}(\mathbf{t})$ (note that $\boldsymbol{\Theta} = \{\boldsymbol{\theta}, \mathbf{Z}(t)\}$) are always modeled in the discrete formula which leads to very high dimensionality (see section 3.3.3.2).

To circumvent the high dimensionality curse, the dynamic response is calculated by the convolution [145, 146] of the impulse response and excitations for linear structures rather than the direct calculation. Consider a deterministic multi-degree structure, the motion equation of which is given by

$$\mathbf{M}\ddot{\mathbf{x}}(t) + \mathbf{C}\dot{\mathbf{x}}(t) + \mathbf{K}\mathbf{x}(t) = \mathbf{G}\mathbf{f}(t), \tag{3.14}$$

where $\mathbf{x}(t)$ is the n-dimensional displacement response vector, $\mathbf{M}$, $\mathbf{C}$ and $\mathbf{K}$ denote the mass, damping and stiffness matrices of dimension $n \times n$ respectively, $\mathbf{f}(t)$ is the N_l-dimensional excitation vector, and $\mathbf{G}$ is a position matrix of dimension $n \times N_l$. Without loss of generality, the solution with zero initial conditions at $t = 0$ is given in the form of convolution, as

$$x_r(t) = \sum_{k=1}^{N_l} \int_0^t h_{rk}(t-\tau) f_k(\tau) d\tau, \tag{3.15}$$

in which $x_r(t)$ represents the displacement at the rth DOF (degree of freedom), $h_{rk}(t)$ is the impulse response at the rth DOF under the excitation at the kth DOF, and $f_k(t)$ is the corresponding excitation.

Thinking of a random structure by entering random structural parameters $\boldsymbol{\theta}$ and replacing the deterministic excitations $\mathbf{f}(t)$ by $\mathbf{Z}(t)$, we have the associated random response

$$x_r(t, \boldsymbol{\theta}, \mathbf{Z}(t)) = \sum_{k=1}^{N_l} \int_0^t h_{rk}(t-\tau, \boldsymbol{\theta}) Z_k(\tau) d\tau. \tag{3.16}$$

For practical applications, the response is always applied in the discrete form due to the discretized modeling of $Z_k(t)$. As long as the time step Δt is sufficiently small, the discrete response will tend to its continuous one. At arbitrary time instant t_s within the time interval $[0, T]$, the response is described as

$$\begin{aligned} x_r(t_s, \boldsymbol{\theta}, \mathbf{Z}(t)) &= \sum_{k=1}^{N_l} \int_0^{t_s} h_{rk}(t_s - t, \boldsymbol{\theta}) Z_k(t) dt \\ &= \lim_{\Delta t \to 0} \sum_{k=1}^{N_l} \sum_{m=1}^{s} h_{rk}(t_s - t_m, \boldsymbol{\theta}) Z_k(t_m) \Delta t \\ &\approx \Delta t \sum_{k=1}^{N_l} \sum_{m=1}^{s} h_{rk}(t_s - t_m, \boldsymbol{\theta}) Z_k(t_m), \quad 0 \le m \le s \le n_T. \end{aligned} \tag{3.17}$$

Apparently, this expression offers a way to consider the uncertainties in the structure and in excitations separately because all the information of a structure is uniquely characterized by the impulse response. It is found that the number of structural random parameters is much less than the one of excitations. With this advantage, it is natural to apply PCE to approximate the impulse response, which is the function of modal properties (natural frequency, modal damping ratio, mode shape or the functions of these values). Then one can use PCE to approximate the modal properties so that the original problem is reduced to the random eigenvalue problem.

Based on different types of the damping, there is no uniform expression of impulse response $h_{rk}(t, \boldsymbol{\theta})$. In this work, we concentrate on linear structures with viscous damping: classically proportional damping and generally viscous damping.

3.3.1.1 Impulse response for structures with proportional damping

For simpleness, we begin with the deterministic problem. In this work the modal superposition principle will be used to evaluate the dynamic response. That implies the

dynamic response in Eq. (3.14) can be represented by

$$\mathbf{x}(t) = \sum_{j=1}^{n} \boldsymbol{\phi}_j \eta_j(t), \tag{3.18}$$

where $\eta_j(t),\ j = 1, \ldots, n$ are the modal responses, and $\boldsymbol{\phi}_j$ denotes the jth mode eigenvector or mode shape, which is obtained by solving the following eigenvalue problem,

$$\mathbf{K}\boldsymbol{\phi} = \lambda \mathbf{M}\boldsymbol{\phi}, \tag{3.19}$$

where λ is the eigenvector. With the orthogonal properties

$$\begin{aligned} \boldsymbol{\phi}_j^{\mathrm{T}} \mathbf{M} \boldsymbol{\phi}_k &= 0, \qquad j \neq k, \\ \boldsymbol{\phi}_j^{\mathrm{T}} \mathbf{M} \boldsymbol{\phi}_k &= 1, \qquad j = k, \\ \boldsymbol{\phi}_j^{\mathrm{T}} \mathbf{K} \boldsymbol{\phi}_k &= 0, \qquad j \neq k, \\ \boldsymbol{\phi}_j^{\mathrm{T}} \mathbf{K} \boldsymbol{\phi}_k &= \omega_j^2, \qquad j = k, \end{aligned} \tag{3.20}$$

in which ω_j represents the jth eigenfrequency of natural frequency following a relation with the associated eigenvalue $\lambda_j = \omega_j^2$, we have the expression in the modal space

$$\ddot{\eta}_j(t) + 2\zeta_j \omega_j \dot{\eta}_j(t) + \omega_j^2 \eta_j(t) = \boldsymbol{\phi}_j^{\mathrm{T}} \mathbf{G}\mathbf{Z}(t), \tag{3.21}$$

where ζ_j denotes the jth modal damping ratio. Then the modal response under a unit impulse applied at the kth DOF at time $t = 0$ is in the form of

$$\eta_j(t) = \frac{\boldsymbol{\phi}_j^{\mathrm{T}} \mathbf{g}_k}{\omega_{dj}} e^{(-\zeta_j \omega_j t)} sin(\omega_{dj} t), \tag{3.22}$$

in which $\mathbf{g}_k$ is the kth column of $\mathbf{G}$, and $\omega_{dj} = \omega_j \sqrt{1 - \zeta_j^2}$ is the jth damped frequency. Then the impulse response can be written as

$$h_{rk}(t) = \sum_{j=1}^{n} \frac{\phi_{rj} \boldsymbol{\phi}_j^{\mathrm{T}} \mathbf{g}_k}{\omega_{dj}} e^{-\zeta_j \omega_j t} sin(\omega_{dj} t), \tag{3.23}$$

where ϕ_{rj} is the rth component of the jth mode shape. The truncated representation [145, 147] is usually used which recalls that only the first few modes contribute most to

the impulse response and the remaining will be ignored, i.e.

$$h_{rk}(t) = \sum_{j=1}^{m \ll n} \frac{\phi_{rj} \boldsymbol{\phi}_j^{\mathrm{T}} \mathbf{g}_k}{\omega_{dj}} e^{-\zeta_j \omega_j t} sin(\omega_{dj} t). \tag{3.24}$$

Considering the random structural parameters $\boldsymbol{\theta}, \boldsymbol{\theta} \in \mathbb{R}^{N_s}$, the associated random impulse response is expressed as

$$h_{rk}(t, \boldsymbol{\theta}) = \sum_{j=1}^{m \ll n} \frac{\phi_{rj}(\boldsymbol{\theta}) \boldsymbol{\phi}_j^{\mathrm{T}}(\boldsymbol{\theta}) \mathbf{g}_k}{\omega_{dj}(\boldsymbol{\theta})} e^{-\zeta_j(\boldsymbol{\theta}) \omega_j(\boldsymbol{\theta}) t} sin(\omega_{dj}(\boldsymbol{\theta}) t). \tag{3.25}$$

All the random modal properties are the solutions of the random eigenvalue problem, described as follows,

$$\mathbf{K}(\boldsymbol{\theta}) \boldsymbol{\phi}(\boldsymbol{\theta}) = \lambda(\boldsymbol{\theta}) \mathbf{M}(\boldsymbol{\theta}) \boldsymbol{\phi}(\boldsymbol{\theta}). \tag{3.26}$$

Physically speaking, the modal properties are supposed to have finite variance. Therefore, it is reasonable to express them by PCE. Similar work can be found in [53, 148]. By means of transformation techniques, the jth set of random eigenvalue and eigenvector can be written in terms of standard normal random variables

$$\lambda_j = \sum_{i=0}^{P-1} a_i \Psi_i(\boldsymbol{\xi}), \qquad \boldsymbol{\phi}_j = \sum_{i=0}^{P-1} \mathbf{b}_i \Psi_i(\boldsymbol{\xi}), \tag{3.27}$$

where a_i and $\mathbf{b}_i$, $\mathbf{b}_i \in \mathbb{R}^n$ are the constant scalar and vector coefficients respectively. Seen from Eq. (3.25), the impulse response is actually the function of random eigenfrequency $\omega_j(\boldsymbol{\theta})$, and the eigenfactor defined as $\phi_{rj}(\boldsymbol{\theta}) \boldsymbol{\phi}_j^{\mathrm{T}}(\boldsymbol{\theta}) \mathbf{g}_k$ similar to the mode factor used in [147]. The work [149] indicated that multiplication or division of two random variables expanded by polynomial chaos can also be expanded by the same order polynomial chaos such that the CPU time is saved. Consequently, we have

$$\omega_j = \sum_{i=0}^{P-1} a_i \Psi_i(\boldsymbol{\xi}), \qquad \phi_{rj} \boldsymbol{\phi}_j^{\mathrm{T}} \mathbf{g}_k = \sum_{i=0}^{P-1} c_i \Psi_i(\boldsymbol{\xi}), \qquad \boldsymbol{\xi} \in \mathbb{R}^{N_s}, \tag{3.28}$$

where c_i is ith constant coefficient with respect to ith eigenfactor.

3.3.1.2 Impulse response for structures with viscous damping

In this case, the deterministic problem is also taken into account first for simpleness. As is well known, the eigenvalue problem is always related to the complex one, i.e.

$$(\bar{\lambda}^2\mathbf{M} + \bar{\lambda}\mathbf{C} + \mathbf{K})\bar{\boldsymbol{\phi}} = 0, \tag{3.29}$$

where $\bar{\lambda}$ and $\bar{\boldsymbol{\phi}}$ are the complex eigenvalue and eigenvector, respectively. Similarly, the dynamic response in linear combination of modal shapes is formed as

$$\mathbf{x}(t) = \sum_{j=1}^{2n} \bar{\boldsymbol{\phi}}_j \vartheta_j(t), \tag{3.30}$$

in which ϑ_j is the modal response that is always evaluated in the state-space. Namely, the originally deterministic problem described in Eq. (3.14) will be solved in the state-space, i.e.

$$\mathbf{A}\dot{\mathbf{y}}(t) + \mathbf{B}\mathbf{y}(t) = \mathbf{Q}(t), \tag{3.31}$$

where

$$\begin{aligned}
\mathbf{A} &= \begin{bmatrix} \mathbf{0} & \mathbf{M} \\ \mathbf{M} & \mathbf{C} \end{bmatrix}_{2n\times 2n}, & \mathbf{B} &= \begin{bmatrix} -\mathbf{M} & \mathbf{0} \\ \mathbf{0} & \mathbf{K} \end{bmatrix}_{2n\times 2n}, \\
\mathbf{y}(t) &= \begin{Bmatrix} \dot{\mathbf{x}}(t) \\ \mathbf{x}(t) \end{Bmatrix}_{2n\times 1}, & \mathbf{Q}(t) &= \begin{Bmatrix} \mathbf{0} \\ \mathbf{G}\mathbf{f}(t) \end{Bmatrix}_{2n\times 1}.
\end{aligned} \tag{3.32}$$

The associated eigenvalue problem in the state space is formulated as

$$\mathbf{B}\boldsymbol{\varphi} = -\bar{\lambda}\mathbf{A}\boldsymbol{\varphi}, \tag{3.33}$$

where $\bar{\lambda}$ is the eigenvalue that is equal to the one of original complex eigenvalue problem and $\boldsymbol{\varphi}$ is the corresponding eigenvector that has the relation

$$\boldsymbol{\varphi} = \begin{Bmatrix} \bar{\lambda}\bar{\boldsymbol{\phi}} \\ \bar{\boldsymbol{\phi}} \end{Bmatrix}_{2n\times 1}. \tag{3.34}$$

The eigenvalues and eigenvectors have the similar orthogonal properties written as

$$\begin{aligned}
&\boldsymbol{\varphi}_i^{\mathrm{T}}\mathbf{A}\boldsymbol{\varphi}_j = 0, \quad i \neq j,\\
&\boldsymbol{\varphi}_i^{\mathrm{T}}\mathbf{A}\boldsymbol{\varphi}_j = \bar{a}_i, \quad i = j,\\
&\boldsymbol{\varphi}_i^{\mathrm{T}}\mathbf{B}\boldsymbol{\varphi}_j = 0, \quad i \neq j,\\
&\boldsymbol{\varphi}_i^{\mathrm{T}}\mathbf{B}\boldsymbol{\varphi}_j = \bar{b}_i, \quad i = j,\\
&\frac{\bar{b}_i}{\bar{a}_i} = -\bar{\lambda}_i.
\end{aligned} \tag{3.35}$$

In the state-space, the jth uncoupled equation is formulated as

$$\dot{\vartheta}_j(t) - \bar{\lambda}_j\vartheta_j(t) = \frac{1}{\bar{a}_j}\bar{\boldsymbol{\phi}}_j^{\mathrm{T}}\mathbf{G}\mathbf{f}(t). \tag{3.36}$$

Its solution with respect to a unit impulse at kth DOF is

$$\vartheta(t) = \frac{\bar{\boldsymbol{\phi}}_j^{\mathrm{T}}\mathbf{g}_k}{\bar{a}_j}e^{(\bar{\lambda}_j t)}. \tag{3.37}$$

Analogically, the truncated representation of impulse response is in the form of

$$h_{rk}(t) = \sum_{j=1}^{2m\ll 2n}\frac{\bar{\phi}_{rj}\bar{\boldsymbol{\phi}}_j^{\mathrm{T}}\mathbf{g}_k}{\bar{a}_j}e^{\bar{\lambda}_j t}, \tag{3.38}$$

where the $\bar{\phi}_{rj}$ is the rth component of the j complex eigenvector. Other expression can be found in [145] by means of state-space method as well.

By entering the uncertainties, the random impulse response is written as

$$h_{rk}(t) = \sum_{j=1}^{2m\ll 2n}\frac{\bar{\phi}_{rj}(\boldsymbol{\theta})\bar{\boldsymbol{\phi}}_j^{\mathrm{T}}(\boldsymbol{\theta})\mathbf{g}_k}{\bar{a}_j(\boldsymbol{\theta})}e^{\bar{\lambda}_j(\boldsymbol{\theta})t}, \tag{3.39}$$

in which all the random modal properties can be estimated by the associated complex random eigenvalue problem

$$(\bar{\lambda}^2(\boldsymbol{\theta})\mathbf{M}(\boldsymbol{\theta}) + \bar{\lambda}(\boldsymbol{\theta})\mathbf{C}(\boldsymbol{\theta}) + \mathbf{K}(\boldsymbol{\theta}))\bar{\boldsymbol{\phi}}(\boldsymbol{\theta}) = 0, \tag{3.40}$$

In a similar way, PCE is not used to represent the eigenvalue and eigenvector directly, but to represent the real part and imaginary part for modal properties with to be defined

coefficients $d_{re,i}$, $d_{im,i}$ and $e_{re,i}$, $e_{im,i}$, say

$$\begin{aligned} \mathrm{Re}(\bar{\lambda}_j) &= \sum_{i=0}^{P-1} d_{re,i}\Psi_i(\boldsymbol{\xi}), & \mathrm{Im}(\bar{\lambda}_j) &= \sum_{i=0}^{P-1} d_{im,i}\Psi_i(\boldsymbol{\xi}), \\ \mathrm{Re}(\frac{\bar{\phi}_{rj}\boldsymbol{\phi}_j^{\mathrm{T}}\mathbf{g}_k}{\bar{a}_j}) &= \sum_{i=0}^{P-1} e_{re,i}\Psi_i(\boldsymbol{\xi}), & \mathrm{Im}(\frac{\bar{\phi}_{rj}\boldsymbol{\phi}_j^{\mathrm{T}}\mathbf{g}_k}{\bar{a}_j}) &= \sum_{i=0}^{P-1} e_{im,i}\Psi_i(\boldsymbol{\xi}). \end{aligned} \tag{3.41}$$

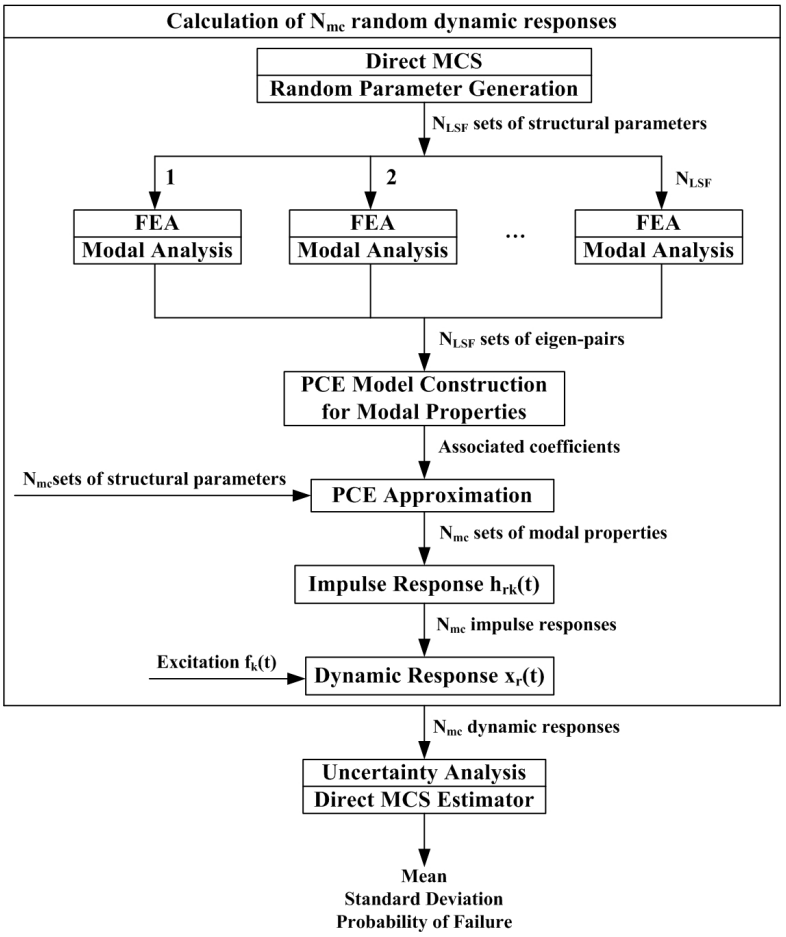

FIGURE 3.1: PCE based MCS for uncertainty analysis

3.3.2 Application procedures

In this section, the approximation of the random dynamic response produced by PCE has been specified, which is summarized as follows:

1. Generating N_{LSF} sets of structural parameters by MCS sampling.

2. Executing the associated N_{LSF} modal analyses to provide N_{LSF} eigen-pairs.

3. Constructing the PCE models for needed modal properties with the N_{LSF} eigen-pairs obtained in step 2.

4. Entering N_{mc} sets of structural parameters into the PCE models to attain the modal properties.

5. Calculating N_{mc} impulse responses and thereafter N_{mc} random dynamic responses.

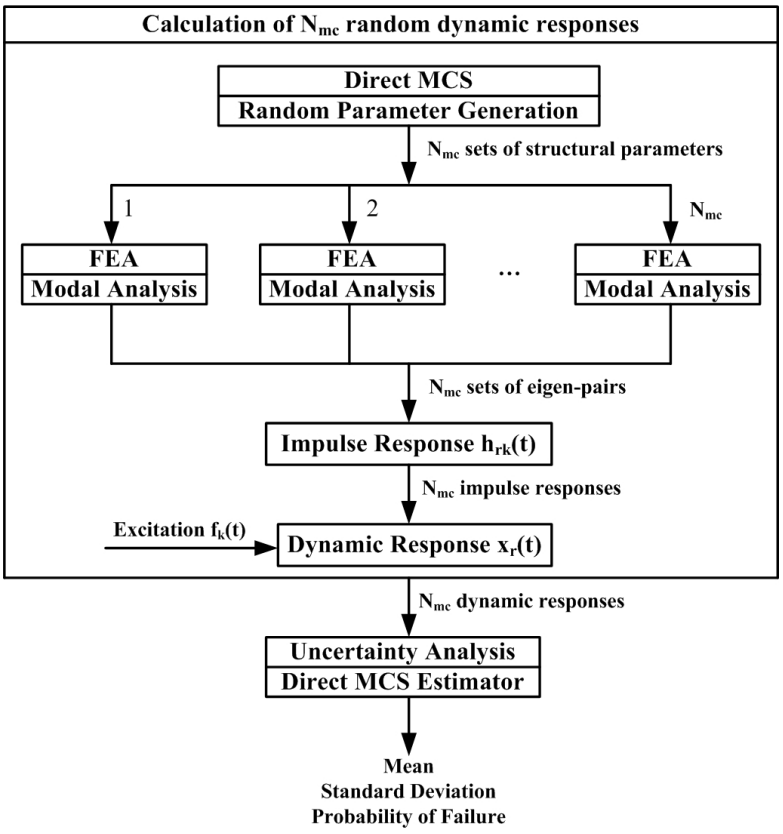

FIGURE 3.2: Direct MCS for uncertainty analysis

Once the samples of the random response have been prepared, the UA can be carried out by direct MCS readily (see Eq. (2.34), Eq. (2.37) and Eq. (2.38) respectively). A flowchart describing the procedure is given in Fig. 3.1.

As calibration, direct MCS is applied in this work, which is illustrated in Fig. 3.2. From these two figures, it is seen that the time consuming N_{mc} modal analyses are replaced by N_{LSF} ones. This always leads to large reduction of CPU time due to $N_{LSF} \ll N_{mc}$, especially for large-scale structures. The rest parts of uncertainty analysis almost consume the same time since the same methods are applied to calculate the dynamic response and the statistical quantities. It will be found in Section 3.5 that

the time associated with the rest parts is much less than the one used for N_{mc} modal analyses.

3.3.3 Fundamentals of reliability analysis

To correctly carry out reliability analysis, the failure mechanism and the associated failure region much be defined first. Remind that the failure mechanism concerned in this work is the over-stress or the first passage failure problem. Corresponding to static problems and dynamic problems, the associated failure regions are defined differently due to the effect of time.

3.3.3.1 Failure region for static problems

The probability of failure in static systems is to determine the probability that any one of q time-invariant outputs $x_i(\boldsymbol{\theta}, \mathbf{Z}),\ i = 1, \ldots, q$ exceeds in magnitude a prescribed threshold $X_i > 0,\ i = 1, \ldots, q$. Hence, the probability of failure is described as

$$P_{F,i} = P(F_i) = P(g_i(\boldsymbol{\theta}, \mathbf{Z}) = X_i - |x_i(\boldsymbol{\theta}, \mathbf{Z})| \leq 0), \tag{3.42}$$

where the failure region related to $x_i(\boldsymbol{\theta}, \mathbf{Z})$ is given by

$$F_i = g_i(\boldsymbol{\theta}, \mathbf{Z}) = X_i - |x_i(\boldsymbol{\theta}, \mathbf{Z})| \leq 0. \tag{3.43}$$

Note that the random inputs $\mathbf{Z}$ is time-invariant which are usually modeled as random variables following some special distribution.

3.3.3.2 Failure region for dynamic problems

In this case, since random outputs vary with time, the first passage problem is always concerned. One needs to determine the probability that any one of q outputs $x_i(\boldsymbol{\theta}, \mathbf{Z}(t)),\ i = 1, \ldots, q$ exceeds in magnitude, ***for the first time***, a prescribed threshold $X_i(t) > 0,\ i = 1, \ldots, q$ within a given time interval $[0, T]$, where $X_i(t)$ could be constant or time-variant. Then the first passage probability is given by

$$P_{F,i} = P(F_i) = P(\exists t \in [0, T] : g_i(\boldsymbol{\theta}, \mathbf{Z}(t)) = X_i(t) - |x_i(\boldsymbol{\theta}, \mathbf{Z}(t))| \leq 0), \tag{3.44}$$

where the associated failure region is given by

$$F_i = \exists t \in [0, T] : g_i(\boldsymbol{\theta}, \mathbf{Z}(t)) = X_i(t) - |x_i(\boldsymbol{\theta}, \mathbf{Z}(t))| \leq 0. \tag{3.45}$$

In practical applications, the random inputs $\mathbf{Z}(t)$ are always modeled by stochastic processes in the discrete formula [86]. Let the sampling be uniform with time spacing $\Delta t = T/(n_T - 1)$, where n_T is the number of time instants so that the sampling time instants are $t_s = (s-1)\Delta t,\ s = 1, \ldots, n_T$. The discrete random input vector is given by $\mathbf{Z}(t) = [Z_1(1), \ldots, Z_{N_l}(1), \ldots, Z_1(n_T), \ldots, Z_{N_l}(n_T)]^{\mathrm{T}}$, $\mathbf{Z}(t) \in \mathbb{R}^{n_T \times N_l}$, the interpretation of which is that there are N_l discrete stochastic excitations. To obtain an accurate result, the time step Δt is relatively small, e.g. $T = 15$s, $\Delta t = 0.01$s and $n_T = 1501$. As a result, the dimension of uncertainties are very high, say $N = N_s + 1501 N_l$.

When the threshold $X_i(t)$ is constant, one can get the simplified failure region, say

$$F_i = \exists t \in [0, T] : g_i(\boldsymbol{\theta}, \mathbf{Z}(t)) = X_i - \max(|x_i(\boldsymbol{\theta}, \mathbf{Z}(t))|) \leq 0. \tag{3.46}$$

3.4 Modal intermixing problem

3.4.1 Problem description

Since the proposed method is based on MCS and modal analysis, there exists a problem named modal intermixing [139] or modal interaction [53, 140] always encountered when using Monte Carlo sampling to solve the random eigenvalue problem. That means, from one simulation to next, the modes may alter whereby the random mode shapes associated with the same order, actually, contain more than one mode. Generally, different modes behave physically different. Such a problem is exacerbated for those structures with closed space eigenfrequencies [53].

In engineering, when concerning random structures, the mean model is usually treated as the reference. The modal behaviors should be consistent with the reference which is very significant for engineers to grasp the inherent properties of random structures. To correctly capture the uncertainties in the modal content by analyzing the modal scatter observed in MCS, it is indispensable to avoid modal intermixing [139]. For this purpose, it is significant to figure out what arouses such a problem.

Fig. 3.3, taking the eigenfrequency as the example, describes the PDFs associated with the two adjacent eigenfrequencies, i.e. mode n and mode $n+1$, in which Fig. 3.3a is with respect to the situation without modal intermixing and Fig. 3.3b depicts the situation with modal intermixing. Comparing with these two situations, we can see that the variances of both eigenfrequencies with modal intermixing are obviously greater than the ones without modal intermixing. Moreover, the overlapping area under modal intermixing is much larger than that when there is no modal intermixing.

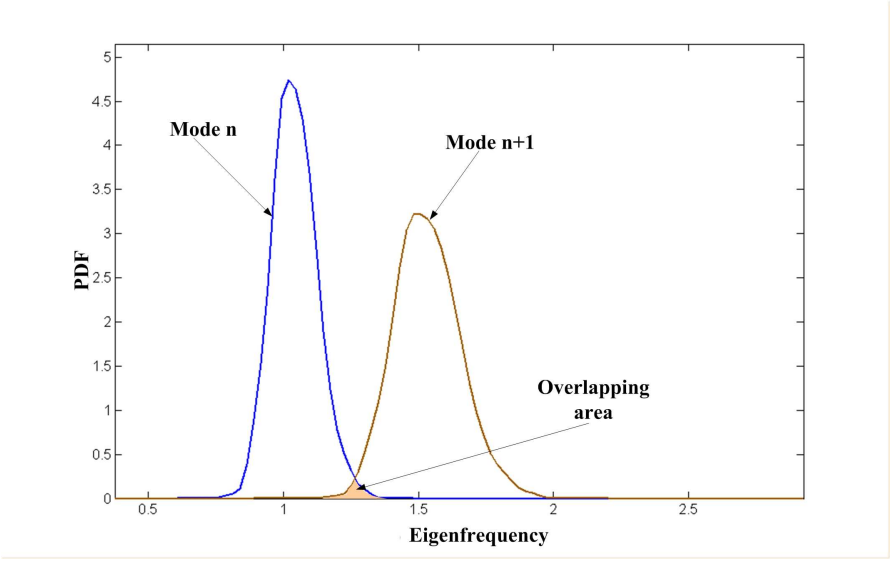

(A) No modal intermixing

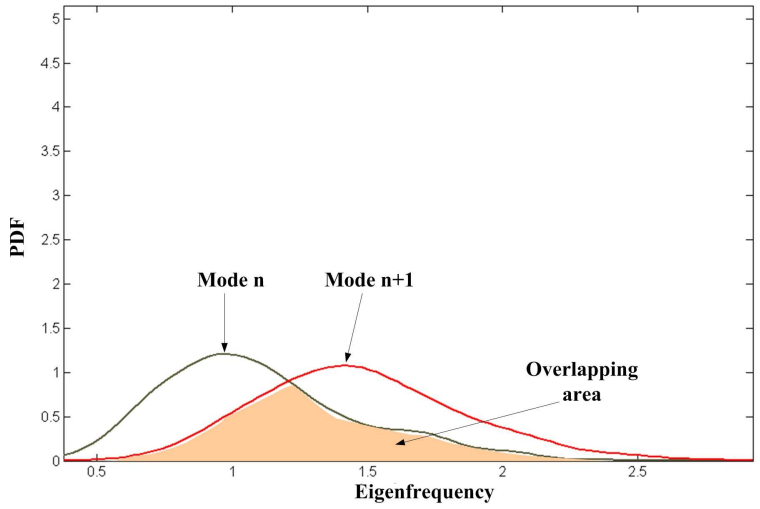

(B) Modal intermixing

FIGURE 3.3: PDF comparison of two adjacent eigenfrequencies

Therefore, it can be concluded that large dispersion of modal solutions can result in the modal intermixing. That is mathematically, because the overlapping area of the PDFs

with respect to adjacent modes becomes larger. However, recall that the presence of large dispersion connected with modal solutions is induced from the large variances of random structural parameters. In Fig. 3.3a, the coefficient of variance of random structural parameter is 2%, while in Fig. 3.3b the coefficient of variance is 20%. Essentially, the modal intermixing is caused by the large dispersion (or variance, standard deviation or COV) of structural parameters.

If one wants to get rid of the modal intermixing, the variance of the eigenfrequency or eigenvector should be small. In some extent, that implies the variances of the random structural parameters are not supposed to be large. The similar issue has been pointed out in the work [141], which denoted that large variances of random parameters may lead to negative quantities (e.g. normal distributed parameters) and thereafter physically meaningless results. Even though all the uncertainties are generated from a distribution supported by positive values, such as lognormal distribution, the large variances may lead to structural parameters very close to zero. In these cases, the random structures are not practically required.

Generally, it is difficult to control the variances. However, based on some criteria, such as the geometry tolerances, the dispersion could be not very large. From this point of view, selection of relatively small variance is not only helpful to avoid the modal intermixing or reduce the associated influences, but also necessary to fulfill practical requirements

3.4.2 MAC factor

To avert the modal intermixing, it would be better get the quantification first. As stated above, the variabilities of random eigenvectors (eigenvalues also) around the ones of mean model ought to be small in order to remove the modal intermixing issue. If this property holds, the random eigenvectors can be interpreted as small rotations with respect to a reference model (i.e. mean model) [150]. Therefore, the rotated eigenvectors can be approximated by a linear combination of m eigenvectors of the mean model. The jth eigenvector of simulation k is formulated as

$$\boldsymbol{\phi}_j^{(k)} = \sum_{i=1}^{m} A_i^{(k)} \boldsymbol{\phi}_i^{(0)}, \qquad 1 \leq j < m, \tag{3.47}$$

where $A_i^{(k)}$ denotes the constant weight coefficient; $\boldsymbol{\phi}_i^{(0)}$ represents the ith eigenvector of the mean model. When the behaviors of random models are identical with the ones of mean model, the effects of the other modes can be ignored, which is interpreted that the most contribution to the sample $\boldsymbol{\phi}_j^{(k)}$ is from the jth mode of the mean model. In this situation, the last equation in the approximate formula is

$$\boldsymbol{\phi}_j^{(k)} \approx A_j^{(k)} \boldsymbol{\phi}_j^{(0)}, \qquad A_j^{(k)} > 0. \tag{3.48}$$

Obviously, the angle between the eigenvector $\boldsymbol{\phi}_j^{(k)}$ and $\boldsymbol{\phi}_j^{(0)}$ will meet $\alpha_{jj}^{(k)} \approx 0$. In conjunction with the last expression, the direction cosine of these two eigenvectors has the property

$$\cos(\alpha_{jj}^{(k)}) = \frac{\boldsymbol{\phi}_j^{(k)} \cdot \boldsymbol{\phi}_j^{(0)}}{\left\|\boldsymbol{\phi}_j^{(k)}\right\| \left\|\boldsymbol{\phi}_j^{(0)}\right\|} \approx 1, \tag{3.49}$$

in which $\boldsymbol{\phi}_j^{(k)} \cdot \boldsymbol{\phi}_j^{(0)}$ denotes the dot product and $\|\cdot\|$ is the Euclidean norm. Eq. (3.49) is the condition to prevent the random models from the modal intermixing. It is actually a variant of the MAC [151] factor, which is defined by

$$f_{\mathrm{MAC}_{jj}}^{(k)} = \frac{(\boldsymbol{\phi}_j^{(k)} \cdot \boldsymbol{\phi}_j^{(0)})^2}{\left\|\boldsymbol{\phi}_j^{(k)}\right\|^2 \left\|\boldsymbol{\phi}_j^{(0)}\right\|^2} = \cos^2(\alpha_{jj}^{(k)}) \approx 1. \tag{3.50}$$

The MAC is the criterion to check the consistency between two modes. In this work, it is used to check the consistency between the random mode $\boldsymbol{\phi}_j^{(k)}$ and the corresponding mean mode $\boldsymbol{\phi}_j^{(0)}$. When the value approaches unity, the consistency is well observed; in contrast, the value is smaller than 1, the behaviors show the violation. The modal intermixing is the right phenomenon from one simulation to another that reflects the violated modes against the mean modes. Therefore, in accordance with Eq. (3.50), the MAC factor is an indicator of the modal intermixing

$$\begin{aligned} f_{\mathrm{MAC}_{jj}}^{(k)} &\approx 1, \quad \text{no modal intermixing,} \\ f_{\mathrm{MAC}_{jj}}^{(k)} &< 1, \quad \text{modal intermixing.} \end{aligned} \tag{3.51}$$

Note that when modal intermixing occurs, the MAC factor usually shows a relatively large difference from 1.

3.4.3 Univariable based strategy

Emphasized again, the modal intermixing is aroused by the large scatter of the random parameters. Generally, some of them may have the large possibility to induce the modal intermixing issue, while the rest parameters may not. So as to check which parameter can cause the modal intermixing, a univariable based strategy is proposed. In this strategy, only one parameter is treated as random variable; others are deterministic. We use the basic concept of the worst case approach (see Section 2.4.2.3) to check whether the intermixing problem is caused referring to the defined worst case.

Most often, designers prefer to prevent the intermixing at a large confidential probability, which corresponds a large confidential interval. We take a normal random variable θ with mean value μ_θ and standard deviation σ_θ as example. Confidential probability 68.3% is related to the confidential interval $\mu_\theta \pm \sigma_\theta$, 95.5% is corresponding to $\mu_\theta \pm 2\sigma_\theta$ and 99.7% is associated with $\mu_\theta \pm 3\sigma_\theta$. In this case, the worst case can be defined at $\mu_\theta \pm 3\sigma_\theta$.

Recall that the worst case does not depends on the distribution types of structural random parameters. Accordingly, when considering the worst case, the type needs not be considered. Based on the above analysis, we set the worst case in the presence of

$$\tilde{\boldsymbol{\theta}} = [\mu_\theta \pm 2\sigma_\theta \quad \mu_\theta \pm 3\sigma_\theta \quad \mu_\theta \pm 4\sigma_\theta]^{\mathrm{T}}, \tag{3.52}$$

where $\tilde{\boldsymbol{\theta}}$ is the worst case vector. The last four elements of $\tilde{\boldsymbol{\theta}}$ suggest the rare events. If all the associated eigenvectors especially the ones corresponding the rare events can meet the condition in Eq. (3.51), σ_θ is a proper standard deviation for averting the modal intermixing.

This strategy is useful to check which parameter can cause the modal intermixing, but is not a rigorous optimization process to obtain a reasonably maximum COV. When an improper COV is investigated, one just needs to reduce the value directly according to the engineering experiences until a fair one is found. To this end, this strategy is also suited to find a proper COV.

Again, it is underlined that the modal intermixing is caused by the large dispersion of random structural parameters. From this view, it is reasonable to use a relatively small

variance to model the uncertainties. Although the variance is difficult to fix or control, however the scatter of structural parameters is usually small to fulfill the practical engineering, e.g. the geometry tolerance. Therefore, it is not rigorously conflicting between the usage of small variance or COV (always not greater than 10%) and the practical engineering.

3.5 Numerical examples

Since this work aims to apply PCE in UA for both static and dynamic problems, four examples, i.e. plate-beam, simply supported beam, mass-spring and an oscillator have been tested in 5 cases respectively, which are listed in Table 3.1.

TABLE 3.1: Cases description

Model	Excitation	Response	N_s	N	Δt(s)	T(s)	Case
Plate-Beam	Dynamic	Displacement	4	1505	0.01	15	Case I
Plate-Beam	Static	Stress	4	5	–	–	Case II
Beam	Static	Stress	5	6	–	–	Case III
Mass-Spring	Dynamic	Displacement	2	1503	0.01	15	Case IV
Oscillator	Dynamic	Displacement	30	4031	0.005	20	Case V

The stress is expanded by the PCE directly following Eq. (3.7) and the displacement is calculated by the discrete convolution in Eq. (3.17). For clarity, the dimension of structural parameters N_s and total number of the random variables N, time step Δt and duration T are also listed here.

Basically speaking, the accuracy of probability of failure is more difficult to achieve than those of the moments. To this end, most results will be shown in the presence of probability of failure. Conveniently, the probability of failure estimated by direct MCS is denoted by $P_{F,\mathrm{DMCS}}$, while the one evaluated by PCE based MCS is denoted by $P_{F,\mathrm{PCEMCS}}$. The error is defined as $\varepsilon = \frac{|P_{F,\mathrm{DMCS}} - P_{F,\mathrm{PCEMCS}}|}{P_{F,\mathrm{DMCS}}}$.

3.5.1 Case I: Plate-Beam (dynamic problem)

In current case, the reliability analysis of a plate-beam structure under stochastic loads, shown in Fig. 3.4 is carried out. There are 294 nodes in the FE model. The excitation acts at node 14 along positive X. First 10 modes are retained for the response calculation.

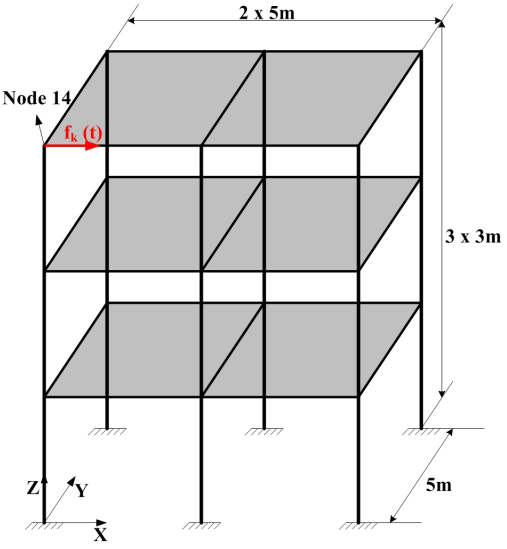

FIGURE 3.4: Plate-Beam model

The damping is assumed as Rayleigh damping. The associated modal damping ratio is calculated by

$$\zeta_j = \frac{\alpha}{2\omega_j} + \frac{\beta\omega_j}{2}, \tag{3.53}$$

where $\alpha = 0.0212$ and $\beta = 0.0182$ are constants. The other parameters are listed in Table 3.2. All the unites belong to SI. The excitation is the modulated Gaussian white noise defined as $Z_k(t_m) = e(t_m)W_k(t_m)$ at the time instant t_m, $m = 1, \ldots, n_T$ within the time interval $[0, T]$. The associated band-limited Gaussian white noise is $W_k(t_m) = \sqrt{2\pi S_k/\Delta t}\boldsymbol{\xi}_k^m$, where $\boldsymbol{\xi}_k^m$ denote independent, identically distributed (i.e. i.i.d.) standard normal random variables at time instant t_m for the kth excitation; $S_k = 3000$ is the associated constant power density. The modulated function is defined as follows

$$e(t_m) = \begin{cases} 0 & t_m \leq 0s \\ (t_m/4)^2 & 0 \leq t_m \leq 4s \\ 1 & 4 \leq t_m \leq 10s \\ e^{-(t_m-10)^2} & 10s \leq t_m \leq T. \end{cases} \tag{3.54}$$

The first passage probability needs to be calculated, and the associated limit state function is given by $g(\boldsymbol{\theta}, \mathbf{Z}(\mathbf{t})) = X_{t,14} - |x_{14}(\boldsymbol{\theta}, \mathbf{Z}(\mathbf{t}))| < 0$, where $x_{14}(\boldsymbol{\theta}, \mathbf{Z}(\mathbf{t}))$ denotes the displacement at node 14 and $X_{t,14}$ is the positive threshold.

Theoretically, PCE can model the second-order random variables with an acceptable convergence. In the light of transformation techniques introduced in section 2.3.2, the

TABLE 3.2: Parameters of plate-beam

Parameter	Symbol	Deterministic/Random	Value/Mean
Poisson's ratio	ν	deterministic	0.3
Density	ρ	random	7.8×10^3
Young's modulus	E	random	2.0×10^{11}
Beam length	BL	random	3
Beam width	BW	deterministic	0.04
Beam height	BH	deterministic	0.04
Plate thickness	PT	random	0.02
Plate length	PL	deterministic	5

applications can be relaxed to other non-Gaussian distributions. However, slow convergence [85] has been observed when the random inputs are non-Gaussian. From this view, it is worth to state the influences of the distributions. Four situations with the same COV= 10% are discussed. 1) Normal: all random parameters are normal; 2) Lognormal: all random parameters are lognormal; 3) Gamma: all random parameters are Gamma; 4)Mixed: ρ and E are lognormal while PT and BL are normal.

TABLE 3.3: First passage probability for plate-beam

Situation	p	P	N_{LSF}	$X_{t,14} = 0.025$m		$X_{t,14} = 0.030$m	
				$P_{F,\text{DMCS}}$	$P_{F,\text{PCEMCS}}$	$P_{F,\text{DMCS}}$	$P_{F,\text{PCEMCS}}$
Normal	1	5	20	2.1×10^{-3}	3.0×10^{-3}	3.2×10^{-4}	5.6×10^{-4}
	2	15	50		2.1×10^{-3}		2.8×10^{-4}
	3	35	100		2.1×10^{-3}		3.2×10^{-4}
Lognormal	1	5	20	2.1×10^{-3}	2.1×10^{-3}	3.0×10^{-4}	3.9×10^{-4}
	2	15	50		2.1×10^{-3}		2.7×10^{-4}
	3	35	100		2.1×10^{-3}		3.1×10^{-4}
Gamma	1	5	20	2.4×10^{-3}	2.9×10^{-3}	3.2×10^{-4}	5.1×10^{-4}
	2	15	50		2.1×10^{-3}		2.7×10^{-4}
	3	35	100		2.3×10^{-3}		3.1×10^{-4}
Mixed	1	5	20	2.3×10^{-3}	3.7×10^{-3}	2.7×10^{-4}	8.8×10^{-4}
	2	15	50		2.1×10^{-3}		2.6×10^{-4}
	3	35	100		2.3×10^{-3}		2.6×10^{-4}

Additionally, the effectiveness of the proposed method may be influenced by the truncated order of the PCE, the modal intermixing problem and the levels of the probability of failure. Combination of all theses influences, the associated results are reported in Table 3.3, based on which some comprehensive comparisons are concluded as follows.

3.5.1.1 Efficiency comparison

The reliability analysis relies on 10^5 random responses, for which there needs $N_{\mathrm{mc}} = 10^5$ modal analyses in direct MCS, while only $N_{\mathrm{LSF}} \approx 3P$ modal analyses are required in PCE based MCS. The number of the modal analyses needed by the proposed method is specified in column #4 corresponding to different order p (or P), among which the largest one is $N_{\mathrm{LSF}} = 100$ to achieve a reasonable accuracy $\varepsilon \leq 5\%$. It is evident that the efficiency is largely improved by the proposed method compared with direct MCS.

Moreover, the CPU time to evaluate the 10^5 random responses (i.e. convolution processes with known modal properties) and the corresponding failure probability for both methods is about 6 minutes. While the time for 10^5 modal analyses (obtained by FEA) equals to 56 hours on average. Consequently, it is apparent that the time used for reliability analysis alone is much less than the time to prepare the random responses.

3.5.1.2 Influences of PCE orders and levels of probability of failure

In the limit state function, two levels of the threshold are considered, $X_{t,14} = 0.025$m and $X_{t,14} = 0.030$m corresponding to the probabilities of failure with order 10^{-3} and 10^{-4} respectively. Since the truncated form of PCE is used, different order may result in different results.

Table 3.3 shows that at least $p = 2$ is required for a larger level of failure probability and $p = 3$ for a smaller one to achieve an acceptable error, say $\varepsilon \leq 5\%$. The reason is that evaluation of relatively small probabilities of failure (e.g. order 10^{-4}), a more accurate approximation in the tails of the distribution with respect to the associated response is essential. As expected, $P_{F,\mathrm{PCEMCS}}$ should converge to $P_{F,\mathrm{DMCS}}$ when the order p fulfills $p \longrightarrow \infty$. To some extent, increasing the order is feasible to achieve reasonable accuracy.

3.5.1.3 Influences of the types of random parameters

For the four sets of random inputs, the convergent rates of the smaller probabilities of failure are equivalent, i.e. the 3rd order PCE is necessary with the error $\varepsilon \leq 5\%$. With respect to larger failure probabilities however, the Gamma and mixed random inputs lead to the slower convergence where $p = 3$ is required; the situation of Lognormal

owns almost the same convergent rate with the normal one. This is not occasional since Lognormal stochastic processes and variables can be reasonably expressed by PCE [67].

Although it is impossible to consider all distribution types, nonetheless we may conclude that increasing the order, in a way, is helpful to obtain a reasonable accuracy. Additionally, a little differences of the first passage probabilities corresponding to the four distinct random inputs have been observed, but the order (10^{-3} and 10^{-4}) is identical. The interpretation is that the four situations have the same COV, which will lead to similar scatter of the random response.

3.5.1.4 Influences of the modal intermixing

Because the modal intermixing is caused by the large COV of random inputs, checking the influence of modal intermixing is equivalent to checking the influence of COV. Therefore, three levels of COV are examined. Taking the random plate thickness as example, Fig. 3.5 schematically gives the MAC factors of the first 10 modes with respect to 6 worst cases under 3 levels of COV.

Observations indicate that with respect to the same worst case, large COV= 20% tends to cause the modal intermixing more easily. Moreover, the worse the case is, the more severe the phenomenon is, as shown in Fig. 3.5e. It is also found that the modal intermixing always occurs related to higher modes and with increase of the COV. The effects are always diffused from higher modes to lower modes.

Comparing the sub-figures on the left to the right, it is shown that the modal intermixing always concerns the random model whose plate thickness is less than the mean value. The explanation is that as the thickness decreases, the flexibility increases since the plate belongs to thin walled structures. The associated structural behaviors can be different from the reference (mean model) more easily. Whereas for thicker plates, the modes have a large probability to agree with the ones of the mean model.

We also discover that when we increase the COVs of density and Young's modulus to 30%, no modal intermixing occurs, the MAC factors of which are always very close to one. This reveals that not all parameters cause the intermixing phenomenon. Note that the worst case associated with Young's modulus up to COV= 30% is set up to $\mu_\theta \pm 3\sigma_\theta$ because the value like $\mu_\theta - 4\sigma_\theta$ will be negative which is physically meaningless.

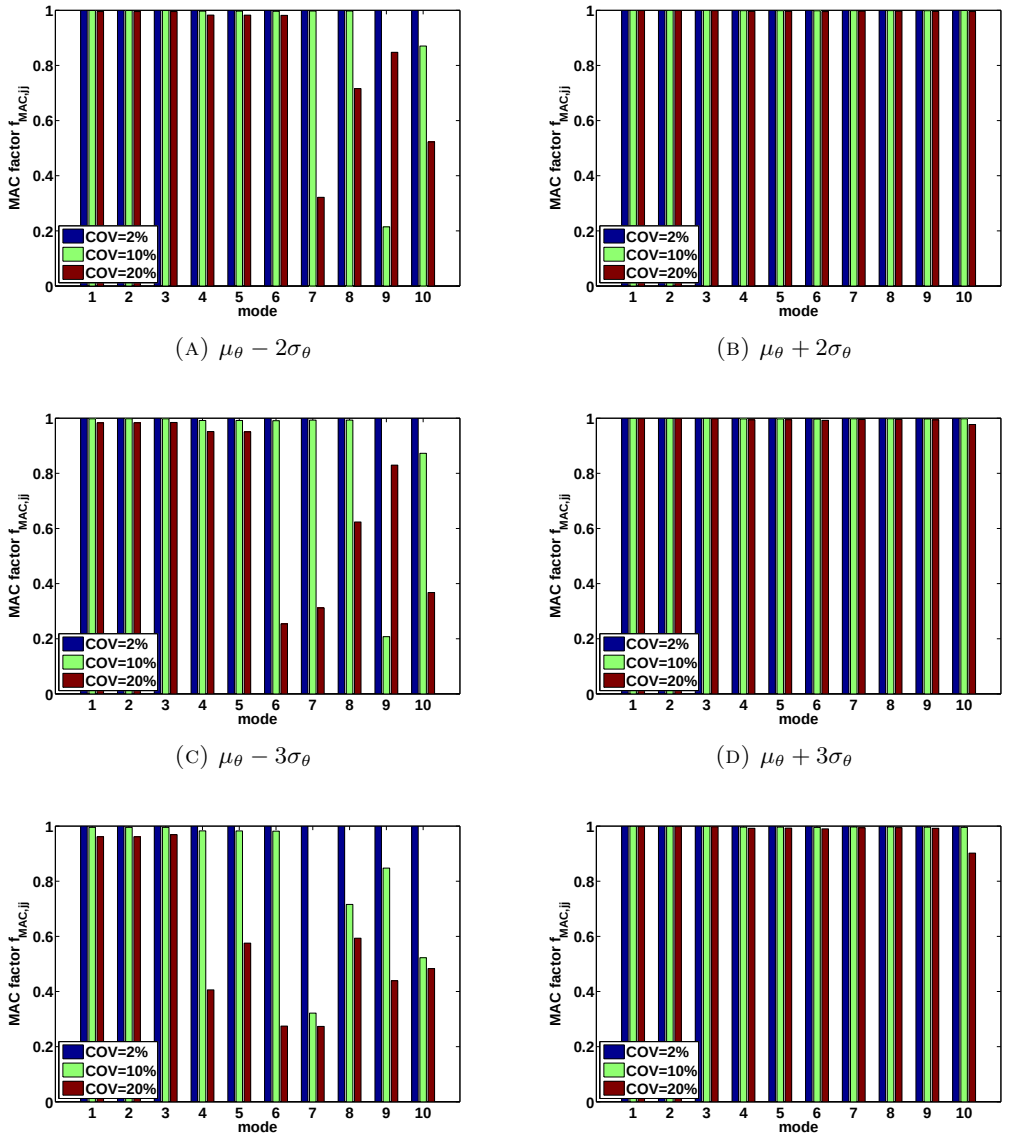

(A) $\mu_\theta - 2\sigma_\theta$ (B) $\mu_\theta + 2\sigma_\theta$

(C) $\mu_\theta - 3\sigma_\theta$ (D) $\mu_\theta + 3\sigma_\theta$

(E) $\mu_\theta - 4\sigma_\theta$ (F) $\mu_\theta + 4\sigma_\theta$

FIGURE 3.5: Comparisons of MAC factor

For reliability analysis, the samples in the tails play more important role than those in the central region. That implies as to small probability of failure (e.g. 10^{-4}), negative samples or very small samples may be generated by MCS sampling due to large variance. In this sense, large COV should be avoided for practical applications.

The instinctive sense for the modal intermixing is schematically illustrated in Fig. 3.6, in which the mode shapes of the 10th mode corresponding to three levels of COV and the mean model are shown respectively. It is clear that the violations are observed for COV= 10% and COV= 20%. While the behavior related to COV= 2% is almost the same with the mean model.

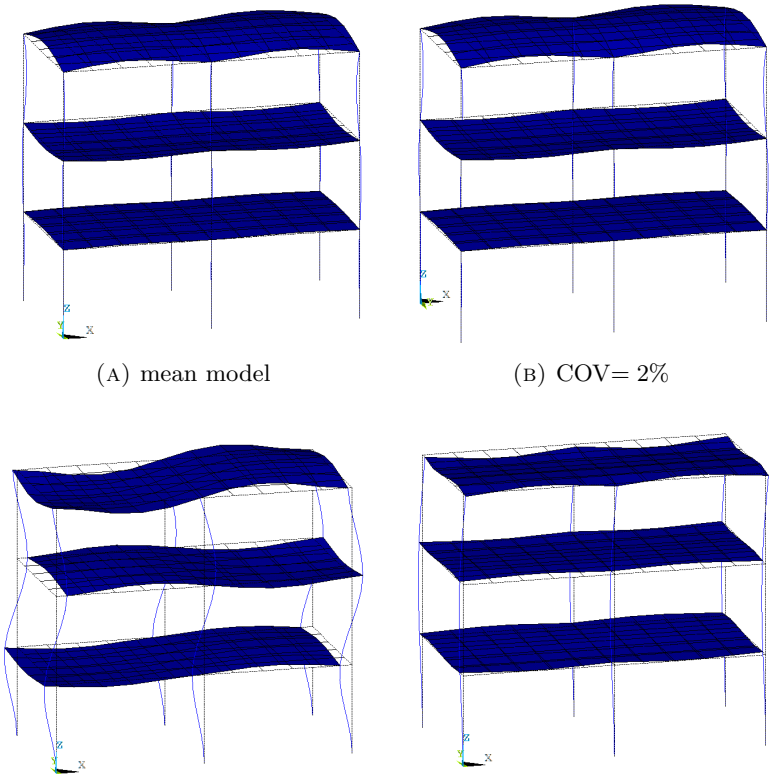

(A) mean model (B) COV= 2%

(C) COV= 10% (D) COV= 20%

FIGURE 3.6: Comparisons of mode shapes

For clarity, the associated probabilities are listed in Table 3.4 under normal random parameters. From Table 3.4, it is found that the probability of failure is monotonic increasing with the increase of COV. Zero probabilities of failure in column #7 and #8 imply that 10^5 samples are insufficient to obtain a much higher reliability level. We can see that the smaller the COV is, the more accurat the results are. Regarding to COV= 10%, although there exists the modal intermixing though (see Fig. 3.5), the consistent results are observed. The reason is that the modal intermixing only appears for the last four modes which contribute the least to the response evaluation.

TABLE 3.4: Influences of the COV

COV*	p	$X_{t,14} = 0.020$m		$X_{t,14} = 0.025$m		$X_{t,14} = 0.030$m	
		$P_{F,\text{DMCS}}$	$P_{F,\text{PCEMCS}}$	$P_{F,\text{DMCS}}$	$P_{F,\text{PCEMCS}}$	$P_{F,\text{DMCS}}$	$P_{F,\text{PCEMCS}}$
2%	2	3.70×10^{-3}	3.70×10^{-3}	1.70×10^{-4}	1.70×10^{-4}	0	0
10%	3	1.46×10^{-2}	1.46×10^{-2}	2.10×10^{-3}	2.10×10^{-3}	3.20×10^{-4}	3.20×10^{-4}
20%	5	7.03×10^{-2}	7.11×10^{-2}	3.07×10^{-2}	3.16×10^{-2}	1.46×10^{-2}	1.56×10^{-2}

* COV= 2% denotes $\delta_E = 10\%$, $\delta_\rho = 10\%$, $\delta_{BL} = 1.75\%$ and $\delta_{PT} = 2\%$; COV= 10% denotes $\delta_E = \delta_\rho = \delta_{BL} = \delta_{PT} = 10\%$; COV= 20% denotes $\delta_E = \delta_\rho = \delta_{BL} = \delta_{PT} = 20\%$.

With respect to COV= 20%, the error is amplified as the threshold increases, even

though the current probability only achieves 10^{-2}. More accurate results are supposed to be obtained by increasing the order of PCE. However, the conflicting results have been shown in Table 3.5 where only the COV= 20% is regarded. Obviously, accuracy improvements have not much benefit from increasing the order since the most accurate results correspond with $p = 5$. It is concluded that bad approximation by PCE will be induced by sever modal intermixing, i.e. fair approximation by PCE can only be obtained provided that the COV is not very large (usually less than 10%), i.e. no severe modal intermixing happens. From this view, the PCE based MCS is capable to solve problem in practical engineering.

TABLE 3.5: Accuracy comparison of the first passage probability with COV= 20%

p	$X_{t,14} = 0.020$m		$X_{t,14} = 0.025$m		$X_{t,14} = 0.030$m	
	$P_{F,\text{DMCS}}$	$P_{F,\text{PCEMCS}}$	$P_{F,\text{DMCS}}$	$P_{F,\text{PCEMCS}}$	$P_{F,\text{DMCS}}$	$P_{F,\text{PCEMCS}}$
4	7.03×10^{-2}	7.38×10^{-2}	3.07×10^{-2}	3.26×10^{-2}	1.46×10^{-2}	1.62×10^{-2}
5		7.11×10^{-2}		3.16×10^{-2}		1.56×10^{-2}
6		7.22×10^{-2}		3.30×10^{-2}		1.72×10^{-2}

3.5.2 Case II: Plate-Beam (static problem)

In this section, the static issue of plate-beam model is taken into account. The static load is modeled by a normal random variable. The limit state function is defined as

$$g(\boldsymbol{\theta}, \mathbf{Z}) = R - S(\boldsymbol{\theta}, \mathbf{Z}) < 0, \tag{3.55}$$

where $R = 160$MPa is the resistance, i.e. the allowable stress in this case and $S(\boldsymbol{\theta}, \mathbf{Z})$ denotes the maximum stress in the structure. Studies focus on normal parameters.

Table 3.6 describes the probabilities under two distinguished COVs. To obtain the same level of probability of failure, the excitations are different. The larger the COV the smaller the excitation is required. More than 99% CPU time is saved, i.e. 800 modal analyses needed in the PCE approximation method compared with 10^5 ones required in direct MCS.

Fig. 3.7 shows the comparisons of the probability density functions (PDFs) of the maximum stress associated with different orders of PCE for COV= 10%. It is evident that the 2end order approximation is not sufficient not only in the tails but also in the

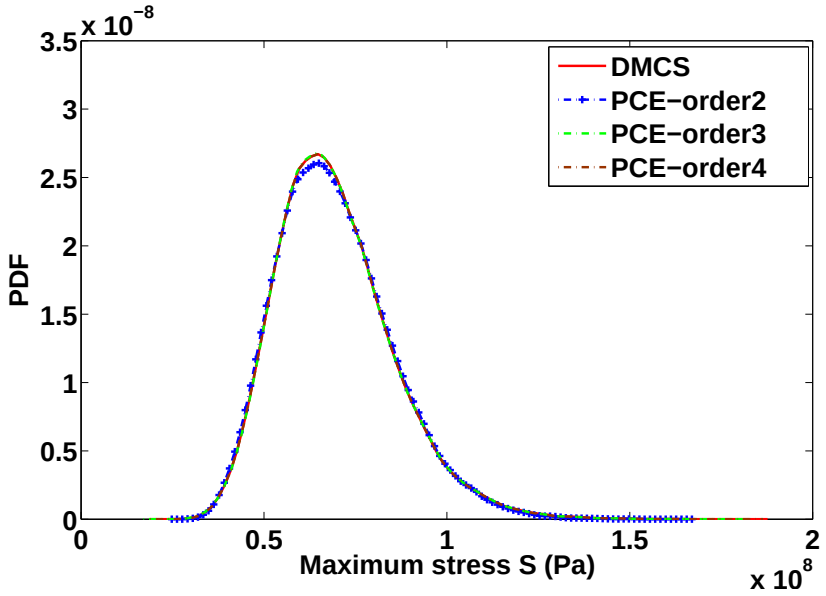

FIGURE 3.7: Comparison of PDFs of the stress for COV= 10%

central region. In the contrary, the 3rd and 4th order both offer better fits through the whole region. Nonetheless, more accurate probability of failure is evaluated with the 4th order PCE which is listed in Table 3.6.

TABLE 3.6: Probabilities of failure for plate-beam

COV	μ_F(N)	p	P	N_{LSF}	$P_{F,\text{DMCS}}$	$P_{F,\text{PCEMCS}}$
10%	2500	2	21	60	1.30×10^{-4}	1.00×10^{-5}
		3	56	200		1.00×10^{-4}
		4	126	400		1.30×10^{-4}
20%	1000	2	21	60	1.10×10^{-4}	0
		3	56	200		8.00×10^{-5}
		4	126	400		1.50×10^{-4}
		5	252	800		1.50×10^{-4}

Because of the modal intermixing problem, the PCE only offers the results with limited accuracy for random eigenvalue problems with the large COV of random parameters, e.g. 20%. Although the response of static problems have no direct relation with the random eigenvalue problem, it has to be noted that the modal properties are associated with the inherent properties of structures. In this sense, large COV may change the position where the maximum stress is located.

The investigations of PDF for COV= 20% are illustrated in Fig. 3.8. The order increased up to 4 is helpful to obtain better fits for both central region and tails. In Table 3.6, zero probability of failure obtained by the 2end PCE is not resulted from the inadequate

samples but the inaccurate approximation in tails. It is evident according to Fig. 3.8 that no data greater than 1.5×10^8 are generated. Again shown in Table 3.6 however, the 4th and 5th order show the same convergence that implies the further increase of the order cannot improve the accuracy effectively.

Note that the 4th order PCE required in current case is one order higher than the corresponding dynamic case (see in Table 3.3). The probable reason is that the excitation uncertainties involved in dynamic problems are not propagated by the PCE model, whereas those within static problems are involved.

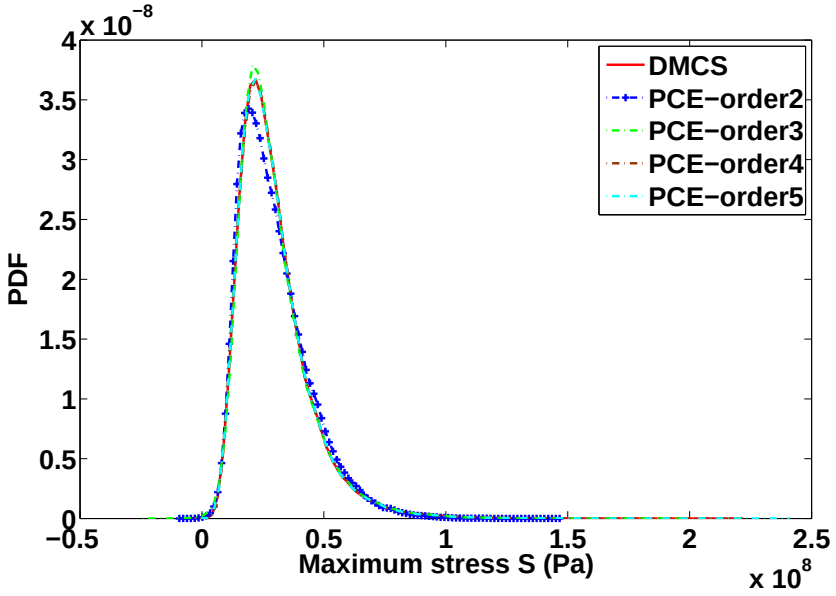

FIGURE 3.8: Comparison of PDFs of the stress for COV= 20%

3.5.3 Case III: Beam

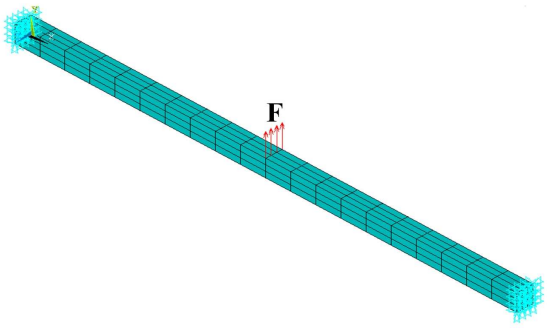

FIGURE 3.9: Beam model

A simply supported beam contains 252 nodes shown in Fig. 3.9. The response is estimated by the superposition of the first three modes. The beam is subjected to

random loads in the middle with direction Y. Deterministic parameters are Poisson's ratio $\nu = 0.3$ and damping ratio $\zeta = 0.05$; the rest parameters are assumed to be statistically independent normal random variables, the mean values of which are $\rho = 7.8 \times 10^3\ kg/m^3$, $E = 2.0 \times 10^{11}$Pa, $L = 2.5$m, $H = 0.1m$, $W = 0.08$m and $F = 6000$N for density, Young's modulus, length, height, width and excitation respectively. All the parameters have the same variability, say COV= 10%.

TABLE 3.7: Probabilities of failure for beam

p	P	N_{LSF}	$P_{F,\text{DMCS}}$	$P_{F,\text{PCEMCS}}$
1	7	20	7.0×10^{-5}	0
2	28	85		0
3	84	250		1.0×10^{-5}
4	210	650		6.0×10^{-5}

The limit state function is also described by Eq. (3.55). Table 3.7 lists the probabilities of failure corresponding different order PCE approximation. In the same manner, 10^5 static analyses are needed in direct MCS. Despite of that the error $\varepsilon > 10\%$, however, the result is still acceptable since the probability of failure is very small, say 10^{-5}. Efficiency is strongly improved by PCE with 650 static analyses compared with direct MCS with 10^5 static analyses.

Although for 10^{-5} probability of failure, 10^5 samples are not adequate, the examples used in this work are to demonstrate the effectiveness of the proposed PCE based MCS method. To reduce the inherent variability due to different sets of samples, the random excitations in this work are generated under the same seed.

3.5.4 Case IV: Mass-Spring

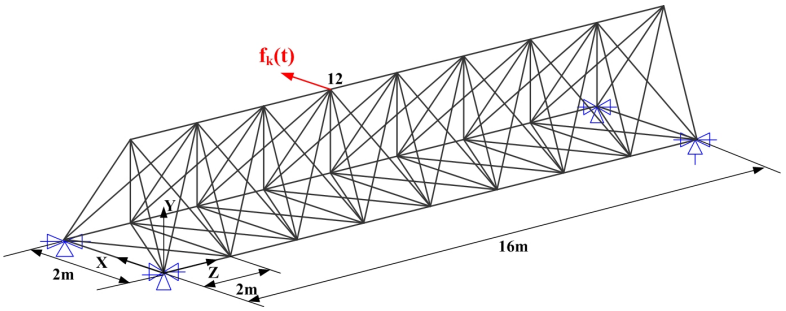

FIGURE 3.10: Mass-spring model

The geometry parameters of the mass-spring are illustrated in Fig. 3.10, in which there are 27 mass elements and 75 spring elements. Four corners in the plane XZ are fixed against the base. The crossing-section is a regular triangle. The mean of the mass and the stiffness are $\mu_m = 1$ kg and $\mu_k = 1000$ N/m. Rayleigh damping is implemented for this model with $\alpha = 0.10$ and $\beta = 0.0036$. First 40 modes are utilized to calculate the response. The lower and upper band of the natural frequency of the mean model are $\omega_1 = 3.47$ rad/s and $\omega_{40} = 55.03$ rad/s. The excitation acts on node 12 along X direction. The stochastic excitation has the same definition in Section 3.5.1 with $S_k = 0.1$. The failure region is defined by

$$g(\boldsymbol{\theta}, \mathbf{Z}(\mathbf{t})) = X_{t,12} - |x_{12}(\boldsymbol{\theta}, \mathbf{Z}(\mathbf{t}))| < 0, \tag{3.56}$$

where $x_{12}(\boldsymbol{\theta}, \mathbf{Z}(\mathbf{t}))$ denotes the displacement at node 12 and $X_{t,12}$ is the positive threshold. In this case, we consider two levels of COV and two distinguished thresholds. The associated results approximated by different order of PCE are given in Table 3.8. It is found that a lot of CPU time is saved since at most 50 modal analyses are required by the PCE based MCS. While 10^5 modal analyses is needed by direct MCS, the average time of which is 76 hours. Moreover, the convergence is achieved up to the 2end order for COV= 5%, while the 3rd order for COV= 10%. The accuracy is guaranteed.

TABLE 3.8: First passage probability for mass-spring

COV	p	P	$N_{t\text{LSF}}$	$X_{t,12} = 0.03$m		$X_{t,12} = 0.035$m	
				$P_{F,DMCS}$	$P_{F,\text{PCEMCS}}$	$P_{F,\text{DMCS}}$	$P_{F,\text{PCEMCS}}$
5%	1	3	10	2.1×10^{-3}	2.0×10^{-3}	1.5×10^{-4}	1.6×10^{-4}
	2	6	20		2.1×10^{-3}		1.5×10^{-4}
	3	10	30		2.1×10^{-3}		1.5×10^{-4}
	4	15	50		2.1×10^{-3}		1.5×10^{-4}
10%	1	3	10	3.5×10^{-3}	3.8×10^{-3}	1.3×10^{-4}	1.5×10^{-4}
	2	6	20		3.5×10^{-3}		1.4×10^{-4}
	3	10	30		3.5×10^{-3}		1.3×10^{-4}
	4	15	50		3.5×10^{-3}		1.3×10^{-4}

The accuracy of the proposed method can also be shown by the moment evaluations. Fig. 3.11 schematically depicts the mean and standard deviation (SD) of the impulse responses with respect to COV= 5% and COV= 10%. It is found that the results obtained by the PCE based MCS are consistent with those obtained by direct MCS, for either COV= 5% or COV= 10%.

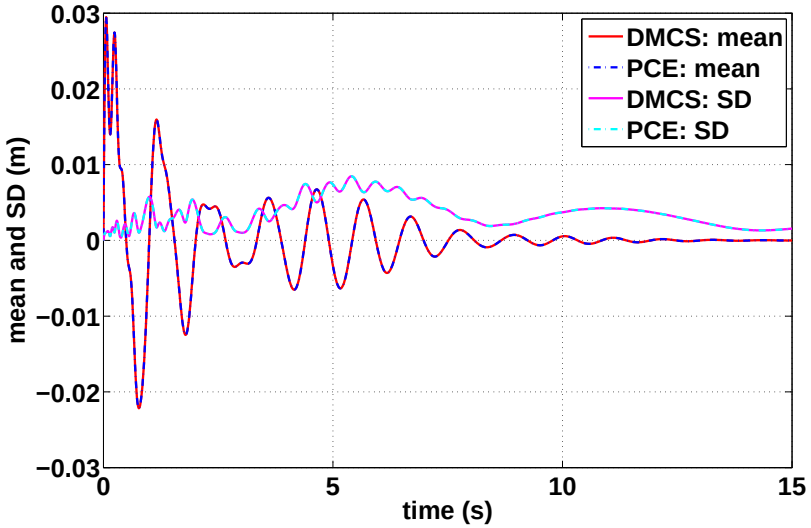

(A) COV= 5%

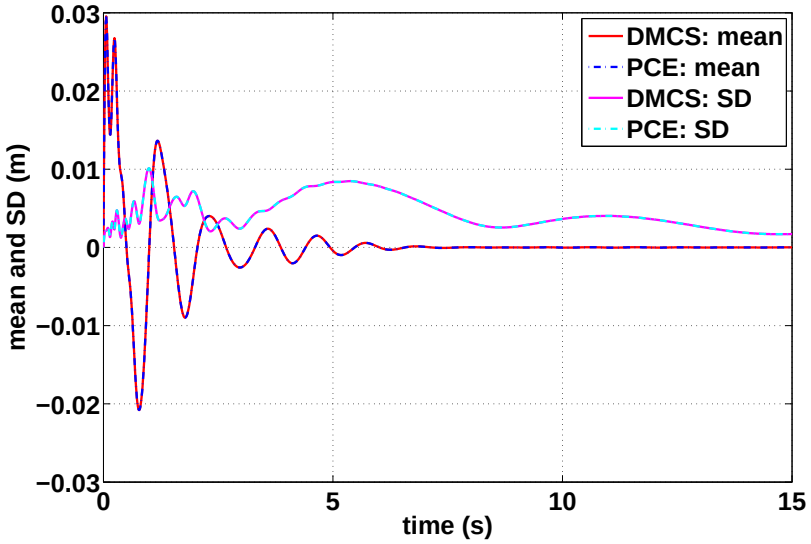

(B) COV= 10%

FIGURE 3.11: Impulse response comparisons

3.5.5 Case V: Ten-degree-of-freedom oscillator (linear simplification)

This model is a ten-degree-of-freedom Duffing type oscillator which has been treated as a benchmark problem in [120]. In this work, we focus on the linear random structures under stochastic excitations. The governing equation is given by

$$\mathbf{M}\ddot{\mathbf{x}}(t) + \mathbf{C}\dot{\mathbf{x}}(t) + \mathbf{K}\mathbf{x}(t) = \mathbf{Z}(t), \tag{3.57}$$

with zero initial conditions, where

$$\mathbf{M}=\begin{bmatrix} m_1 & 0 & 0 & \cdots & 0 \\ 0 & m_2 & 0 & \cdots & 0 \\ \vdots & \vdots & \vdots & \ddots & \vdots \\ 0 & \cdots & 0 & 0 & m_{10} \end{bmatrix}, \quad \mathbf{K}=\begin{bmatrix} k_1+k_2 & -k_2 & 0 & \cdots & 0 \\ -k_2 & k_2+k_3 & -k_3 & \cdots & 0 \\ \vdots & \vdots & \vdots & \ddots & \vdots \\ 0 & \cdots & 0 & -k_{10} & k_{10} \end{bmatrix},$$
$$\mathbf{Z}(t)=p(t)\begin{Bmatrix} m_1 \\ m_2 \\ \vdots \\ m_{10} \end{Bmatrix}, \qquad \mathbf{C}=\begin{bmatrix} c_1+c_2 & -c_2 & 0 & \cdots & 0 \\ -c_2 & c_2+c_3 & -c_3 & \cdots & 0 \\ \vdots & \vdots & \vdots & \ddots & \vdots \\ 0 & \cdots & 0 & -c_{10} & c_{10} \end{bmatrix}. \tag{3.58}$$

The structural parameters are random, the mean and standard deviation are described in Table 3.9. The damping $c_i = 2\zeta_i\sqrt{m_i k_i}$ in this case is the viscous damping but the proportional one. Accordingly, the PCE is used to represent the complex modal properties (see Section 3.3.1.2). The stochastic excitation $p(t)$ is modeled by a modulated filtered Gaussian white noise

$$p(t)=\Omega_{1g}^2 v_{f1}(t)+2\zeta_{1g}\Omega_{1g}v_{f2}(t)-\Omega_{2g}^2 v_{f3}(t)-2\zeta_{2g}\Omega_{2g}v_{f4}(t), \tag{3.59}$$

where

$$\frac{d}{dt}\begin{Bmatrix} v_{f1}(t) \\ v_{f2}(t) \\ v_{f3}(t) \\ v_{f4}(t) \end{Bmatrix}=\begin{bmatrix} 0 & 1 & 0 & 0 \\ -\Omega_{1g}^2 & -2\zeta_{1g}\Omega_{1g} & 0 & 0 \\ 0 & 0 & 0 & 1 \\ \Omega_{1g}^2 & 2\zeta_{1g}\Omega_{1g} & -\Omega_{2g}^2 & -2\zeta_{2g}\Omega_{2g} \end{bmatrix}\begin{Bmatrix} v_{f1}(t) \\ v_{f2}(t) \\ v_{f3}(t) \\ v_{f4}(t) \end{Bmatrix}+\begin{Bmatrix} 0 \\ w(t) \\ 0 \\ 0 \end{Bmatrix}, \tag{3.60}$$

and

$$h(t)=\begin{cases} 0 & t\le 0s, \\ t/2 & 0\le t\le 2s, \\ 1 & 2\le t\le 10s, \\ e^{-0.1(t-10)} & 10s\le t\le T. \end{cases} \tag{3.61}$$

$w(t)$ stands for a modulated Gaussian white noise with autocorrelation function $E[w(t)w(t+\tau)] = S\delta(\tau)h^2(t)$ and S denotes the intensity of the white noise. The values $\Omega_{1g} = 15.0\text{rad/s}$, $\zeta_{1g} = 0.8$, $\Omega_{2g} = 0.3\text{rad/s}$, $\zeta_{2g} = 0.995$, and $S = 0.08\text{m}^2/\text{s}^3$ have been used

to model the filter. The impulse of each discrete time step has zero mean and standard deviation $h(t)\sqrt{S\Delta t}$.

TABLE 3.9: Statistical properties of the structural parameters

Variables	Mean	Standard Deviation
$m_1, \ldots, m_{10}$	10 Mg	1.0 Mg
k_1, k_2, k_3	40 MN/m	4.0 MN/m
k_4, k_5, k_6	36 MN/m	3.6 MN/m
k_7, k_8, k_9, k_{10}	32 MN/m	3.2 MN/m
$\zeta_1, \ldots, \zeta_{10}$	0.04	0.004

We are interested in the first passage probability that the relative maximum displacement of the first DOF is greater than the threshold 0.057m; on the other hand, the probability that the relative maximum displacement between the ninth DOF and tenth DOF exceeds the threshold 0.013m is concerned. First 8 modes are used to evaluate the response. The corresponding quantities of the mean model are $\lambda_{1,2} = -0.0548 \pm i9.1440$, $\lambda_{3,4} = -0.4699 \pm i28.3350$, $\lambda_{5,6} = -1.2672 \pm i43.3092$ and $\lambda_{7,8} = -2.3774 \pm i59.0970$.

TABLE 3.10: First passage probability for oscillator

Threshold	$P_{F,\text{PCEMCS}}$	Reference value*
0.057m	8.6×10^{-5}	9.8×10^{-5}
0.013m	7.1×10^{-5}	6.0×10^{-5}

* results in [120].

Based on the analysis for the last four cases, to achieve an acceptable result for problem with COV= 10%, at least 2end order PCE ought to be applied. The order up to 4th may supply more accurate results. Note that the dimension of structural parameters of this case is high somehow, say $N_s = 30$ which needs more computational effort to determine the PCE model. Accordingly, a fair tradeoff should be counted for between the accuracy and economy. To that end, the 2end order PCE (i.e. $N_{\text{LSF}} = 1500$) is used to approximate the modal properties in Eq. (3.41). First passage probabilities concerning with 10^6 approximate random responses can be found in Table 3.10. It is observed that the obtained results are close to the reference ones, which can satisfy the practical requirements. The reasonable inference for the differences between the probabilities is to applying low order PCE.

This case study here mainly shows the capability of the PCE for large dimensional problems with reasonable solutions. The efficiency, especially for the large-degree-of-freedom structures, could be improved in two aspects. The modal superposition method could save the CPU time than the direct methods, e.g. Newmark method; for the other thing, the PCE can provide a fast calculation of modal properties by avoiding repeated modal analyses. This benchmark study is only a ten-degree-of-freedom structure, so the first advantage is weakened. About 90% CPU time is mainly saved from the application of PCE approximation.

3.6 Summary

In this chapter, a PCE based MCS method for UA is proposed in the framework of mechanical engineering. The efficiency is improved in manner of approximating the random response by PCE (HPCE is mainly concerned).

For a considered structure under static loads, the PCE is used to approximate the random response directly. To overcome the curse of high dimensionality caused by the stochastic excitation that is usually specified by a finitely large number of random inputs, we use the convolution form to compute the dynamic response. The PCE is applied to approximate the modal properties but the response so that the dimension of uncertainties is reduced since only random structural parameters are considered.

Case studies exhibit that the proposed method has the capability to cope with UA for both static and dynamic problems related to relatively large COV, e.g. 10%, as well as for the problems with small probability of failure, e.g. 10^{-4} or 10^{-5}. It is found that this method can achieve reasonable accuracy and greater efficiency compared with direct MCS. Depending on the case studies, at least the 2end order PCE is necessary.

To correctly capture the uncertainties in the modal content by analyzing the modal scatter observed in MCS, the encountered modal intermixing problem should be avoided or reduced. For this purpose, the MAC factor is used to quantify the modal intermixing between some random mode and the corresponding mean mode. And then, based on the concept of worst case, we develop a univariable based method to check which parameter can leads to the modal intermixing and to avert it by reducing the COV.

Although the variance (or COV) is not easy to fix or control, the small one fulfills the practical applications, from the view of generating positive samples and grasping the consistently inherent properties of random models with the mean model. Based on simulations, it is found that when the COV of random structural parameters is not greater than 10%, there is no sever modal intermixing.

Chapter 4

Sequential formulation for RBRDO

4.1 Introduction

In this chapter, the efficiency of RBRDO (RBDO is also included) is further improved by the sequential formulation, which is usually related to decoupling the reliability analysis from the optimization loop by converting probabilistic constraints into the equivalent deterministic ones. As to aforementioned sequential formulations, a variety of methods have been developed (see Section 2.4.1.3). It is found that most of these methods rely on the information about the MPP, which signifies FORM/SORM is applied for reliability analysis. However, if FORM/SORM is not available, MCS will dominate due to its facility and accuracy. In this vein, alternative sequential RBRDO in conjunction with MCS is necessary to develop since MCS provides none of MPPs.

In order to realize this, response surface approximations between the probability of failure and the design variables have been developed, among which the exponential function is useful to give a global approximation [152] or a local approximation [153]. Although no formal proof has been stated regarding the convergence of the optimization procedure in conjunction with the exponential approximation, numerical experience has indicated that this approach is most suitable [4, 153, 154]. One of the main challenges for this method is the estimation of the coefficients, which can be obtained in the least square sense [153]. However, the numerical effort associated with LSM will be increased with increase of the dimension of design variables since more and more reliability analyses are required. In these cases, efficient approaches are needed to overcome this disadvantage.

From the algorithm point of view, two ways can achieve this target. One is to utilize advanced reliability methods, e.g. the PCE based MCS method proposed in Chapter 3; and the other one is to reduce the number of reliability analyses. Note that if the approximation of probability of failure is in the presence of "first-order" design variables,

such as the first Taylor expansion method [132], reliability sensitivity analysis is capable to provide the coefficients (i.e. the derivatives or sensitivities of the probability of failure with respect to the design variables) within one reliability analysis. Such sensitivities can be utilized to construct the approximate representation of the probability of failure as an explicit function of the design variables efficiently.

Based on simulation methods, an efficient reliability sensitivity approach [155] is proposed. The main advantage is that only one reliability analysis is carried out, whereas their applicable scope may be restricted to a low number of design variables[155], i.e. less than 3. Wu *et al.* [156, 157] developed another reliability sensitivity method that is not confined to the number of the design variables. Unfortunately, it is not applicable within the scope of deterministic design variables. Nonetheless, this weakness can be removed. For this purpose, we propose an auxiliary distribution based sensitivity analysis method, in which the deterministic design variables are assumed to be be random variables following some random distribution. Although, the auxiliary uncertainties will influence the results of reliability analysis, when the given variance is small, it is found that the influence can be neglected according to the simulation investigations.

On the other hand, sequential strategy should be extended into a wider scope in the context of RBRDO. That is because the objective is to reduce the variability of the performance (usually characterized by the random response), which means the design objective robustness must be taken into account and the associated first and second order moments of the random response are required.

Practically, most of the random responses are available in numerical manner which usually do not have an explicit relation with the design variables. In this occasion, during each function evaluation with respect to the optimization procedure, substantial repeated structural analyses are needed to determine the desired moments. In this dissertation, the random response is approximated by the PCE, and the time of the repeated analyses is largely reduced. Even so, in cases where the convergence rate is slow, the number of moment evaluations will be increased, and the computational burden is somehow heavy. To this end, decoupling the moment evaluations from the optimization procedure would be useful to accelerate the entire optimization process.

For the sake of decoupling the moment evaluations from the optimization procedure, the locally exponential approximation is also applied to establish the relation between

the moments and the design variables. To determine the corresponding coefficients efficiently, we propose a PCE based moment sensitivity analysis with respect to the design variables, which is capable to provide the coefficients within one moment evaluation procedure. This method is still developed based on assumptions of random design variables. If deterministic design variables are involved, such a limitation can be removed by applying the auxiliary distribution method, the concept of which is consistent with the one mentioned above for the reliability sensitivity analysis.

In conclusion therefore, the final target of this chapter is to decouple UA (both the reliability analysis and the moment evaluation are included) from the design optimization. Numerical examples demonstrate that the developed sequential RBRDO is computationally affordable and reasonably accurate.

4.2 Approximation of probabilistic constraints

In respect that the decoupling concepts for the design objective robustness (i.e. the concerned moment evaluations) and the design feasibility robustness (i.e. the required reliability analysis) are identical, all details will be specified in the context of the approximating probabilistic constraints.

4.2.1 Local optimization

Basically speaking, construction of the equivalent constraint is to find an approximate probability of failure as an explicit function of the design variables, i.e. the original one $P_F(\mathbf{d})$ (i.e. $P_F(\mathbf{d}, \boldsymbol{\Theta})$, in which the uncertainty vector $\boldsymbol{\Theta}$ is omitted for simplicity) is replaced by $\bar{P}_F(\mathbf{d})$,

$$P_F(\mathbf{d}) \approx \bar{P}_F(\mathbf{d}), \quad \mathbf{d} \in \mathbb{R}^{N_d}. \tag{4.1}$$

The approximation in the last equation is a global and ideal approximation. Generally, such an approximation is not feasible, as the relation between the probability of failure and the design variables can be very complicated, and it is not an easy task to find a properly surrogate function. The most probable explanation is that significant discontinuities in probability of failure arise due to changes in curvature of the limit state surface

with design changes [158]. In this sense, it might be much more tractable to construct a local approximation around a current optimal design $\mathbf{d}^k$, say

$$P_F(\mathbf{d}) \approx \bar{P}_F(\mathbf{d}, \mathbf{d}^k), \quad \mathbf{d} \in \bar{\mathbb{R}}_k^{N_d}, \quad \bar{\mathbb{R}}_k^{N_d} \subset \mathbb{R}^{N_d}, \tag{4.2}$$

where $\bar{\mathbb{R}}_k^{N_d}$ is a neighborhood of the design $\mathbf{d}^k$ and is also a subdomain of the entire design domain $\mathbb{R}^{N_d}$. This approximation is used to produce an improved design that makes the current probability of failure approach the target. After some repeated sub-sequential-procedures (see 2.4.1.3), it is possible to find a local optimum of the original RBRDO problem.

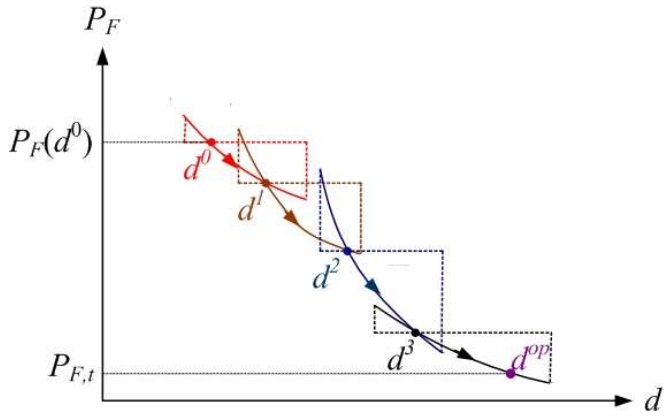

FIGURE 4.1: Sequential procedure for a local optimum search. d is the design variable, $P_F(d^0)$ and $P_{F,t}$ are initial and target probability of failure, respectively.

For a better understanding, the whole procedure is illustrated by a one-dimensional problem schematically shown in Fig. 4.1. In this figure, each solid line depicted by distinguished color represents an approximate relation between the probability of failure and the design variables that are in the neighborhood of d^k, $k = 0, 1, 2, 3$ (assume that the local optimum is found in the neighborhood of d^3). The associated colored dash line describes the bound (or the neighborhood) of the design variable. Most often, in each sub-sequential-optimization problem, the relation is not exactly the same, which implies there needs to reconstruct the relation for each sub-problem, schematically shown by the solid lines with different colors.

In Fig. 4.1, it is not difficult to image that such approximations may be more accurate in a relatively small subdomain. Actually, the accuracy of the original optimization problem depends on selections of this subdomain.

4.2.2 Exponential representation

As stated in the very beginning of this chapter, the probability of failure can be reasonably represented as an explicitly exponential function of the design variables around a current design $\mathbf{d}^k$, i.e.

$$P_F(\mathbf{d}) \approx \bar{P}_F(\mathbf{d}, \mathbf{d}^k) = \mathbf{e}^{a_0 + \sum_{i=1}^{N_d} a_i (d_i - d_i^k)}, \quad \mathbf{d} \in \bar{\mathbb{R}}_k^{N_d}, \quad \bar{\mathbb{R}}_k^{N_d} \subset \mathbb{R}^{N_d}, \tag{4.3}$$

where $a_i : i = 0, 1, \ldots, N_d$ denote the constant coefficients. It is evident that the original optimization problem is converted into an approximate one by replacing the probabilistic constraint as the equivalently deterministic constraint. In the same manner, approximations for the mean and standard deviation of the objective function can also be approximated locally as

$$\mu_f(\mathbf{d}) \approx \bar{\mu}_f(\mathbf{d}, \mathbf{d}^k) = \mathbf{e}^{b_0 + \sum_{i=1}^{N_d} b_i (d_i - d_i^k)}, \quad \mathbf{d} \in \bar{\mathbb{R}}_k^{N_d}, \quad \bar{\mathbb{R}}_k^{N_d} \subset \mathbb{R}^{N_d}, \tag{4.4}$$

$$\sigma_f(\mathbf{d}) \approx \bar{\sigma}_f(\mathbf{d}, \mathbf{d}^k) = \mathbf{e}^{c_0 + \sum_{i=1}^{N_d} c_i (d_i - d_i^k)}, \quad \mathbf{d} \in \bar{\mathbb{R}}_k^{N_d}, \quad \bar{\mathbb{R}}_k^{N_d} \subset \mathbb{R}^{N_d}. \tag{4.5}$$

The RBRDO problem described in Eq. (2.65) is then approximated by the local optimization problem as

$$\begin{aligned} \text{find} \quad & \mathbf{d} \\ \text{minimize} \quad & f(\mathbf{d}, \boldsymbol{\Theta}) = w_1 \frac{\bar{\mu}_f(\mathbf{d}, \mathbf{d}^k)}{\mu^*} + w_2 \frac{\bar{\sigma}_f(\mathbf{d}, \mathbf{d}^k)}{\sigma^*} \\ \text{subject to} \quad & \bar{P}_F(\mathbf{d}, \mathbf{d}^k) - P_{F_{t,i}} \leq 0, \ i = 1, 2, \ldots, N_g \\ & \mathbf{d}^{\mathrm{L}} \leq \mathbf{d} \leq \mathbf{d}^{\mathrm{U}}, \end{aligned} \tag{4.6}$$

where $\bar{P}_F(\mathbf{d}, \mathbf{d}^k)$, $\bar{\mu}_f(\mathbf{d}, \mathbf{d}^k)$ and $\bar{\sigma}_f(\mathbf{d}, \mathbf{d}^k)$ are the local exponential approximations for the probability of failure, the mean and standard deviation of the objective function depicted by Eq. (4.3) to Eq. (4.5) respectively.

Two important issues of this approximate problem must be considered. One is the convergence and the other is the coefficient evaluation. The former is related to the selection of the bounds of the design variables, in which the local approximation is valid, while the latter concerns how to determine the coefficients efficiently. We will discuss them in sequence.

4.2.3 Adaptive bounds

The practical implementation of the local approximation requires the selection of appropriate neighborhood $\bar{\mathbb{R}}_k^{N_d}$ or the bound $\mathbf{d}^{\mathrm{L}}$ and $\mathbf{d}^{\mathrm{R}}$. If the approximation is relatively accurate, large bounds can be chosen. In contrast, it would be better to choose small ones. A possible selection proposed in [153] is described as follows

$$\bar{\mathbb{R}}_k^{N_d} = \{\mathbf{d} : d_i \in [(1-\delta_i)d_i^k, (1+\delta_i)d_i^k],\ i = 1, \ldots, N_d\}, \quad \bar{\mathbb{R}}_k^{N_d} \subset \mathbb{R}^{N_d}, \tag{4.7}$$

where $\delta_i,\ i = 1, \ldots, N_d$ control the size of the subdomain, within a typical range $[10\%, 50\%]$ [153]. This bound definition can be treated as an adaptive bound since it is changed with the current design variables.

From the point of the worst case, it can be expected that for some special problems the probability of failure will achieve the maximum and minimum corresponding to $\mathbf{d} = [(1-\delta_1)d_1^k, \ldots, (1-\delta_{N_d})d_{N_d}^k]^{\mathrm{T}}$ and $\mathbf{d} = [(1+\delta_1)d_1^k, \ldots, (1+\delta_{N_d})d_{N_d}^k]^{\mathrm{T}}$ respectively. This means the larger the design variables are, the smaller the associated probability of failure is. A typical example is the cross section design of a beam in the context of sizing optimization problems. It can be expected that the larger the cross section, the safer the beam is. In this case, to accelerate the optimization process the asymmetric bound would be a more appropriate choice, i.e.

$$\bar{\mathbb{R}}_k^{N_d} = \{\mathbf{d} : d_i \in [(1-\delta_i^{\mathrm{L}})d_i^k, (1+\delta_i^{\mathrm{R}})d_i^k],\ i = 1, \ldots, N_d\}, \quad \delta_i^{\mathrm{L}} \leq \delta_i^{\mathrm{R}}, \quad \bar{\mathbb{R}}_k^{N_d} \subset \mathbb{R}^{N_d}, \tag{4.8}$$

where δ_i^L and δ_i^R control the left and right bound of the local problem respectively. The side constraint is given by $\mathbf{d}^{\mathrm{L}} = \{\mathbf{d} : d_i = (1-\delta_i^{\mathrm{L}})d_i^k,\ i = 1, \ldots, N_d\}$ and $\mathbf{d}^{\mathrm{U}} = \{\mathbf{d} : d_i = (1+\delta_i^{\mathrm{R}})d_i^k,\ i = 1, \ldots, N_d\}$.

Be aware that no matter what approximation is exploited, higher accuracy can be captured in a relatively small bound. Unfortunately, small bound signifies the relatively slow convergence rate. To overcome this problem, the start point is usually in the failure domain, which approaches the regions with the probabilities of failure not very far from the desired one. In fact, different start points may lead to different local optimum. However, these properties do not impose a serious limitation, as usual engineering criteria and the knowledge on the problem at hand provide guidelines for judging the quality of the optimum [154].

There exists another problem that is needed to be noted. When determining the right bound, zero probability of failure should be averted. The reason is that zero probability will result in ill approximation during the process of coefficient evaluations. Hence, the right bound controlling coefficient δ_i^{R} should be chosen with caution. It can be imagined that when the probability of failure corresponding to the current design is close to the target one (especially the target one is small, e.g. 10^{-4}), the large value of δ_i^{R} may lead to zero probability of failure. According to the simulation investigations, the recommended range of controlling coefficients are defined as

$$0 < \delta_i^{\mathrm{L}} \leq \delta_i^{\mathrm{R}} \leq 10\%. \tag{4.9}$$

4.2.4 Coefficient evaluation and sensitivity analysis

4.2.4.1 Least square method

To determine the coefficients in Eq. (4.3) - Eq. (4.5), one may refer to the LSM, in which the probabilities of failure or moments are usually calculated at a grid of points (see Fig. 4.2). Selections like this can cover the probability information in the associated subdomain as far as possible. The number of experimental points is about $2N_d$ or $3N_d$ to obtain relatively accurate results.

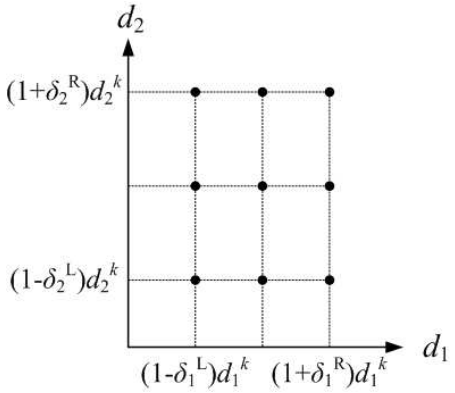

FIGURE 4.2: Principles of selection of experimental points in LSM. d_1 bounded in $[(1-\delta_1^{\mathrm{L}}),(1+\delta_1^{\mathrm{R}})]$, and d_2 bounded in $[(1-\delta_2^{\mathrm{L}}),(1+\delta_2^{\mathrm{R}})]$ are the two design variables. The "•" represents the experimental point.

However, the main drawback of this method is the low efficiency caused by the large dimension of the design variables. To overcome this, we propose the (auxiliary distribution based) reliability sensitivity analysis method and the PCE based moment sensitivity

analysis method so that the associated coefficients will be estimated in one reliability analysis and one moment evaluation procedure respectively.

4.2.4.2 Reliability sensitivity analysis

From Eq. (4.3), the coefficients can be calculated by the information on the reliability analysis and the associated sensitivity analysis, i.e.

$$a_0 = \ln(P_F(\mathbf{d}^k)), \tag{4.10}$$

$$a_i = \frac{1}{P_F(\mathbf{d}^k)} \frac{\partial P_F(\mathbf{d})}{\partial d_i}\bigg|_{\mathbf{d}=\mathbf{d}^k}, \quad i = 1, \ldots, N_d. \tag{4.11}$$

In the last two expressions, the main challenge is to determine the derivatives of the probability with respect to the design variables. Consider the definition of the probability of failure described in Eq. (2.27), i.e.

$$P_F = P(F) = \int_F q(\mathbf{\Theta}) d\mathbf{\Theta}. \tag{4.12}$$

where F represents the failure region and the $q(\mathbf{\Theta})$ is the joint PDF. If the design variables $\mathbf{d}$ are assumed as the distribution parameters of the design random variables $\mathbf{\Theta}$, the associated sensitivity of P_F with respect to the ith design variable can be formulated:

$$\frac{\partial P_F}{\partial d_i} = \int_F \frac{\partial q(\mathbf{\Theta})}{\partial d_i} d\mathbf{\Theta}, \tag{4.13}$$

The last equation can be represented by an expectation function,

$$\frac{\partial P_F}{\partial d_i} = \int_F \frac{P_F \partial q(\mathbf{\Theta})}{q(\mathbf{\Theta}) \partial d_i} \left(\frac{q(\mathbf{\Theta})}{P_F} d\mathbf{\Theta} \right) = E\left[\frac{P_F \partial q(\mathbf{\Theta})}{q(\mathbf{\Theta}) \partial d_i} \right]_F, \tag{4.14}$$

in which $q(\mathbf{\Theta})/P_F$ is the reconstructed sampling density in the domain F and $E[\cdot]_F$ is the expectation or average supported in F and zero elsewhere. In this dissertation, the distribution parameter is confined to the mean values. Accordingly, the sensitivity determination is actually connected with the derivatives of the probability of failure with respect to the mean value, i.e. $\partial P_F/\partial d_i = \partial P_F/\partial \mu_i$. Based on Eq. (4.14), the normalized mean sensitivity is described as

$$S_{\mu_i} = \frac{\partial P_F / P_F}{\partial \mu_i / \sigma_i}, \tag{4.15}$$

where $\mu_i = d_i$ and σ_i are the mean and standard deviation of the random variable Θ_i. For independent variables, the joint PDF of $\boldsymbol{\Theta}$ is a product of the PDF of Θ_i. Substituting Eq. (4.14) into Eq. (4.15), we have

$$\begin{aligned} S_{\mu_i} &= E\left[\frac{\sigma_i \partial q(\boldsymbol{\Theta})}{q(\boldsymbol{\Theta})\partial \mu_i}\right]_F \\ &= E\left[\frac{\sigma_i}{q(\boldsymbol{\Theta})}\frac{\partial q_i(\Theta_i)}{\partial \mu_i}\frac{q(\boldsymbol{\Theta})}{q_i(\Theta_i)}\right]_F \\ &= E\left[\frac{\sigma_i}{q_i(\Theta_i)}\frac{\partial q_i(\Theta_i)}{\partial \mu_i}\right]_F . \end{aligned} \tag{4.16}$$

In the same manner, if Θ_i is assumed to be normally distributed, the normalized mean sensitivity in the standard normal space can be simplified to [156]

$$S_{\mu_{\xi_i}} = \frac{\partial P_F/P_F}{\partial \mu_{\xi_i}/\sigma_{\xi_i}} = E[\xi_i]_F, \tag{4.17}$$

in which μ_{ξ_i} and σ_{ξ_i} are the calculated mean value and standard deviation of the standard normal variable ξ_i, not exactly the nominal values 1 and 0. According to chain rule,

$$S_{\mu_i} = \frac{\partial P_F/P_F}{\partial \mu_i/\sigma_i} = (\frac{\partial P_F/P_F}{\partial \mu_{\xi_i}/\sigma_{\xi_i}})(\frac{\partial \mu_{\xi_i}/\partial \mu_i}{\sigma_{\xi_i}/\sigma_i}) = S_{\mu_{\xi_i}}(\frac{\partial \mu_{\xi_i}/\partial \mu_i}{1/\sigma_i}), \tag{4.18}$$

the originally normalized sensitivity is in the presence of the one in the standard normal space. When Θ_i is a normal random variable, based on the transformation

$$\xi_i = \frac{\Theta_i - \mu_i}{\sigma_i}, \tag{4.19}$$

the derivative is found, i.e. $\partial \mu_{\xi_i}/\partial \mu_i = 1/\sigma_i$, we get

$$S_{\mu_i} = S_{\mu_{\xi_i}} = E[\xi_i]_F = \frac{1}{N_F}\sum_{j=1}^{N_F}\frac{\Theta_i^{(j)} - \mu_i}{\sigma_i}, \tag{4.20}$$

where N_F is the number of samples in the failure region F. At last, the mean sensitivity is written as

$$\frac{\partial P_F}{\partial \mu_i} = \frac{P_F}{\sigma_i}S_{\mu_i} = \frac{P_F}{\sigma_i}E[\xi_i]_F. \tag{4.21}$$

Eq. (4.21) can be realized by direct MCS or the importance sampling method. In this context, direct MCS is applied. Note that Eq. (4.21) is obtained under the assumption that all the random variables are independently normally distributed. In other cases, the transformation methods introduced in Section 2.3.2 are required to re-deduce the

Eq. (4.17) to Eq. (4.21). Substituting Eq. (4.21) into Eq. (4.11), the coefficients are calculated by

$$a_i = \frac{1}{\sigma_i} E[\xi_i]_F, \quad i = 1, \ldots, N_d. \tag{4.22}$$

Pay attention that the expectation $E[\xi_i]_F$ is obtained in the failure region F at the design variables $\boldsymbol{\mu} = \boldsymbol{\mu}_k$ (i.e. $\mathbf{d} = \mathbf{d}^k$).

Apart from the random design variables (i.e. the associated distribution parameters), they also can be deterministic. However, the aforementioned sensitivity method is not proper since it concentrates on the former type of the design variables. Under this circumstance, we develop the auxiliary method to make this method available.

Generally, the deterministic design variables are assumed as random variables following some probabilistic distribution. For simplicity, normal distribution is preferred. It is not difficult to deduce that the larger the scatter of the design variable, the larger the probability of failure is. To this end, the variance of the auxiliary distribution should not be large. On the other hand, the value is not supposed to be very small to avoid inaccuracy of the sensitivity (see Eq. (4.21)). Based on the simulation investigations, the recommended scope depending on the value of the probability of failure is given by

$$P_{F,t} \leq \sigma_i \leq 10 P_{F,t}, \tag{4.23}$$

where $P_{F,t}$ is relatively small, e.g. $P_{F,t} = 1 \times 10^{-5}$. If the target probability of failure is relatively large, e.g. $P_{F,t} = 1 \times 10^{-1}$, the proposed standard deviation is

$$\sigma_i = 0.001 \mu_i. \tag{4.24}$$

4.2.4.3 Moment sensitivity analysis

Analogically, the coefficients in Eq. (4.4) and Eq. (4.5) can be also obtained by the derivatives with respect to the design variables, as is done in Eq. (4.10) and Eq.(4.11), i.e.

$$b_0 = \ln(\mu_f(\mathbf{d}^k)), \tag{4.25}$$

$$b_i = \frac{1}{\mu_f(\mathbf{d}^k)} \frac{\partial \mu_f(\mathbf{d})}{\partial d_i}\bigg|_{\mathbf{d}=\mathbf{d}^k}, \quad i = 1, \ldots, N_d, \tag{4.26}$$

and

$$c_0 = \ln(\sigma_f(\mathbf{d}^k)) \tag{4.27}$$

$$c_i = \frac{1}{\sigma_f(\mathbf{d}^k)} \frac{\partial \sigma_f(\mathbf{d})}{\partial d_i}\bigg|_{\mathbf{d}=\mathbf{d}^k}, \quad i = 1, \ldots, N_d. \tag{4.28}$$

In the context of RBRDO, the objective function is always the function of the random response, the variability of which needs to be reduced. Accordingly, moment evaluations and the associated sensitivities for the objective function is equivalent to those for the random response. For simplicity, only one random response $x(\mathbf{d}^k)$ of interest is involved in the objective function $f(\mathbf{d})$, i.e. $f(\mathbf{d}) = x(\mathbf{d})$, $\mu_f(\mathbf{d}) = \mu_x(\mathbf{d})$ and $\sigma_f(\mathbf{d}) = \sigma_x(\mathbf{d})$. Then the last four equations can be rewritten as

$$b_0 = \ln(\mu_x(\mathbf{d}^k)), \tag{4.29}$$

$$b_i = \frac{1}{\mu_x(\mathbf{d}^k)} \frac{\partial \mu_x(\mathbf{d})}{\partial d_i}\bigg|_{\mathbf{d}=\mathbf{d}^k}, \quad i = 1, \ldots, N_d, \tag{4.30}$$

and

$$c_0 = \ln(\sigma_x(\mathbf{d}^k)) \tag{4.31}$$

$$c_i = \frac{1}{\sigma_x(\mathbf{d}^k)} \frac{\partial \sigma_x(\mathbf{d})}{\partial d_i}\bigg|_{\mathbf{d}=\mathbf{d}^k}, \quad i = 1, \ldots, N_d. \tag{4.32}$$

Apparently, the original problem is converted to calculating the moments of the random response and the associated derivatives related to the design variables. The design variables $\mathbf{d}$ are seen as the mean values of the random design variables $\boldsymbol{\Theta}$, i.e. $d_i = \mu_i$. For convenience, we denote the random response as $x(\mathbf{d}) = x(\boldsymbol{\Theta})$. Consider the definition of the moments in Eq. (2.28) and Eq. (2.29), that is

$$\mu_x = \int_{\mathbb{R}^N} x(\boldsymbol{\Theta}) q(\boldsymbol{\Theta}) d\boldsymbol{\Theta}. \tag{4.33}$$

$$V_x = \sigma_x^2 = \int_{\mathbb{R}^N} (x(\boldsymbol{\Theta}) - \mu_x)^2 q(\boldsymbol{\Theta}) d\boldsymbol{\Theta}, \tag{4.34}$$

where V_x is the variance, and $q(\boldsymbol{\Theta})$ is the joint PDF.

In order to improve efficiency of moment evaluations, the PCE based MCS is applied. That implies the random response is approximated by the PCE, which is exactly the

function of the corresponding independent standard normal variables $\boldsymbol{\xi}$, i.e.

$$\mu_x = \int_{\mathbb{R}^N} x(\boldsymbol{\xi}) Q(\boldsymbol{\xi}) d\boldsymbol{\xi}, \tag{4.35}$$

$$V_x = \sigma_x^2 = \int_{\mathbb{R}^N} (x(\boldsymbol{\xi}) - \mu_x)^2 Q(\boldsymbol{\xi}) d\boldsymbol{\xi}, \tag{4.36}$$

where $Q(\boldsymbol{\xi})$ is the joint PDF for standard normal variables. If Θ_i is normally distributed, based on the transformation described in Eq. (4.19), we can get the derivatives as follows

$$\frac{\partial \Theta_i}{\partial \mu_i} = 1, \qquad \frac{\partial \Theta_i}{\partial \xi_i} = \sigma_i. \tag{4.37}$$

Then the sensitivities can be obtained by the chain rule, say

$$\frac{\partial \mu_x}{\partial d_i} = \frac{\partial \mu_x}{\partial \mu_i} = \frac{\partial \mu_x}{\partial \Theta_i}\frac{\partial \Theta_i}{\partial \mu_i} = \frac{\partial \mu_x}{\partial \Theta_i} = \frac{\partial \mu_x}{\partial \xi_i}\frac{\partial \xi_i}{\partial \Theta_i} = \frac{1}{\sigma_i}\frac{\partial \mu_x}{\partial \xi_i}, \tag{4.38}$$

$$\frac{\partial \sigma_x}{\partial d_i} = \frac{\partial \sigma_x}{\partial \mu_i} = \frac{\partial \sigma_x}{\partial \Theta_i}\frac{\partial \Theta_i}{\partial \mu_i} = \frac{\partial \sigma_x}{\partial \Theta_i} = \frac{\partial \sigma_x}{\partial \xi_i}\frac{\partial \xi_i}{\partial \Theta_i} = \frac{1}{\sigma_i}\frac{\partial \sigma_x}{\partial \xi_i}. \tag{4.39}$$

From Eq.(4.35), we can get $\partial \mu_x / \partial \xi_i$ readily, i.e.

$$\frac{\partial \mu_x}{\partial \xi_i} = \int_{\mathbb{R}^N} \frac{\partial x(\boldsymbol{\xi})}{\partial \xi_i} Q(\boldsymbol{\xi}) d\boldsymbol{\xi} + \int_{\mathbb{R}^N} x(\boldsymbol{\xi}) \frac{\partial Q(\boldsymbol{\xi})}{\partial \xi_i} d\boldsymbol{\xi}. \tag{4.40}$$

In respect that $\boldsymbol{\xi}$ consists of independent standard normal variables, the joint PDF is then represented by $Q(\boldsymbol{\xi}) = \phi(\xi_1) \cdots \phi(\xi_N)$. Accordingly, the associated derivative is given by

$$\frac{\partial Q(\boldsymbol{\xi})}{\partial \xi_i} = -\xi_i Q(\boldsymbol{\xi}). \tag{4.41}$$

Substituting Eq. (4.41) into Eq. (4.40), the original derivative can be approximated by the associated Monte-Carlo estimator as

$$\frac{\partial \mu_x}{\partial \xi_i} \approx E[\frac{\partial x(\boldsymbol{\xi})}{\partial \xi_i}] - E[x(\boldsymbol{\xi})\xi_i], \tag{4.42}$$

where $E[\cdot]$ is the expectation of average defined in the sampling space but the nominal mean. For example, the average of a standard normal variable ξ is $E[\xi] = \sum_{j=1}^{N_{\text{mc}}} \xi^{(j)} / N_{\text{mc}}$ but zero, in which N_{mc} is the number of samples. The coefficient b_i is given by

$$b_i = \frac{1}{\mu_x(\mathbf{d}^k)\sigma_i}(E[\frac{\partial x(\boldsymbol{\xi})}{\partial \xi_i}] - E[x(\boldsymbol{\xi})\xi_i]), \quad i = 1, \ldots, N_d. \tag{4.43}$$

Note that the average is estimated at $\boldsymbol{\mu} = \boldsymbol{\mu}_k$ (i.e. $\mathbf{d} = \mathbf{d}^k$). Since the random response

is represented by the PCE, the derivative in the last equation is easily attained. Taking the static response (see Eq. (3.7)) as example, the derivative is written as

$$\frac{\partial S}{\partial \xi_i} = \sum_{i=0}^{P-1} S_i \frac{\partial \Psi_i(\boldsymbol{\xi})}{\partial \xi_i}. \tag{4.44}$$

All the information needed in this derivative estimation can be found in the PCE model of the random response. In the same manner, we will give the expression of the coefficient c_i concerned with the standard deviation of the random response. From Eq. (4.36), two relations are obtained, i.e.

$$\frac{\partial \sigma_x}{\partial \xi_i} = \frac{1}{2\sigma_x} \frac{\partial V_x}{\partial \xi_i}, \tag{4.45}$$

and

$$\begin{aligned} \frac{\partial V_x}{\partial \xi_i} = &+ \int_{\mathbb{R}_N} 2x(\boldsymbol{\xi}) \frac{\partial x(\boldsymbol{\xi})}{\partial \xi_i} Q(\boldsymbol{\xi}) d\boldsymbol{\xi} \\ &- \int_{\mathbb{R}_N} x^2(\boldsymbol{\xi}) \xi_i Q(\boldsymbol{\xi}) d\boldsymbol{\xi} \\ &- 2\mu_x \int_{\mathbb{R}_N} \frac{\partial x(\boldsymbol{\xi})}{\partial \xi_i} Q(\boldsymbol{\xi}) d\boldsymbol{\xi} \\ &+ 2\mu_x \int_{\mathbb{R}_N} x(\boldsymbol{\xi}) \xi_i Q(\boldsymbol{\xi}) d\boldsymbol{\xi} \\ &- \mu_x^2 \int_{\mathbb{R}_N} \xi_i Q(\boldsymbol{\xi}) d\boldsymbol{\xi}. \end{aligned} \tag{4.46}$$

Substituting Eq. (4.39) and Eq. (4.45) into Eq. (4.32), the coefficient c_i is finally obtained as

$$c_i = \frac{1}{2\sigma_x^2(\mathbf{d}^k)\sigma_i} \frac{\partial V_x}{\partial \xi_i}\bigg|_{\mathbf{d}=\mathbf{d}^k}, \quad i = 1, \ldots, N_d, \tag{4.47}$$

where $\partial V_x / \partial \xi_i$ is rewritten in the form of the average as

$$\begin{aligned} \frac{\partial V_x}{\partial \xi_i}\bigg|_{\mathbf{d}=\mathbf{d}^k} \approx &+ 2E[x(\boldsymbol{\xi}) \frac{\partial x(\boldsymbol{\xi})}{\partial \xi_i}] \\ &- E[x^2(\boldsymbol{\xi}) \xi_i] \\ &- 2\mu_x(\mathbf{d}^k) E[\frac{\partial x(\boldsymbol{\xi})}{\partial \xi_i}] \\ &+ 2\mu_x(\mathbf{d}^k) E[x(\boldsymbol{\xi}) \xi_i] \\ &- \mu_x^2(\mathbf{d}^k) E[\xi_i]. \end{aligned} \tag{4.48}$$

In this equation, all the definitions are consistent with Eq. (4.42) and Eq. (4.43).

Pay attention that the coefficient expressions (see Eq. (4.43) and Eq. (4.48)) are obtained based on the assumption that only random design variables are considered. In cases where deterministic design variables are involved, such coefficient evaluations cannot be used. However, as is done in Section 4.2.4.2, the auxiliary distribution method can be applied. The associated principles are identical with Section 4.2.4.2.

For clarity and convenience, we summarize the sensitivity based sequential strategy as follows:

1. Construct the approximate RBRDO formulation with use of the locally exponential approximation, as

$$\begin{aligned} \text{find} \quad & \mathbf{d} \\ \text{minimize} \quad & f(\mathbf{d},\boldsymbol{\Theta}) = w_1 \frac{\bar{\mu}_f(\mathbf{d},\mathbf{d}^k)}{\mu^*} + w_2 \frac{\bar{\sigma}_f(\mathbf{d},\mathbf{d}^k)}{\sigma^*} \\ \text{subject to} \quad & \bar{P}_F(\mathbf{d},\mathbf{d}^k) - P_{F_{t,i}} \leq 0, \ i = 1,2,\ldots,N_g \\ & \mathbf{d}^{\mathrm{L}} \leq \mathbf{d} \leq \mathbf{d}^{\mathrm{U}}, \end{aligned}$$

   where

$$\begin{aligned} P_F(\mathbf{d}) \approx \bar{P}_F(\mathbf{d},\mathbf{d}^k) &= \mathbf{e}^{a_0+\sum_{i=1}^{N_d} a_i(d_i-d_i^k)}, \quad \mathbf{d} \in \bar{\mathbb{R}}_k^{N_d}, \quad \bar{\mathbb{R}}_k^{N_d} \subset \mathbb{R}^{N_d}, \\ \mu_f(\mathbf{d}) \approx \bar{\mu}_f(\mathbf{d},\mathbf{d}^k) &= \mathbf{e}^{b_0+\sum_{i=1}^{N_d} b_i(d_i-d_i^k)}, \quad \mathbf{d} \in \bar{\mathbb{R}}_k^{N_d}, \quad \bar{\mathbb{R}}_k^{N_d} \subset \mathbb{R}^{N_d}, \\ \sigma_f(\mathbf{d}) \approx \bar{\sigma}_f(\mathbf{d},\mathbf{d}^k) &= \mathbf{e}^{c_0+\sum_{i=1}^{N_d} c_i(d_i-d_i^k)}, \quad \mathbf{d} \in \bar{\mathbb{R}}_k^{N_d}, \quad \bar{\mathbb{R}}_k^{N_d} \subset \mathbb{R}^{N_d}. \end{aligned}$$

2. Determine the associated coefficients with reliability analysis and moment evaluations, and the associated sensitivities, i.e.

$$\begin{aligned} a_0 &= \ln(P_F(\mathbf{d}^k)), \\ a_i &= \frac{1}{P_F(\mathbf{d}^k)} \frac{\partial P_F(\mathbf{d})}{\partial d_i}\bigg|_{\mathbf{d}=\mathbf{d}^k} = \frac{1}{\sigma_i} E[\xi_i]_F, \quad i = 1,\ldots,N_d, \\ b_0 &= \ln(\mu_x(\mathbf{d}^k)), \\ b_i &= \frac{1}{\mu_x(\mathbf{d}^k)} \frac{\partial \mu_x(\mathbf{d})}{\partial d_i}\bigg|_{\mathbf{d}=\mathbf{d}^k} = \frac{1}{\mu_x(\mathbf{d}^k)\sigma_i} (E[\frac{\partial x(\boldsymbol{\xi})}{\partial \xi_i}] - E[x(\boldsymbol{\xi})\xi_i]), \quad i = 1,\ldots,N_d, \\ c_0 &= \ln(\sigma_x(\mathbf{d}^k)) \\ c_i &= \frac{1}{\sigma_x(\mathbf{d}^k)} \frac{\partial \sigma_x(\mathbf{d})}{\partial d_i}\bigg|_{\mathbf{d}=\mathbf{d}^k} = \frac{1}{2\sigma_x^2(\mathbf{d}^k)\sigma_i} \frac{\partial V_x}{\partial \xi_i}\bigg|_{\mathbf{d}=\mathbf{d}^k}, \quad i = 1,\ldots,N_d, \end{aligned}$$

where $f(\mathbf{d}) = x(\mathbf{d})$, and

$$\begin{aligned}\left.\frac{\partial V_x}{\partial \xi_i}\right|_{\mathbf{d}=\mathbf{d}^k} \approx &+ 2E[x(\boldsymbol{\xi})\frac{\partial x(\boldsymbol{\xi})}{\partial \xi_i}] \\ &- E[x^2(\boldsymbol{\xi})\xi_i] \\ &- 2\mu_x(\mathbf{d}^k)E[\frac{\partial x(\boldsymbol{\xi})}{\partial \xi_i}] \\ &+ 2\mu_x(\mathbf{d}^k)E[x(\boldsymbol{\xi})\xi_i] \\ &- \mu_x^2(\mathbf{d}^k)E[\xi_i].\end{aligned}$$

4.2.5 Enhanced convergent condition

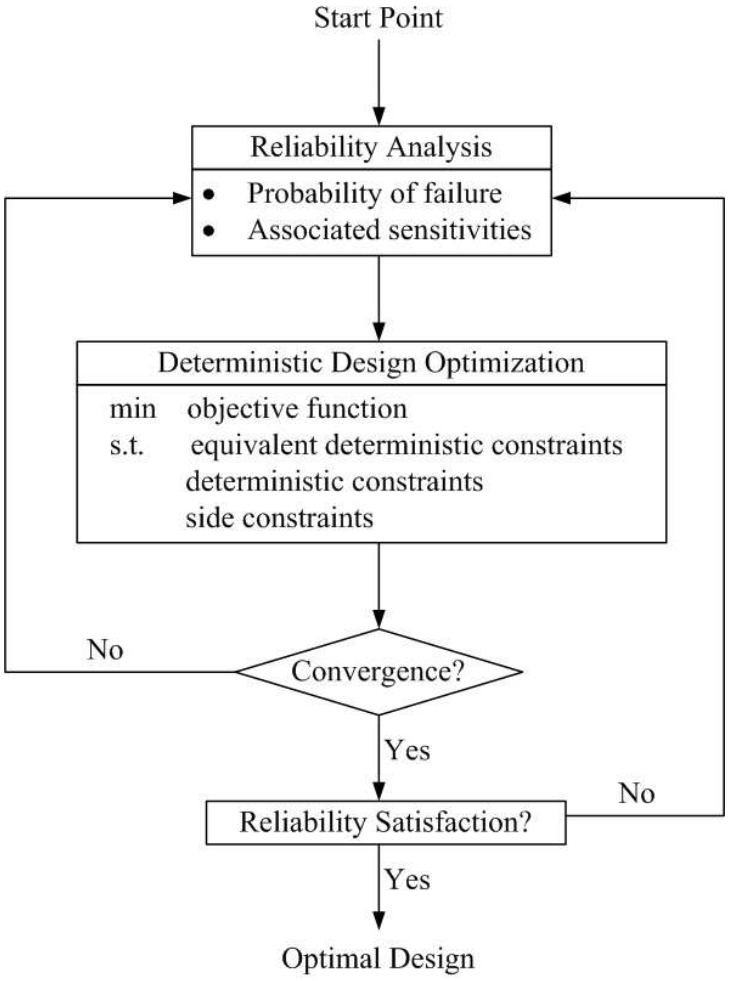

FIGURE 4.3: Sequential RBDO based on reliability sensitivity

As the equivalent deterministic constraints or the moments of the objective function are only approximated representations with respect to the design variable, the optimal designs obtained by the equivalent deterministic optimization might not satisfy the real

probabilistic constraints, even if the optimization procedure is converged. In this sense, it is necessary to execute the reliability analysis after each convergent sub-optimization procedure to check if the current design is the desired one.

The sensitivity based sequential RBDO and RBRDO are schematically depicted respectively in Fig. 4.3 and Fig. 4.4. For the former, the sequential strategy is to decouple the reliability from the optimization; while for the latter, both reliability analysis and moment evaluations are independent from the optimization.

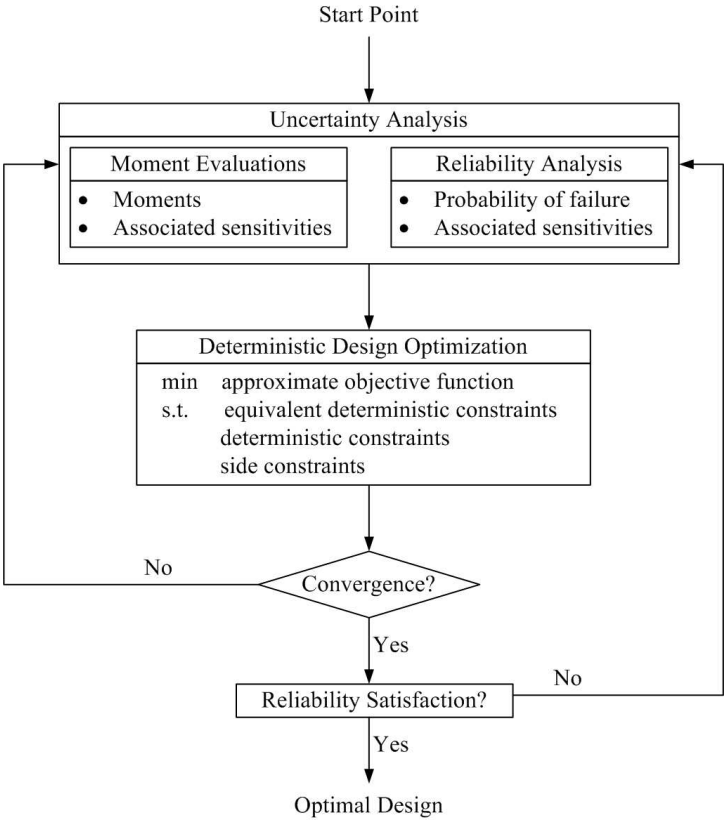

FIGURE 4.4: Sequential RBRDO based on reliability and moment sensitivity

4.3 Numerical examples

In this section, several methods have been applied to solve RBRDO or RBDO problem for comparative purposes, among which the methods in the context of MCS are mainly concerned since the main contributions in this chapter are to develop MCS based RBRDO. For clarity, these approaches are listed as follows:

- **Approach I**. PMA based nested RBDO.

- **Approach II**. MCS based nested RBDO.
- **Approach III**. MCS based sequential RBDO, in which the coefficients with respect to the probability of failure are obtained by the LSM involved in several reliability analyses.
- **Approach IV**. MCS based sequential RBDO, in which the coefficients with respect to the probability of failure are obtained by the (auxiliary distribution based) reliability sensitivity analysis within on reliability analysis.
- **Approach V**. MCS based sequential RBRDO, in which the coefficients with respect to the moments and probability of failure are obtained by the LSM involved in several moment evaluation procedures and reliability analyses, respectively.
- **Approach VI**. MCS based sequential RBRDO, in which the coefficients with respect to the moments and probability of failure are obtained by the PCE Based moment sensitivity analysis and the (auxiliary distribution based) reliability sensitivity analysis within one reliability analysis and one moment evaluation procedure, respectively.

4.3.1 Cantilever: a static RBDO

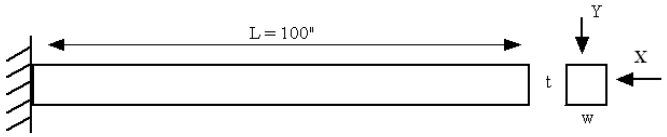

FIGURE 4.5: Cantilever beam model

In this section, the RBDO problem is studied by investigating a cantilever beam [131], which is schematically represented in Fig. 4.5. The objective is to minimize the weight characterized by the cross section under two uncertain constraints. The optimization problem is formulated as

$$\begin{aligned} \text{minimize} \quad & f(\mathbf{d}) = d_1 d_2 \\ \text{subject to} \quad & P_{F_i} = P(g_i(\mathbf{d}, \boldsymbol{\Theta}) \leq 0) \leq P_{F_{t,i}},\ i = 1, 2 \\ & (1 - \delta_i^{\mathrm{L}}) d_i^k \leq d_i \leq (1 + \delta_i^{\mathrm{R}}) d_i^k,\ i = 1, 2, \end{aligned} \tag{4.49}$$

where two deterministic design variables are $d_1 = w$ and $d_2 = t$, $P_{F_{t,i}} = 0.0013$, $\delta_i^{\mathrm{L}} = 3\%$ and $\delta_i^{\mathrm{R}} = 5\%$, and the uncertain constraints (yielding stress at the fixed end and the tip displacement) are described as

$$\begin{aligned} g_1(R, X, Y, w, t) &= R - (\frac{600}{wt^2}Y + \frac{600}{w^2t}X), \\ g_2(E, X, Y, w, t) &= D_t - \frac{4L^3}{Ewt}\sqrt{(\frac{Y}{t^2})^2 + (\frac{X}{w^2})^2}, \end{aligned} \tag{4.50}$$

in which $D_t = 2.5$ is the allowable tip displacement, the random variables are the random yield strength $Z_1 = R$, random external forces $Z_2 = X$ and $Z_3 = Y$, and random Young's modulus $\theta_1 = E$ (Note that $\mathbf{\Theta} = \{\boldsymbol{\theta}, \mathbf{Z}\}$). All the random variables are independent normal variables, i.e. $R \sim N(40000, 2000)$ psi, $X \sim N(500, 100)$ lb, $Y \sim N(1000, 100)$ lb and $E \sim N(29 \times 10^6, 1.45 \times 10^6)$psi.

To show the effectiveness of the proposed methods, this cantilever has been studied by 4 approaches, respectively, the results of which are specified sequentially:

- The optimization procedure begin with the point $w = 3,\ t = 3$. The optimal designs provided by **Approach I** are $w = 2.4460,\ t = 3.8922,\ f = 9.5052,\ P_{F_1} = 0.0013$ and $P_{F_2} = 5 \times 10^{-5}$. Obviously, the first constraint is more significant. These results are treated as the reference.

- Using **Approach II**, the start point is selected as $w = 5,\ t = 5$ (the optimization procedure is out of convergence with the start point $w = 3,\ t = 3$). The optimal designs are $w = 3.1204,\ t = 3.1204$ and $f = 9.7371$, with $P_{F_1} = 0.0012$ and $P_{F_2} = 3 \times 10^{-6}$. The active constraint is exactly the first one. It is obvious that the associated optimum is safer than the one obtained by PMA based method. The number of function evaluation (NFE) is 128 and so is the number of reliability analysis (NRA). The efficiency is mainly measured by NRA since reliability analysis is the most computationally expensive.

- The optimization procedure starts in the failure region, i.e. $w = 3,\ t = 3$. After one sub-sequential-optimization, **Approach III** converges, providing the optimum $w = 3.1068,\ t = 3.1500,\ f = 9.7863,\ P_{F_1} = 8.52 \times 10^{-4}$ and $P_{F_2} = 3 \times 10^{-6}$. The CPU time is characterized by NFE= 21 and NRA= 20. For each equivalent deterministic constraint, 9 reliability analyses are used to calculate the coefficients with respect to the exponential approximation, and one is to check if the current

optimum satisfies the constraints. This method is more efficient than **Approach II**. Moreover, the results are closer to **Approach II** than to **Approach I**, which signified the design is more security.

- In **Approach IV**, the start point is also $w = 3,\ t = 3$. The results are listed in Table 4.1. After 3 sub-sequential optimizations, the final weight is $f = 9.7044$. From Table 4.1, it is observed that the first optimization procedure is not converged (note that "$-$" represents no reliability analysis is carried out); the second optimization procedure is converged but the first probabilistic constraint is not satisfied. NRA is 10 in total for the entire optimization procedure, which demonstrates **Approach IV** is the most efficient compared with **Approach II** and **Approach III**.

TABLE 4.1: Optimum obtained by **Approach IV** for cantilever

Sub-Optimization	Design Variables		Probability of failure		NFE	NRA
	w	t	P_{F_1}	P_{F_2}		
1	3.1512	3.1292	–	–	202	2
2	3.1087	3.0353	0.0063	1.05×10^{-4}	21	4
3	3.0449	3.1871	0.0012	4.00×10^{-6}	15	4

Additionally, the deterministic design variables are assumed normally distributed with the standard deviation is $\sigma_i = 10^{-3} d_i \in [0.0013, 0.013],\ i = 1, 2$ (see Eq.(4.23)). Based on the results, it is found that the small variance assumption is proper since there is not much influence on the final optimum.

From the above comparisons, it can be concluded that **Approach III** and **Approach IV** are more robust than **Approach II**. That is because the start point in **Approach II** is uncontrollable. The used start point is selected after some simulation investigations. Although it is located in the safe region, not all points in the safe region can make the optimization converged, e.g. $w = 4,\ t = 4$. It can be deduced that if an improper start point is used, the convergence rate may be very slow or there no convergence achieves.

On the contrary, in despite that the sequential strategy only provides the local minimum, the start points and the final designs can be judged by the designers depending on the information of the problem right in hand or engineering experiences. Hence, the sequential RBDO is not only more efficient, but also more robust than the MCS based nested RBDO.

4.3.2 Plate-Beam: a dynamic RBDO

In this section, the RBDO problem for dynamic structures is studied by a plate-beam model. The deterministic design variables are the beam width $d_1 = BW$, and height $d_2 = BH$. The objective is to minimize the cross section of the beam $f = d_1 d_2$. The constraints are the probabilistic constraint $P_{F_t} = P(0.03 - |x_{14}(\boldsymbol{\theta}, \mathbf{Z}(t))| \leq 0) \leq 10^{-4}$ and the side constraint. More details can be found in Section 3.5.1.

Both **Approach III** and **Approach IV** are used to solve this RBDO problem. Because the design variables are deterministic, the auxiliary method is applied. The selected variance is $\sigma_i = 1\% d_i \in [P_{F,t}, 10P_{F,t}] = [0.0001, 0.001],\ i = 1, 2$ (see Eq. (4.23)). The controlling coefficients are chosen as $\delta_i^{\mathrm{L}} = 3\%$ and $\delta_i^{\mathrm{R}} = 5\%$.

In **Approach III**, 9 reliability analyses are required to construct the exponential approximation for each sub-sequential-optimization. Table 4.2 summarizes the results obtained by **Approach III** with start point $[0.0405, 0.0405]$. Apparently, there needs 4 sub-sequential-optimization loops and the first two equivalent deterministic optimization loops are not converged. The third sub-sequential-optimization is converged, but the probabilistic constraint is violated. In this sense, it is necessary to check the reliability after each converged sub-optimization to ensure the real convergence. Finally, the optimal design is obtained in the fourth sub-sequential-optimization.

TABLE 4.2: Optimum obtained by **Approach III** for plate-beam ($[0.0405, 0.0405]$)

Sub-Optimizatoin	Design Variables		f	P_F	NFE	NRA
	BW	BH				
0	0.0405	0.0405	0.001625	2.92×10^{-4}	–	–
1	0.0428	0.0428	0.001835	–	6	9
2	0.0451	0.0451	0.002090	–	9	9
3	0.0454	0.0437	0.001986	1.04×10^{-4}	6	10
4	0.0457	0.0445	0.002035	9.20×10^{-5}	6(30)	10(38)

While in **Approach IV**, only one reliability analysis is wanted to evaluate the coefficients. In Table 4.3, the results under the same start point obtained by **Approach IV** are listed. The entire optimization procedure is composed of 6 sub-sequential-optimization loops. Comparing those results in Table 4.2 and Table 4.3 however, **Approach IV** is more efficient than **Approach III** since only 9 reliability analyses are utilized, while the number of reliability analyses in **Approach III** is 38. And seen

from the final probabilities of failure $P_F = 9.2 \times 10^{-5}$ and $P_F = 9.4 \times 10^{-5}$ for these two approaches respectively, the optimum is close to each other as the both final cross sections approach to 0.00200.

TABLE 4.3: Optimum obtained by **Approach IV** for plate-beam ($[0.0405, 0.0405]$)

Sub-Optimizatoin	Design Variables		f	P_F	NFE	NRA
	BW	BH				
0	0.0405	0.0405	0.001625	2.92×10^{-4}	–	–
1	0.0389	0.0429	0.001690	–	9	1
2	0.0408	0.0417	0.001700	–	9	1
3	0.0413	0.0437	0.001807	2.20×10^{-4}	12	2
4	0.0434	0.0439	0.001904	1.70×10^{-4}	9	2
5	0.0417	0.0464	0.001938	–	6	1
6	0.0436	0.0450	0.001966	9.40×10^{-5}	9(54)	2(9)

Note that the selected start point is very close to the optimal design, since the initial probability of failure 2.92×10^{-4} is close to the target one 1.00×10^{-4}. There is a possibility when the start point is far away from the optimum, the convergence rate will be slower. In this situation, investigations on convergence with respect to start points $[0.02, 0.02]$ and $[0.03, 0.03]$ are carried out. The corresponding optimization procedures are specified in Table 4.4 and Table 4.5, respectively.

TABLE 4.4: Optimum obtained by **Approach IV** for plate-beam ($[0.03, 0.03]$)

Sub-Optimization	Design Variables		f	P_F	NFE	NRA
	BW	BH				
0	0.0300	0.0300	0.000900	1.76×10^{-2}	–	–
1	0.0338	0.0338	0.001140	–	18	1
2	0.0362	0.0362	0.001312	–	9	1
3	0.0385	0.0385	0.001483	–	11	1
4	0.0372	0.0406	0.001512	–	12	1
5	0.0392	0.0428	0.001672	–	21	1
6	0.0418	0.0455	0.001904	–	6	1
7	0.0406	0.0469	0.001901	1.08×10^{-4}	6	2
8	0.0407	0.0492	0.002000	9.20×10^{-5}	18(101)	2(10)

If the convergence rate of **Approach IV**is characterized by the number of sub-optimization, the comparison is shown in Figure 4.6. It is observed that the farther the start point the more sub-optimizations are required. Comparing the number of reliability analysis from Table 4.3 to Table 4.5, the more reliability analyses are derived from the start point farther from the optimum. However, the increment of reliability analysis is acceptable.

In other word, the convergence rate of **Approach IV** depends on the start point, but the latter will not arouse limited applications. It is also found that the final values of objective function under different start points are all close to 0.002. In this sense, the proposed **Approach IV** achieve the local optimization with different start point, regardless of farther one or closer one related to the optimum.

TABLE 4.5: Optimum obtained by **Approach IV** for plate-beam ($[0.02, 0.02]$)

Sub-Optimization	Design Variables		f	P_F	NFE	NRA
	BW	BH				
0	0.0200	0.0200	0.000400	3.83×10^{-1}	–	–
1	0.0282	0.0282	0.000796	–	33	1
2	0.0331	0.0331	0.001096	–	30	1
3	0.0365	0.0365	0.001328	–	9	1
4	0.0391	0.0391	0.001528	–	6	1
5	0.0414	0.0414	0.001714	–	9	1
6	0.0402	0.0416	0.001670	2.94×10^{-4}	12	2
7	0.0425	0.0439	0.001864	–	9	1
8	0.0412	0.0453	0.001868	1.28×10^{-4}	9	2
9	0.0433	0.0463	0.002000	9.20×10^{-5}	9(126)	2(12)

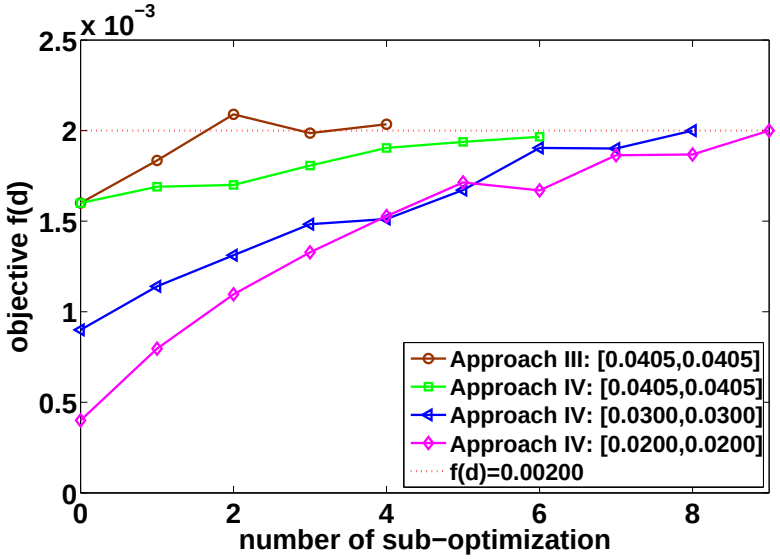

FIGURE 4.6: Convergence comparisons

Remind that in a local optimization problem, there usually exist multi local optima, which is schematically described in Figure 4.7 based on the results in Table 4.3 to Table 4.5. The multi local optima are caused by different start point. From this view, the start point has effects on the optimum, but not on the convergence denoted in the above.

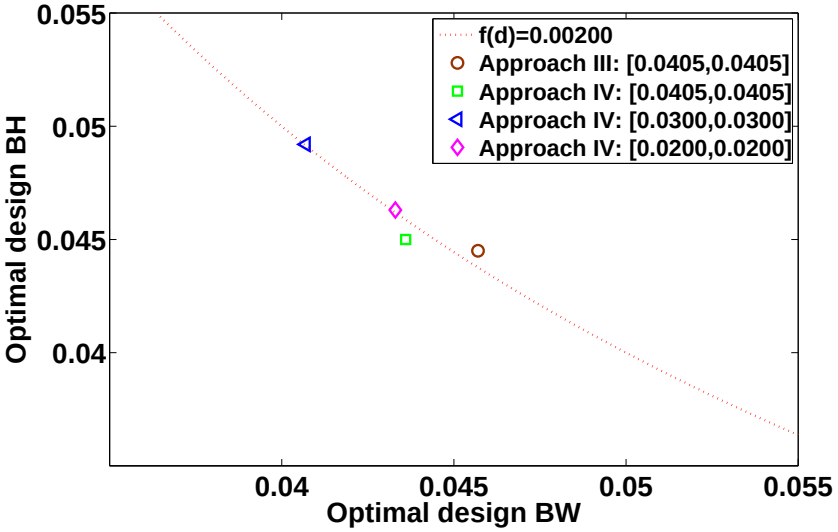

FIGURE 4.7: Multi local optima investigations

In the last two numerical examples, i.e. cantilever and plate-beam, it is observed that more sub-sequential-optimization loops trends to be executed by **Approach IV** than **Approach III**. The probable explanation is that the sensitivity reflects more information around the current design, but not the whole subdomain. Whereas, the LSM gives a global fit throughout the whole domain due to the grid selection of experimental points. In this sense, in a selected subdomain, **Approach III** can somehow supply a relatively "global" optimum than **Approach IV**.

4.3.3 Simply supported beam: a static RBRDO

This example is to study the RBRDO problem, in which both the weight (or cross section) and the maximum deformation of a simply supported beam are the objectives. Mathematically, the RBRDO problem is formulated as

$$\begin{aligned} \text{minimize} \quad & f(\mathbf{d}) = w_1 \frac{M}{M^*} + w_2 \frac{\sigma_{D_{max}}}{\sigma^*_{D_{max}}} \\ \text{subject to} \quad & P_F = P(g(\mathbf{d}, \boldsymbol{\Theta}) = R - S(\mathbf{d}, \boldsymbol{\Theta}) \leq 0) \leq 10^{-4} \\ & \mathbf{d}^{\mathrm{L}} \leq \mathbf{d} \leq \mathbf{d}^{\mathrm{U}}, \end{aligned} \tag{4.51}$$

in which w_1 and w_2 are the weight factors, $M = d_1 d_2$ is the cross section in the mean sense since d_1 and d_2 are the mean value of the width W and height H respectively, R is the allowable stress, $S(\mathbf{d}, \boldsymbol{\Theta})$ is the maximum stress in the beam, $\sigma_{D_{max}}$ is the

standard deviation of the maximum deformation D_{max} in the beam, M^* is obtained at the start point and $\sigma^*_{D_{max}}$ is calculated in the same manner for the computational purposes. Other concerns can be found in Section 3.5.3, except that the mean value of the excitation is 6500N.

Both of the deformation and the stress are obtained by FEA, which means there is no explicit relation with the design variables. Therefore, the sequential strategy is applied to decouple the standard deviation estimation and reliability analysis from the optimization procedure (see Fig. 4.4). The start point is $d_1 = 0.08,\ d_2 = 0.1$, and the weight factors are fixed as $w_1 = 0.5$ and $w_2 = 0.5$ (how to choose the weights is not the task in this work).

TABLE 4.6: Optimal results obtained by **Approach V**and **Approach VI** for beam

Methods	Design variables		M		$D_{\max}$		P_F
	d_1	d_2	μ_M	σ_M	$\mu_{D_{\max}}$	$\sigma_{D_{\max}}$	
Initial	0.0800	0.1000	0.0080	0.0012	0.0018	8.5145×10^{-4}	1.3×10^{-4}
Approach V	0.0776	0.1050	0.0081	0.0016	0.0016	7.5934×10^{-4}	7.4×10^{-5}
Approach VI	0.0776	0.1037	0.0080	0.0012	0.0016	7.8881×10^{-4}	9.2×10^{-5}

Table 4.6 shows the results by **Approach V** and **Approach VI**, in which the mean value and standard deviation are listed respectively for the weight and the maximum deformation. It is found that the optimum obtained by **Approach V** is more conservative than the one obtained by **Approach VI** since the former has a smaller final probability of failure. That is why the reduction of the variability of the deformation by **Approach VI** is less than the one of **Approach V**. Note that **Approach VI** (NRA=2) is more efficient than **Approach V** (NRA=10). From this point of view, **Approach VI** is more attractive for practical purposes.

4.4 Summary

In this chapter, the sequential formulation for RBRDO in the context of MCS is concentrated on, which is not only valuable to improve efficiency of RBRDO procedure, but also helpful to overcome the non-convergence problem encountered in MCS based nested double loop RBRDO due to the improper start point.

Different from the conventional sequential strategy, the one considered here aims to decouple both the reliability analysis and moment evaluations from the optimization procedure since the moment evaluations are usually computationally expensive.

To realize the sequential RBRDO, locally "first-order" exponential approximation around the current design is implemented to construct the equivalently deterministic objective functions and probabilistic constraints. The associated coefficients can be evaluated by the LSM. However, the efficiency is always challenged by high dimension of the design variables. In this case, advanced UA method is used to reduce the computational expense for one UA process, i.e. the PCE based MCS method. On the other hand, we develop the (auxiliary distribution based) reliability sensitivity analysis and the PCE based moment sensitivity analysis to calculate the associated coefficients such that the number of UA is reduced.

Numerical examples demonstrate that the proposed sequential RBRDO is computational efficient and reasonably accurate. Convergence investigations are studied with different start point. It turns out that the local convergence is achieved. Multi local optima are also observed due to different start point. However, these properties do not impose a serious limitation, as usual engineering criteria and the knowledge on the problem at hand provide guidelines for judging the quality of the optimum [154].

Chapter 5

Application of RBRDO on passive vibration control: optimal design of tuned mass dampers

5.1 Introduction

An important task in the field of mechanical engineering is to suppress the vibrations of dynamic structures. To this end, passive or active vibration control techniques have been developed. One of the most widely used strategies for passive vibration control is based on applications of the tuned mass damper (**TMD**). A typical TMD, consisting of a mass, a damping and a spring, is commonly attached to a protected primary structure for suppressing undesirable vibrations induced by external excitations.

Through intensive researches and developments in recent years, the TMD has been accepted as an effective vibration control device to enhance the performances of the protected structures [159–162]. For the TMD is one of the simplest and most reliable passive control devices, the study on optimal design of the TMD is still an ongoing topic. Since Den Hartog [163] first proposed an optimal design for the TMD for an undamped single DOF (SDOF) structure, many optimal design methods for the TMD have been developed to control the structural vibration under various types of excitation sources [162, 164–168]. The optimal design of the TMD is obtained by the above methods with assumptions of deterministic structural parameters. This problem is always characterized as conventional SDO (**CSDO**).

However, the assumption that uncertainties in structural systems have negligible effects on response can become unacceptable in many real situations [169]. The effectiveness of the TMD may be therefore drastically reduced [126]. It is reported that the uncertainties in structural parameters might have equal or even greater influence on response

than uncertainty in excitation [170]. Moreover, Jensen [171] indicated that different designs are attained due to the influences of parameter uncertainties. In this sense, the uncertainties must be considered.

Recently, much attention has been drawn on vibration control problems with both structural uncertainties and random excitations. The optimal design can be captured by two main approaches [172]. One from the risk point of view is RBDO [125], which aims to minimize the probability of failure with respect to the random response of the protected structure; the other is to reduce the sensitivity of the performances to the variabilities, which is achieved by RDO [172]. The optimal design by the former method concentrates on the rare events at the tails of the PDF and thereafter can confine the amplitude within some threshold, while the latter guarantees the quality. Both measurements could be very valuable in design optimization of the TMD. To our knowledge, nevertheless, there is little research work that is concerned about both properties for the TMD optimization.

Therefore, in this chapter we will focus on application of RBRDO to optimally design the TMD with consideration of structural uncertainties as well as stochastic excitations. Quite often, the objective function of RBRDO is constructed by minimizing the mean and standard deviation of the random response with respect to the protected structure simultaneously. Nonetheless, mean minimization for the TMD design can be eliminated since the response level is, in a way, limited by the threshold required in the probabilistic constraint. In this case, the original multi-objective optimization is reduced to a single-objective optimization. For completeness and comparison, CSDO and RBRDO for deterministic structures are also regarded.

5.2 CSDO

An ideal mechanical TMD system (see Fig. 5.1) is composed of a protected primary structure represented by a SDOF system with mass m_S, stiffness k_S and damping c_S, and a passive TMD with mass m_T, stiffness k_T and damping c_T. All the parameters of interest are time-invariant. In case of the TMD system excited by a base acceleration, the structural response is determined by solving the motion equations

$$\mathbf{M}\ddot{\mathbf{X}}(t) + \mathbf{C}\dot{\mathbf{X}}(t) + \mathbf{K}\mathbf{X}(t) = \mathbf{Z}(t), \tag{5.1}$$

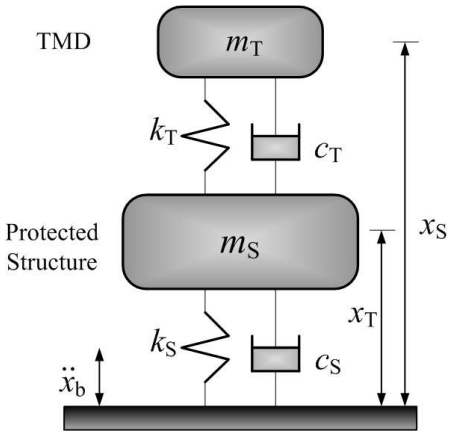

FIGURE 5.1: TMD system

where the mass matrix $\mathbf{M}$, stiffness matrix $\mathbf{C}$, damping matrix $\mathbf{K}$ and the excitation are described respectively as

$$\mathbf{M} = \begin{bmatrix} m_T & 0 \\ 0 & m_S \end{bmatrix}, \ \mathbf{C} = \begin{bmatrix} c_T & -c_T \\ -c_T & c_S + c_T \end{bmatrix}, \ \mathbf{K} = \begin{bmatrix} k_T & -k_T \\ -k_T & k_T + k_S \end{bmatrix}, \ \mathbf{Z}(t) = \ddot{x}_b(t) \begin{Bmatrix} m_T \\ m_S \end{Bmatrix}, \tag{5.2}$$

and $\mathbf{X} = [x_T, x_S]^{\mathrm{T}}$ is the displacement vector relative to the base, x_T is the relative displacement of the TMD, and x_S is concerned with the protected structure. Introducing the state space vector $\mathbf{Y}_S = [x_T, x_S, \dot{x_T}, \dot{x_S}]^{\mathrm{T}}$, the original problem is converted into the state space is

$$\dot{\mathbf{Y}}_S(t) = \mathbf{A}_S \mathbf{Y}_S(t) + \mathbf{r}_Z \ddot{x}_b(t), \tag{5.3}$$

where $\mathbf{r}_Z = [0, 0, 1, 1]^{\mathrm{T}}$, and

$$\mathbf{A}_S = \begin{bmatrix} \mathbf{0} & \mathbf{I} \\ \mathbf{H}_K & \mathbf{H}_C \end{bmatrix}, \tag{5.4}$$

$$\mathbf{H}_K = \mathbf{M}^{-1}\mathbf{K} = \begin{bmatrix} -\omega_T^2 & \omega_T^2 \\ \gamma\omega_T^2 & -(\omega_S^2 + \gamma\omega_T^2) \end{bmatrix}, \tag{5.5}$$

$$\mathbf{H}_C = \mathbf{M}^{-1}\mathbf{C} = \begin{bmatrix} -2\zeta_T\omega_T & 2\zeta_T\omega_T \\ 2\gamma\zeta_T\omega_T & -(2\zeta_S\omega_S + 2\gamma\zeta_T\omega_T) \end{bmatrix}. \tag{5.6}$$

In the last three expressions, $\mathbf{0}$ and $\mathbf{I}$ are the zero and unit matrices with dimension 2×2, and the structural parameters are defined as

$$\omega_T = \sqrt{\frac{k_T}{m_T}}, \quad \omega_S = \sqrt{\frac{k_S}{m_S}}, \quad \zeta_T = \frac{c_T}{2\sqrt{m_T k_T}}, \quad \zeta_S = \frac{c_S}{2\sqrt{m_S k_S}}, \quad \gamma = \frac{m_T}{m_S}. \tag{5.7}$$

The seismic acceleration $\ddot{x}_b(t)$ is modeled by the Kanai-Tajimi stationary stochastic process [173]. The filter is considered as an elastically suspended mass with a natural frequency ω_f and damping ratio ζ_f. The acceleration $\ddot{x}_b(t)$ is expressed as

$$\begin{aligned} &\ddot{x}_f(t) + 2\zeta_f\omega_f\dot{x}_f(t) + \omega_f^2 x_f(t) = -w(t), \\ &\ddot{x}_b(t) = \ddot{x}_f(t) + w(t) = -(2\zeta_f\omega_f\dot{x}_f(t) + \omega_f^2 x_f(t)), \end{aligned} \tag{5.8}$$

in which $w(t)$ is a stationary Gaussian zero mean white noise process whose intensity is S_0. The global state space vector is introduced as

$$\mathbf{Y} = [x_T, x_S, x_f, \dot{x}_T, \dot{x}_S, \dot{x}_f]^{\mathrm{T}}. \tag{5.9}$$

The state space covariance matrix $\mathbf{R_{YY}}$ in the stationary case is then obtained as the solution of the Lyapunov equation [174], which is represented as an algebraic matrix equation of size 6×6,

$$\mathbf{A}\mathbf{R_{YY}} + \mathbf{R_{YY}}\mathbf{A}^{\mathrm{T}} + \mathbf{B} = \mathbf{0}, \tag{5.10}$$

where

$$\mathbf{A} = \begin{bmatrix} 0 & 0 & 0 & 1 & 0 & 0 \\ 0 & 0 & 0 & 0 & 1 & 0 \\ 0 & 0 & 0 & 0 & 0 & 1 \\ -\omega_T^2 & \omega_T^2 & \omega_f^2 & -2\zeta_T\omega_T & 2\zeta_T\omega_T & 2\zeta_f\omega_f \\ \gamma\omega_T^2 & -(\omega_S^2 + \gamma\omega_T^2) & \omega_f^2 & 2\gamma\zeta_T\omega_T & -(2\zeta_S\omega_S + 2\gamma\zeta_T\omega_T) & 2\zeta_f\omega_f \\ 0 & 0 & -\omega_f^2 & 0 & 0 & -2\zeta_f\omega_f \end{bmatrix}, \tag{5.11}$$

and the matrix $\mathbf{B}$ has all null elements except for the last one on the main diagonal, $[\mathbf{B}]_{6,6} = 2\pi S_0$. In the same manner, the covariance matrix $\mathbf{R}_{\mathbf{Y}_0\mathbf{Y}_0}$ of the unprotected structure is obtained by solving the following Lyapunov equation

$$\mathbf{A}_0\mathbf{R}_{\mathbf{Y}_0\mathbf{Y}_0} + \mathbf{R}_{\mathbf{Y}_0\mathbf{Y}_0}\mathbf{A}_0^{\mathrm{T}} + \mathbf{B}_0 = \mathbf{0}, \tag{5.12}$$

where the state space vector is

$$\mathbf{Y}_0 = [x_S, x_f, \dot{x}_S, \dot{x}_f]^{\mathrm{T}}, \tag{5.13}$$

the system matrix is

$$\mathbf{A}_0 = \begin{bmatrix} 0 & 0 & 1 & 0 \\ 0 & 0 & 0 & 1 \\ -\omega_S^2 & \omega_f^2 & -2\zeta_S\omega_S & 2\zeta_f\omega_f \\ 0 & -\omega_S^2 & 0 & -2\zeta_f\omega_f \end{bmatrix}, \tag{5.14}$$

and the 4×4 matrix $\mathbf{B}_0$ has only one non-zero element as $[\mathbf{B}]_{4,4} = 2\pi S_0$.

Then we can get the root of the mean square of the displacement, σ_S and σ_S^0, associated with the protected structure and unprotected structure respectively, i.e.

$$\sigma_S = \sqrt{[\mathbf{R}_{\mathbf{YY}}]_{2,2}}, \tag{5.15}$$

$$\sigma_S^0 = \sqrt{[\mathbf{R}_{\mathbf{Y}_0\mathbf{Y}_0}]_{1,1}}. \tag{5.16}$$

The primary concept of the optimal design for the TMD is to find optimal TMD parameters to suppress the vibration as far as possible. Then the design variables are $\mathbf{d} = [m_T, k_T, \zeta_T]^{\mathrm{T}}$. Sometimes, researchers prefer to fix the mass ratio to control the mass of the TMD. In this sense, the design variables are reduced to $\mathbf{d} = [k_T, \zeta_T]^{\mathrm{T}}$.

In CSDO, the optimization problem is constructed as un unconstraint one by minimizing the mean square response $f(\mathbf{d}) = \sigma_S^2$, based on which the analytical formula for the optimal TMD parameters, also termed as the optimal frequency ratio Ω_{opt} (or the optimal frequency $\omega_{T,\text{opt}}$) and the optimal damping ratio $\zeta_{T,\text{opt}}$, are given by the following simple analytical expressions [164] by assuming $\zeta_S = 0$ as

$$\Omega_{\text{opt}} = \frac{\omega_{T,\text{opt}}}{\omega_S} = \sqrt{\frac{2-\gamma}{2(\gamma+1)^2}}, \tag{5.17}$$

$$\zeta_{T,\text{opt}} = \sqrt{\frac{\gamma(3\gamma+4)}{2(\gamma+1)(\gamma+2)}}, \tag{5.18}$$

These expressions have been found to be accurate even for non-zero, but small values of ζ_S. The optimal TMD parameters depend on the mass ratio γ only. Namely, when the system is considered to be deterministic, and is with light damping, the optimal design of the TMD can be obtained readily.

Keeping in mind that the optimum obtained by CSDO is under the hypothesis of stationary excitations, which in a way is reasonable. For earthquake loads, for example,

the broadband assumption is usually well justified. Therefore, this assumption will be throughout this chapter.

5.3 RBRDO

In RBRDO, design makers aim to reduce variability of the random response with respect to the protected structure, and meanwhile to make sure a small probability of failure that the random response of the protected structure exceeds a prescribed threshold. To realized the former target, the objective function (or the performance) is always based on minimizing the mean square response (or the associated root) for deterministic structures as is done in CSDO, or in the case of uncertain ones, on minimizing the expected valued of the mean square response [171]. The latter is always involved in constraints. Namely, RBRDO is actually a constraint optimization problem. For simplicity and clarity, the RBRDO problem for deterministic structures is termed by **RBRDO-I**, and **RBRDO-II** denotes the RBRDO problem for uncertain structures.

5.3.1 RBRDO-I

If the protected structure is assumed to be deterministic and subjected to stationary excitations, the objective function can be defined in a dimensionless way as the ratio between the root of the mean square of the protected structure σ_S and the unprotected one σ_S^0 [172]. This definition represents a direct statistical index of vibration protection effectiveness, which shows the protection effectiveness when its value is smaller than one. Obviously, the smaller the value is, the better the effectiveness is. Then the optimization problem is constructed as

$$\begin{aligned} \text{minimize} \quad & f(\mathbf{d}) = \frac{\sigma_S(\mathbf{d})}{\sigma_S^0} \\ \text{subject to} \quad & P_F(\mathbf{d}) = P(g(\mathbf{d}, \mathbf{Z}) = x_{S,t} - \max|x_S(\mathbf{d}, \mathbf{Z})| \leq 0) \leq P_{F,t}, \end{aligned} \tag{5.19}$$

where $\mathbf{d}$ is the design variable vector, $\mathbf{Z}$ represents the random variables in excitations, P_F is the first passage probability of failure with respect to the protected structure that the maximum response $\max|x_S(\mathbf{d}, t)|$ exceeds the prescribed threshold $x_{S,t}$ in the time interval $[0, T]$, and $P_{F,t}$ is the target probability of failure.

Quantities like $\sigma_S(\mathbf{d})$ and σ_S^0 (see Eq. (5.15) and Eq. (5.16) respectively) involved in this optimization problem can be obtained easily. Thanks of the low DOF, P_F is also computationally tractable to calculate in the context of MCS. However, RBRDO will be quite expensive if reliability analysis is nested in the optimization procedure. To tackle this, the sequential strategy proposed in Chapter 4 is used to decouple reliability analysis from the optimization loop and thereafter reduce the number of reliability analysis.

5.3.2 RBRDO-II

To consider uncertainties in both structure and excitation, in a simple way, three parameters are treated as uncertainties: the protected structure frequency ω_S, the damping ratio ζ_S and the mass ratio γ, which are caused by inaccurate measurements or degradation varying with time.

Essentially, these aforementioned uncertainties are induced by the variability in the mass m_S, stiffness k_S and the damping c_S of the protected structure. Then it is possible to introduce the random vector which collects the following uncertain parameters $\boldsymbol{\theta} = [m_S, k_S, c_S, \omega_f, \zeta_f]^{\mathrm{T}}$, provided that the excitation parameters ω_f and ζ_f are always supposed to be uncertain.

For the same reason, if the probable changes in the TMD parameters are also considered, the uncertainties will be extended to $\boldsymbol{\theta} = [m_S, k_S, c_S, m_T, k_T, c_T, \omega_f, \zeta_f]^{\mathrm{T}}$. For convenience, c_S and c_T will be replaced by ζ_S and ζ_T.

Difficulties are brought on evaluating the root of the mean square by entering the parameter uncertainties, which cannot be obtained by Eq. (5.15) since it is based on the classic vibration theory that none of uncertainties are considered in Eq. (5.11). If the system is treated as deterministic system for each set of realizations $\hat{\boldsymbol{\theta}}$ of $\boldsymbol{\theta}$, i.e. $\sigma_S(\mathbf{d}, \hat{\boldsymbol{\theta}})$ can be calculated by Eq. (5.15), one can utilize the average of $\sigma_S(\mathbf{d}, \boldsymbol{\theta})$ [171] to construct the objective function. The associated Monte Carlo estimator is written as

$$E[\sigma_S(\mathbf{d}, \boldsymbol{\theta})] \approx \sum_{k=1}^{N_{\mathrm{mc}}} \sigma_S(\mathbf{d}, \boldsymbol{\theta}^{(k)}), \tag{5.20}$$

where $\boldsymbol{\theta}^{(k)}$ is equivalent to $\hat{\boldsymbol{\theta}}$. Then the optimization problem is finally described in a dimensionless way as

$$\begin{aligned} \text{minimize} \quad & f(\mathbf{d}) = \frac{E[\sigma_S(\mathbf{d},\boldsymbol{\theta})]}{\sigma_S^0} \\ \text{subject to} \quad & P_F(\mathbf{d}) = P(g(\mathbf{d},\boldsymbol{\Theta}) = x_{S,t} - \max|x_S(\mathbf{d},\boldsymbol{\Theta})| \leq 0) \leq P_{F,t}, \end{aligned} \tag{5.21}$$

in which $\boldsymbol{\Theta} = \{\mathbf{Z}, \boldsymbol{\theta}\}$ contains all uncertainties in both excitations and structures.

To obtain $E[\sigma_S(\mathbf{d},\boldsymbol{\theta})]$, N_{mc} Lyapunov equations (see Eq.(5.11) and Eq. (5.20)) have to be solved repeatedly. This is usually not computationally efficient. Be aware that $E[\sigma_S(\mathbf{d},\boldsymbol{\theta})]$ is the function of $\boldsymbol{\theta}$, the maximum dimension of which is 8. In this occasion, $E[\sigma_S(\mathbf{d},\boldsymbol{\theta})]$ can be calculated by the PCE based MCS method proposed in Chapter 3. Other computational issues are similar to those in Section 5.3.1.

5.4 Numerical examples

The purpose of the numerical study is twofold, i.e. demonstration of the effectiveness of RBRDO for the TMD with respect to both deterministic and uncertain structures. The protected structure has the characteristics: $\mu_{m_S} = 100$kg, $\mu_{k_S} = 19460.25$N/m, $\mu_{\omega_S} = 13.95$rad/s, and the excitation parameters are described as $\mu_{\omega_f} = 18.62$rad/s as well as $\mu_{\zeta_f} = 0.4$. All the uncertainties of interest are assumed to be independent normal variables. Other details will be specified in the following.

To show the ability of vibration control of the well designed TMD, two aspects are considered: the performance represented by the objective function $f^{\text{opt}} = \sigma_S/\sigma_S^0$ or $f^{\text{opt}} = E(\sigma_S)/\sigma_S^0$, and the probability of failure associated with the optimal design P_F. The former corresponds to the dispersion reduction of the random response, and the latter presents the structural safety with respect to some prescribed threshold.

5.4.1 RBRDO-I versus CSDO

In this part, the effectiveness of RBRDO for deterministic structures (i.e. RBRDO-I) is examined, and is demonstrated by comparing with CSDO. To carry out RBRDO-I, the target probability of failure and the corresponding threshold must be defined first.

Although no reliability information is produced during CSDO, such information can still be provided by the results of CSDO. One just needs to fix the TMD system with respect to each set of optimal design provided by CSDO (see Eq. (5.17) and Eq. (5.18)), depending on which the associated probability of failure under some prescribed threshold can be obtained.

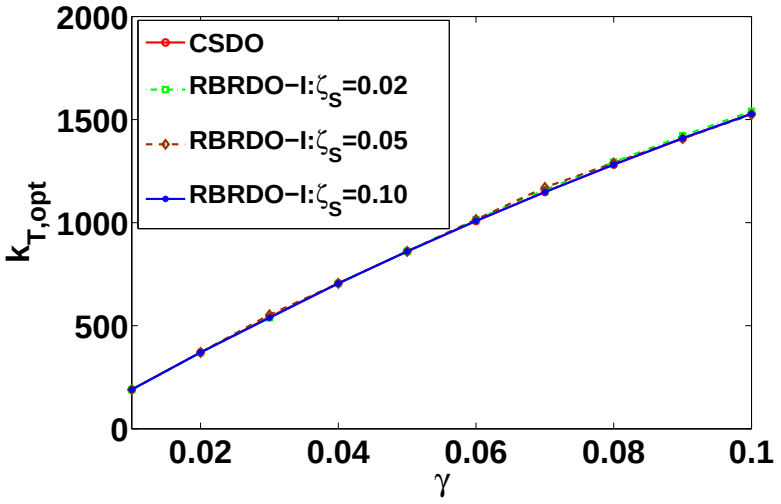

(A) Optimal stiffness

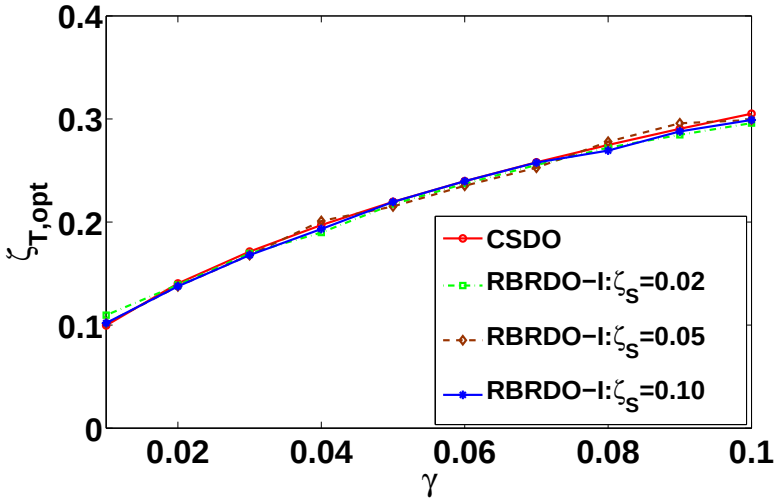

(B) Optimal damping ratio

FIGURE 5.2: Comparisons of optimal designs between CSDO and RBRDO-I for deterministic structure with variation of the mass ratio γ under $x_{S,t} = 0.02$m

Fig. 5.2 compares the optimal results provided by CSDO and RBRDO-I with respect to three damping ratios of the protected structure, i.e. $\zeta_S = 0.02, 0.05, 0.10$. The threshold is chosen as $x_{S,t} = 0.02$m. Obviously, the results provided by RBRDO-I and CSDO are very close to each other. This implies that RBRDO-I is equivalent to CSDO, and that

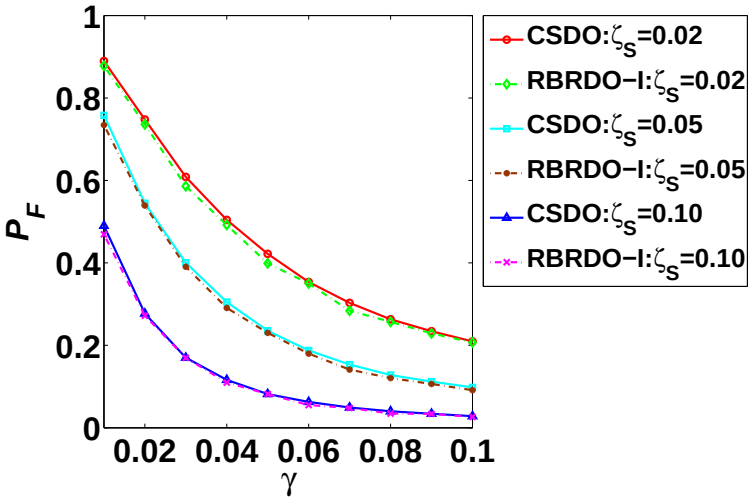

(A) Probability of failure

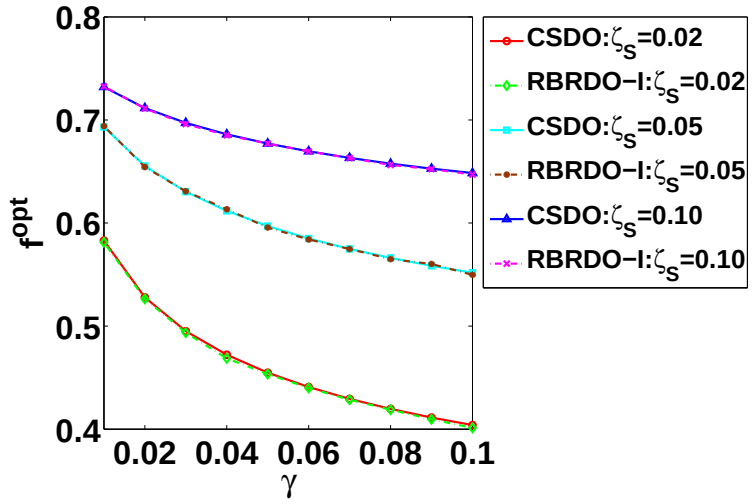

(B) Performance

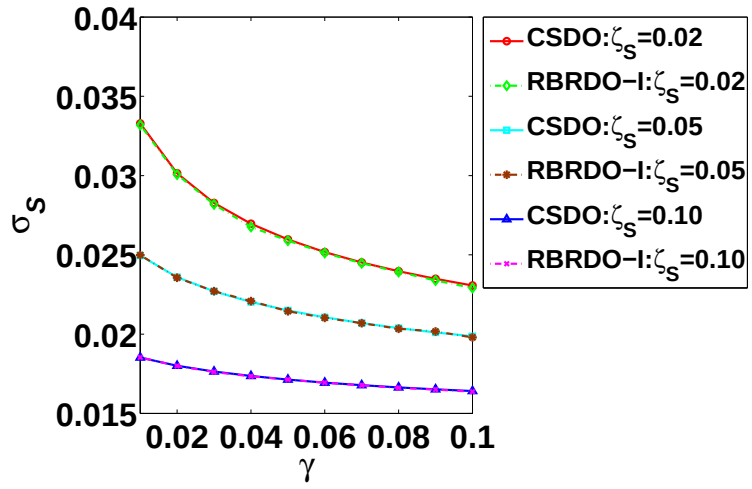

(C) Root of the mean square

FIGURE 5.3: Comparisons of effectiveness between CSDO and RBRDO-I for deterministic structure with variation of the mass ratio γ under $x_{S,t} = 0.02$m.

the protected structure damping has little influence on the optimal designs obtained by RBRDO-I or CSDO. The similar results has been observed in the work [125].

Little fluctuations of the optimal designs between CSDO and RBRDO-I shown in Fig. 5.2 are induced by final probabilities of failure provided by RBRDO-I that are not exactly the same (actually smaller than the target ones) with those of CSDO corresponding to the same ζ_S and γ. This is illustrated in Fig. 5.3a, from which we can also see that the probabilities are apparently distinguished due to different levels of ζ_S, and meanwhile the larger the ζ_S is, the smaller the probability of failure is. One conclusion is that the level of ζ_S has significant influences on the level of probability of failure.

Seen from Fig. 5.3b, the variability of the response is reduced as all the ratios are less than one. However, it appears that the smaller ζ_S is, the better the effectiveness is. Actually, this is not true since the roots of the mean square of the unprotected structure are different due to distinguished ζ_S , i.e. $\sigma_S^0 = 0.0571, 0.0360, 0.0253$ corresponding to $\zeta_S = 0.02, 0.05, 0.10$, respectively. More directly, the final roots are compared in Fig. 5.3c. Obviously, larger ζ_S is helpful to reduce the variability in the response.

Based on studies of the effects of ζ_S, the optimal designs of RBRDO-I are not sensitive to the damping ratio of the protected structure ζ_S. However, the latter bring significant influences on the effectiveness of the TMD. Quite often, large ζ_S leads to high reliability and robustness. It is not difficult to image when ζ_S is random, changes of effectiveness cannot be perceived directly since the optimal designs of CSDO are independent of ζ_S. This implies uncertainties should be considered for more reliable or more robust designs.

In the above studies, we concentrate on the effects of ζ_S under unique threshold $x_{S,t} = 0.02$m, which leads to large probabilities of failure even for $\gamma = 0.1$ (see Fig. 5.3a). In these cases, the associated optimal designs of RBRDO-I are very close to those of CSDO. However, there is a possibility that lower probabilities of failure may bring large deviations between the results of CSDO and RBRDO-I. From this view, low level should be taken into account. Generally, large thresholds signify high reliability. To this end, the threshold is selected as $x_{S,t} = 0.03$m.

Table 5.1 lists the final probabilities of failure computed by RBRDO-I, as well as the target ones provided by CSDO. The final probabilities of failure in RBRDO-I are smaller

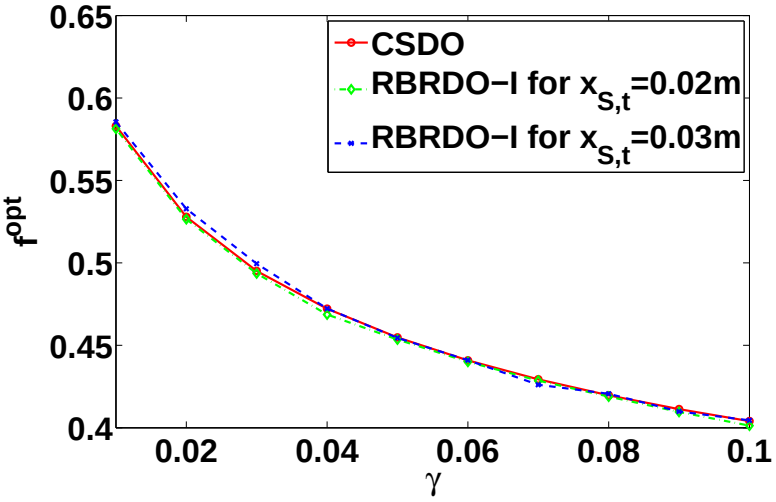

(A) Performance

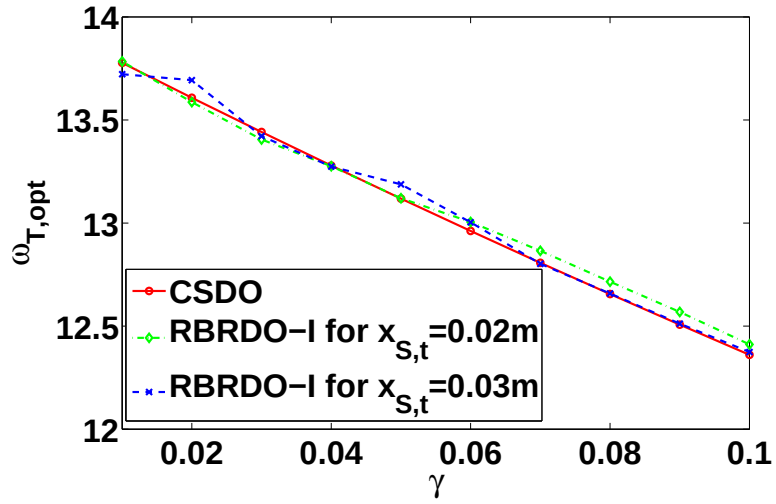

(B) Optimal frequency

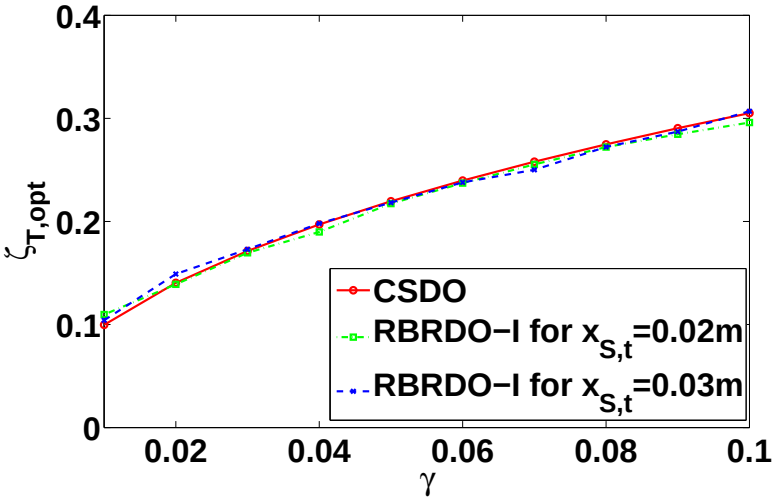

(C) Optimal damping ratio

FIGURE 5.4: Comparisons of effectiveness and optimal designs between CSDO and RBRDO-I for deterministic structure with variation of the mass ratio γ under $\zeta_S = 0.02$

than those of CSDO, such that the former method gives a safer design. Note that these results are obtained under $\zeta_S = 0.02$.

TABLE 5.1: Probabilities of failure provided by CSDO and RBRDO-I associated with $x_{S,t} = 0.03$m and $\zeta_S = 0.02$

Method	γ									
	0.01	0.02	0.03	0.04	0.05	0.06	0.07	0.08	0.09	0.10
CSDO	0.1871	0.0571	0.0209	0.0111	0.0059	0.0031	0.0020	0.0017	0.0013	0.0009
RBRDO-I	0.1819	0.0544	0.0202	0.0086	0.0047	0.0029	0.0017	0.0014	0.0012	0.0008

The performance f^{opt} is also compared, which is illustrated in Fig. 5.4a. It is evident that the dispersion reductions of RBRDO-I with respect to both thresholds $x_{S,t} = 0.02$m and $x_{S,t} = 0.03$m are almost identical with the ones of CSDO. The same things can be found from the optimal solutions $\omega_{T,\text{opt}}$ and $\zeta_{T,\text{opt}}$ that are respectively depicted in Fig. 5.4b and Fig. 5.4c. We can then conclude that RBRDO-I is equivalent to CSDO as long as they own the same probabilistic constraint, i.e $P_{F,t}$ and the associated $x_{S,t}$.

In addition, an important property should be stressed: regardless of other conditions, large mass ratio γ is liable to reduce both of the probability of failure P_F and the performance f^{opt}, which would be helpful for the TMD design for uncertain structures.

5.4.2 RBRDO-II versus CSDO

Effects of parameter uncertainties are investigated first, which are shown by comparisons of the probabilities of failure under the optimal designs obtained by CSDO. Namely, optimal designs of the uncertain structures are obtained by CSDO in the mean sense. Parameter uncertainties $\boldsymbol{\theta}$ will be studied under two cases. One is related to **Case 1**, $\boldsymbol{\theta} = [m_S, k_S, c_S, \omega_f, \zeta_f]^{\mathrm{T}}$ with COV= 5%, and the other is connected with **Case 2**, $\boldsymbol{\theta} = [m_S, k_S, c_S, m_T, k_T, c_T, \omega_f, \zeta_f]^{\mathrm{T}}$ with COV= 5%. The design variables are chosen as $\mathbf{d} = [m_T, k_T, \zeta_T]^{\mathrm{T}}$ for Case 1, and $\mathbf{d} = [\mu_{m_T}, \mu_{k_T}, \mu_{\zeta_T}]^{\mathrm{T}}$ for Case 2.

Comparisons of the probabilities of failure under each set of optimal designs with respect to CSDO are shown in Fig. 5.5. The damping ratio of the protected structure is chosen as $\zeta_S = 0.02$, and the threshold is $x_{S,t} = 0.02$m. It is observed that Case 2 corresponds to the largest probabilities of failure which means the higher level of the uncertainties, the lower the reliability is. For uncertain structures, if one wants to pursue the same reliability with deterministic structures, the obtained designs by CSDO are not optimal

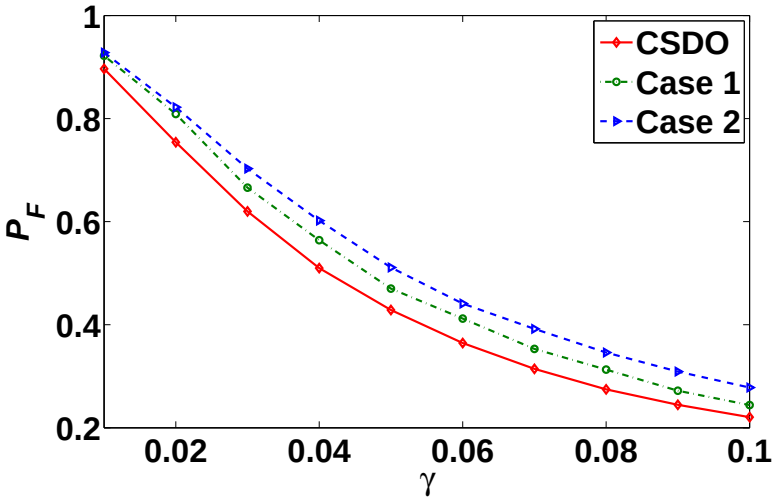

FIGURE 5.5: Comparisons of probabilities of failure with variation of the mass ratio γ under threshold $x_{S,t} = 0.02$m and $\zeta_S = 0.02$ with/without uncertainties

any more and new ones must be searched. Next, we will use RBRDO-II to realize optimal designs under parameter uncertainties.

Take the probabilities of failure of the deterministic structure as the target probabilities of failure (see the red solid line in Fig. 5.5), the values of which are calculated under each set of optimal designs provided by CSDO, i.e. each optimal set is obtained by fixing the mass ratio γ. In CSDO, if the mass ratio γ is fixed, all the other quantities are determined. That is, one target probability of failure is correlated with one fixed mass ratio γ. Accordingly, the compared studies (i.e. in Fig. 5.6 and Fig. 5.7) will be also shown based on the mass ratio γ, which actually represents the different levels of probability of failure provided by CSDO. For convenience and distinction, the mass ratio in CSDO is denoted as γ, while in RBRDO-II it is represented as the nominal value $\gamma_N = \mu_{m_T}/\mu_{m_S}$.

Fig. 5.6a compares the final probabilities of failure obtained by RBRDO-II with respect to Case 1 and Case 2 and the target ones supplied by CSDO, respectively. Results show that RBRDO-II can achieve the target by adapting parameters of the TMD. The associated performance f^{opt} is schematically described in Fig. 5.6b. It is found that the variability obtained by RBRDO-II is always smaller than the one of CSDO, regardless of the level of uncertainties.

From Fig. 5.6, we can conclude that the effectiveness of vibration control of new designs of RBRDO-II is improved and RBRDO-II is a powerful tool for the TMD design under

parameter uncertainties. For one thing, new designs achieve the same target reliability with CSDO in consideration of parameter uncertainties. For another, the performance is better than CSDO.

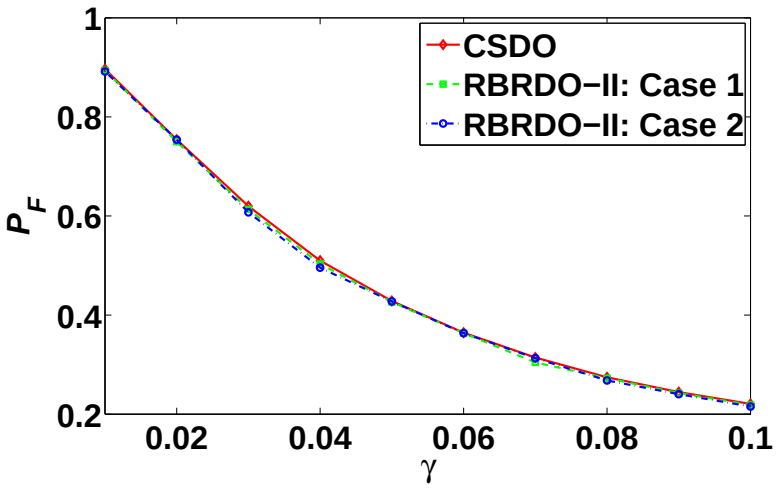

(A) Probability of failure

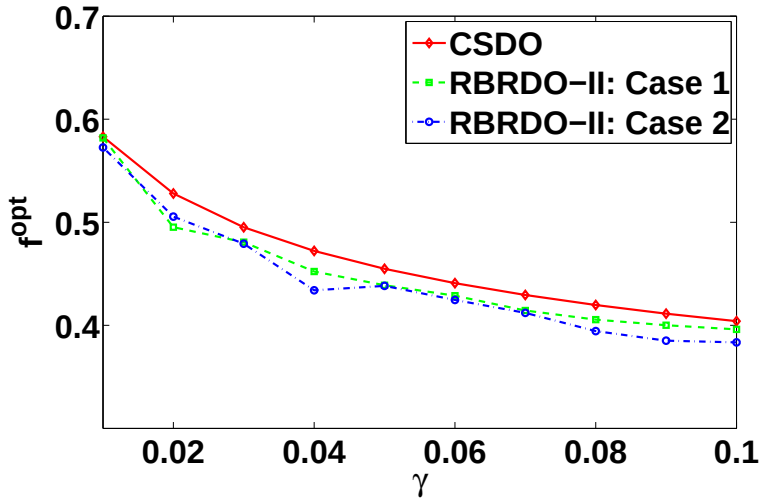

(B) Performance

FIGURE 5.6: Comparisons of effectiveness between CSDO and RBRDO-II with variation of the mass ratio γ for uncertain structure under $x_{S,t} = 0.02$m and $\zeta_S = 0.02$

In Fig. 5.7a, the associated optimal mass ratios $\gamma_N = \mu_{m_T}/\mu_{m_S}$ of RBRDO-II are found to be greater than those of CSDO. This is not occasional since increasing the mass ratio is helpful to obtain high reliability which has been demonstrated in Section 5.4.1.

The corresponding optimal frequency and the damping ratio are given in Fig. 5.7b and Fig. 5.7c. There is no monotonic increasing or decreasing relation with variation of the mass ratio γ (i.e. the target probability of failure). However, optimal values of these

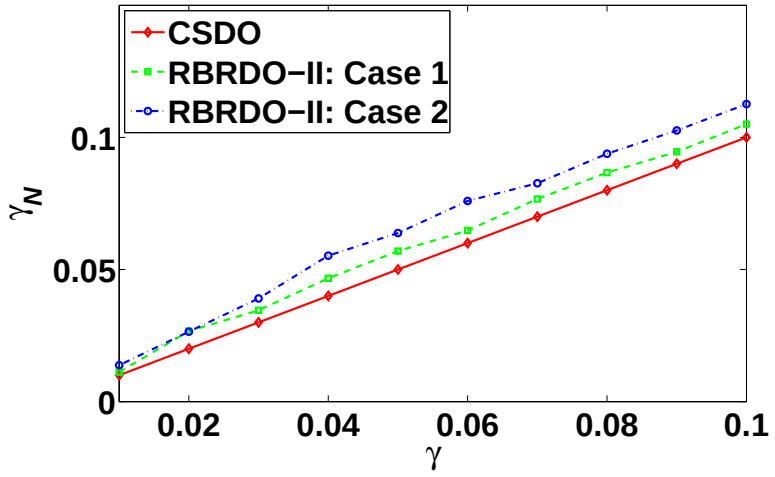

(A) Mass ratio

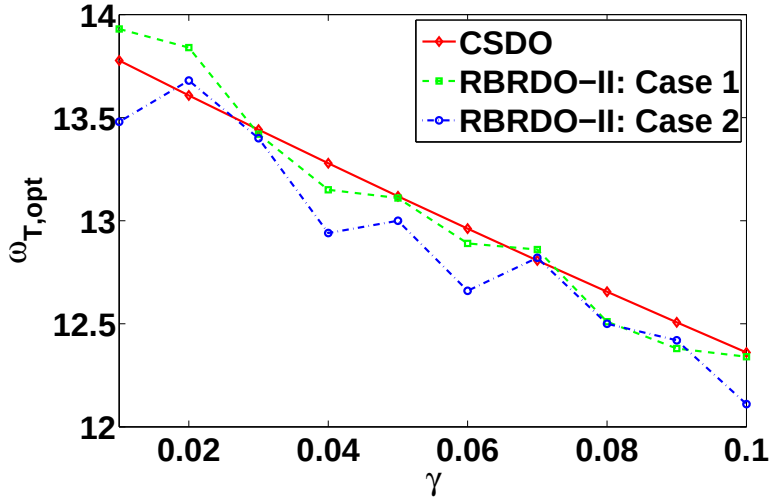

(B) Optimal frequency

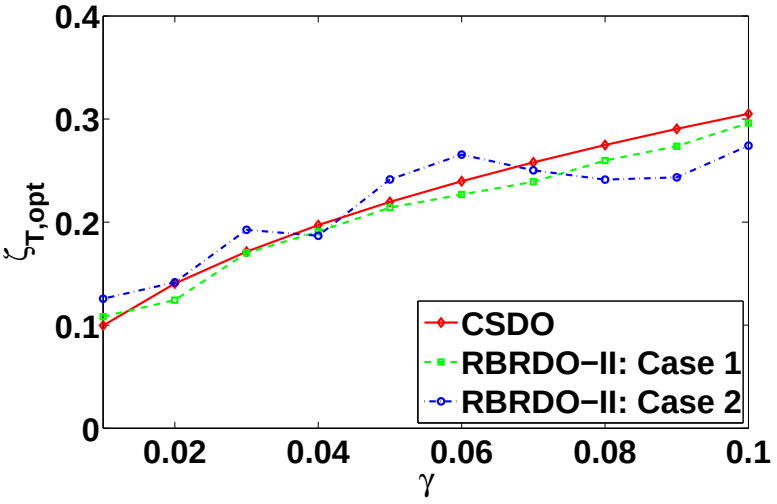

(C) Optimal damping ratio

FIGURE 5.7: Comparisons of optimal designs between CSDO and RBRDO-II with variation of the mass ratio γ for uncertain structure under $x_{S,t} = 0.02$m and $\zeta_S = 0.02$.

two quantities are all close to the values of CSDO. This property is very important for the TMD design when considering structural uncertainties. Roughly speaking, under the same probability of failure with respect to the same threshold, one can capture the optimal designs of uncertain structures by setting the optimal frequencies and the damping ratio of the TMD around the associated values provided by CSDO, and by keeping the mass greater than the one in CSDO.

Note that in the above investigations, the target probabilities of failure are provided by CSDO for comparative purposes, and they are relatively large and different from each other with distinguished mass ratio. In the following studies, uniquely smaller values independent from CSDO will be chosen to show more general cases. All the parameters are considered to be random, i.e. $\boldsymbol{\theta} = [m_S, k_S, \zeta_S, m_T, k_T, \zeta_T, \omega_f, \zeta_f]^{\mathrm{T}}$. The associated COV is 10%, which is characterized as **Case 3**.

For practical applications, the mass of the TMD is usually not very large, i.e. $\gamma \leq 10\%$. In this sense, the mass is usually pre-fixed according to the mass ratio $\gamma = \mu_{M_T}/\mu_{M_S}$. As well known, the frequency of the TMD plays a significant role in vibration control. To show effects of uncertainties on the optimal frequency $\omega_{T,\mathrm{opt}}$, we will fix the the damping ratio with three levels $\mu_{\zeta_T} = 0.05, 0.10, 0.20$. Then, only the mean value of the stiffness μ_{K_T} is seen as the design variable. The target probability of failure is $P_{F,t} = 0.01$ with the displacement threshold $x_{S,t} = 0.07$m and the damping ratio of the protected structure is $\mu_{\zeta_S} = 0.1$. In these circumstances, the optimal frequency $\omega_{T,\mathrm{opt}}$ of the TMD are compared in Fig. 5.8.

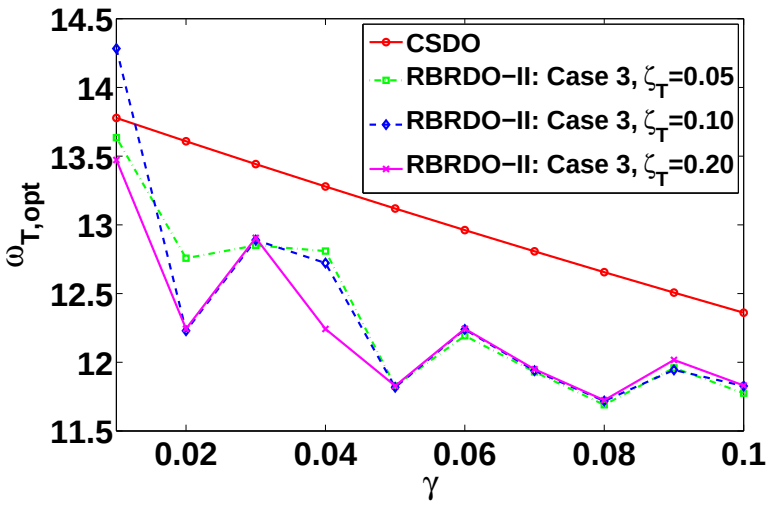

FIGURE 5.8: Comparisons of optimal frequency $\omega_{T,\mathrm{opt}}$ with variation of the mass ratio γ under the target probability of failure $P_{F,t} = 0.01$ related to the threshold $x_{S,t} = 0.07$m.

From Fig. 5.8, almost all the optimal frequencies are smaller than those of CSDO. To this end, reduction of the TMD frequency is useful to suppress the vibration. For each damping level the optimal frequency trends to be decreased, but not monotonic. The reason is that the final probabilities of failure corresponding to these designs are all smaller than $P_{F,t} = 0.01$ but not the same. It is found that optimal frequencies corresponding to each fixed damping ratio under the same mass ratio are somehow close to each other. From this sense, the optimal frequencies are not very sensitive to the TMD damping ratio.

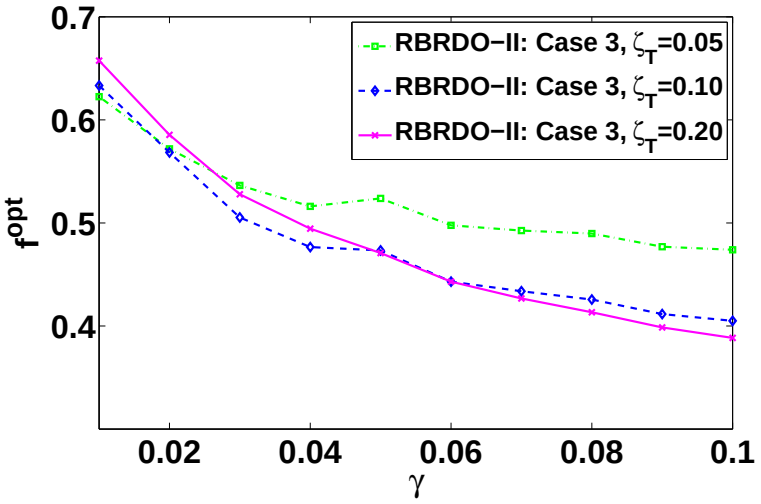

FIGURE 5.9: Comparisons of the performance f^{opt} with variation of the mass ratio γ under the target probability of failure $P_{F,t} = 0.01$ related to the threshold $x_{S,t} = 0.07$m.

The associated performance is described in Fig. 5.9. The effectiveness of variability reduction becomes better as the mass ratio increases. This is identical with the results obtained by CSDO shown in Fig. 5.4a. After $\gamma = 0.05$ especially, the larger the damping is, the more reduction can be observed. A possible conclusion is that the large damping of the TMD is valuable for the robust design. In summary, under the same target probability of failure associated with the same threshold, different ζ_T brings not much influence on the optimal frequencies $\omega_{T,\text{opt}}$, while large ζ_T is useful to improve the quality.

The studies mentioned above are only related to $P_{F,t} = 0.01$ and $x_{S,t} = 0.07$m. Depending on these simulations, the effects of the threshold are not clear. To this end, besides $x_{S,t} = 0.07$m, another two thresholds $x_{S,t} = 0.05$m and $x_{S,t} = 0.06$m are also concerned. The target probability of failure is set as $P_{F,t} = 0.005$. As the new reliability level is difficult to achieve when $\gamma < 0.05$, the relations in these two figures are described from

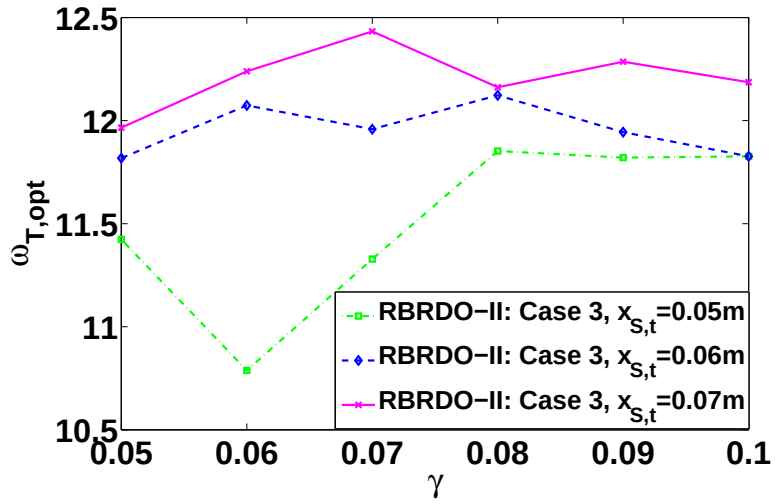

FIGURE 5.10: Comparisons of optimal frequency $\omega_{T,\text{opt}}$ with variation of the mass ratio γ under the target probability of failure $P_{F,t} = 0.005$ and the fixed damping $\mu_{\zeta_T} = 0.1$.

$\gamma = 0.05$ to $\gamma = 0.1$. Fig. 5.10 and Fig. 5.11 give the optimal solutions of the optimal frequencies and the performances under these new circumstances.

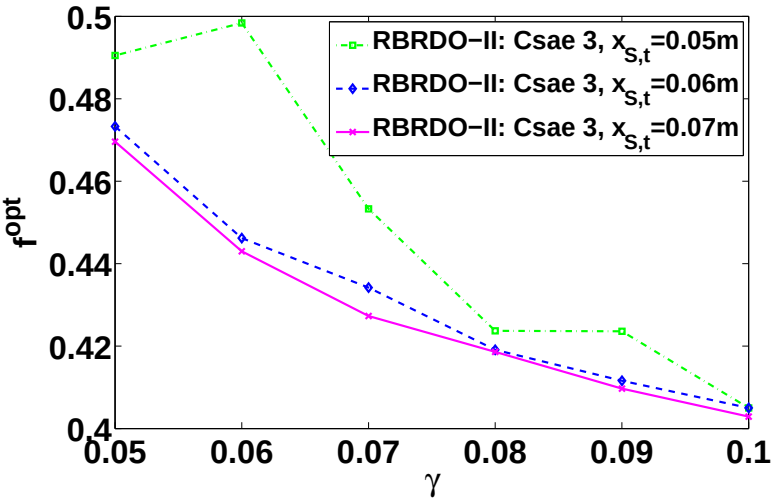

FIGURE 5.11: Comparison of the performance f^{opt} with variation of the mass ratio γ under the target probability of failure $P_{F,t} = 0.005$ and the fixed damping $\mu_{\zeta_T} = 0.1$.

In Fig. 5.10, to achieve the target probability of failure, the smallest frequencies of the TMD are required corresponding to the smallest threshold $x_{S,t} = 0.05$m. Whereas in this case, the largest standard deviation is obtained (see Fig. 5.11). This situation is not occasional according to the study in Section 2.4.3.2. It is found that smaller mean value of the random response usually corresponds to larger standard deviation of the random response. In the framework of RBRDO for the TMD, the objective is to minimize the standard deviation but the mean. However, the latter is somehow equivalent to the

threshold in reliability analysis. This is why when the smallest threshold is connected with the largest standard deviation compared with the other larger ones. We can see again that large mass ratios are useful to reduce the variability of the random response, no matter what threshold is applied.

TABLE 5.2: Sequential strategy of RBRDO for the TMD

Sub-optimization	μ_{m_T}	μ_{k_T}	μ_{ζ_T}	f^{opt}	P_F
$0^\star$	5.0000	1000.0	0.0500	1.6223	$1.45E-2$
1	5.5032	1003.6	0.0418	1.5731	$-^{\star\star}$
2	5.9537	903.25	0.0462	2.1750	$-$
3	6.5499	812.93	0.0516	1.1908	$-$
4	7.1633	889.07	0.0530	0.8261	$9.90E-4$

* stands for the start point;
** denotes the sub-optimization is not converged.

At last, we consider the a RBRDO problem with Case 3 under the target probability is $P_{F,t} = 0.001$ corresponding to the threshold $x_{S,t} = 0.06$m. This procedure is realized by the sequential strategy, the whole procedure of which is described in Table 5.2. Comparing the reliability and the performance in conjunction with the initial condition and the optimal design, it is found that: 1) the final frequency of the TMD is smaller than the initial one, i.e 11.14rad/s vs 13.14rad/s; 2) the mass ratio is increased since this property is useful to reduce the mean square.

5.5 Summary

Due to the uncertainties involved in both structures and excitations, CSDO is not appropriate for random structures since the uncertainties in structures can bring bad influences of the control ability of the TMD. Therefore, in this chapter, RBRDO is applied to design the TMD for uncertain structures. In RBRDO, not only the quality of the protected structure is considered, but also the safety is taken into account. The former connected with the design objective robustness is quantified by the mean value of the mean square response; the latter is realized by achieving a low probability of failure corresponding to some prescribed threshold.

Compared with CSDO, numerical results demonstrated that RBRDO-I is equivalent to CSDO as long as they own the same probabilistic constraint, i.e $P_{F,t}$ and the associated $x_{S,t}$. Furthermore, the effectiveness of vibration control of the TMD designed by

RBRDO-II is improved because the same target reliability with CSDO is achieved by taking parameter uncertainties into account. For uncertain structures, some properties related to the performance f^{opt}, by studying a SDOF system, are concluded as follows:

- More variability reduction with respect to the random response will be realized as the mass ratio increases.
- Large damping ratios ζ_T and ζ_S are helpful to reduce f^{opt}.
- To achieve the same target probability of failure $P_{F,t}$, the smaller the associated threshold $x_{S,t}$ is, the larger the the structural performance f^{opt} is, and vise versa.

Chapter 6

Conclusion

6.1 Conclusions

In this dissertation, we study the design optimization for random structural systems under stochastic excitations in the framework of RBRDO, in which both quality and safety are regarded. From the view of safety, reliability analysis is required to ensure a low probability of failure corresponding to the response exceeding a prescribed threshold. With respect to quality, the concept of robustness is applied, which aims at reducing the performance sensitivity to uncertainties. In an extended scope, RBDO is also involved. Two main aspects have been considered to make RBRDO mathematically robust and computationally efficient: advanced methods for UA and sequential formulations of RBRDO which decouple both reliability analysis and moment evaluations from the optimization procedure.

6.1.1 PCE based MCS method for UA

A PCE based MCS method is developed to carry out UA, which connects with not only reliability analysis for design feasibility robustness but also moment evaluations for design objective robustness. In this method, the PCE is applied to approximate the random response so that large quantities of structural analyses are avoided, leading to the enhanced efficiency.

However, implementations of the PCE are always confined to random dynamic responses due to the curse of high dimensionality induced by the stochastic excitations. Therefore, we use the convolution form to compute the dynamic response, in which the PCE is applied to approximate the modal properties so that the dimension of uncertainties is reduced since only structural random parameters are considered.

Case studies exhibit that the proposed method has the capability to cope with UA for both static and dynamic problems with relatively large COV, e.g. 10%, and with small probability of failure, e.g. 10^{-4} or 10^{-5}. It is found that this method can achieve reasonable accuracy and greater efficiency compared with direct MCS. Depending on the case studies, at least the 2nd order PCE is necessary.

6.1.2 Modal intermixing problem

As the PCE based method is associated with modal analysis and MCS, the modal intermixing problem is also regarded since it is always encountered within MCS sampling. Investigations show that the modal intermixing is aroused by the large dispersion of random structural parameters. To correctly capture the uncertainties in the modal content by analyzing the modal scatter observed in MCS, it is indispensable to avoid this problem. Namely, the modal behaviors of random models should agree with those of the mean model as far as possible.

For this purpose, the MAC factor is used to quantify the modal intermixing between some random mode and the corresponding mean mode. And thereafter, based on the concept of worst case, a univariable based method is proposed to check which parameter leads to this problem and to avert it by reducing the COV. Although the variance (i.e. COV) is not easy to fix or control, the small one fulfills the practical applications, from the view of generating positive samples and grasping the consistently inherent properties of random models with the mean model. Based on simulations, it is found that when the COV of random structural parameters is not greater than 10%, there is no sever modal intermixing.

6.1.3 Sequential RBRDO

The sequential formulation of RBRDO is developed. The main advantages of this formulation are to improve efficiency, and to overcome the non-convergence problem encountered in nested MCS based RBRDO. Different from conventional sequential strategy that mainly aims to decouple the reliability analysis from the optimization procedure, we also concentrate on making the moment evaluations independent from the optimization procedure for computational purposes.

To realize the sequential RBRDO, locally "first-order" exponential approximation around the current design is implemented to construct the equivalently deterministic objective functions and probabilistic constraints. The associated coefficients can be evaluated by the LSM. However, the efficiency is always challenged by high dimension of the design variables. Hence, the auxiliary distribution based reliability sensitivity analysis and the PCE based moment sensitivity analysis are developed to calculate the associated coefficients within one reliability analysis and one moment evaluation procedure, respectively.

Since the sequential RBRDO is an approximation of the original problem, some respects must be taken into account:

1. Adaptive bounds. According to significant discontinuities in probability of failure due to design changes, the local approximation concept is applied. In this sense, the optimum is supposed to be located in the subdomain (or bounds) of the current design point. Note that more accurate results can be obtained in a relatively small subdomain. To make the approximation available, the controlling coefficients are recommended as $0 < \delta_i^{\mathrm{L}} \leq \delta_i^{\mathrm{R}} \leq 10\%$ depending on numerical investigations.

2. Start point. In spite of that the relatively small bound is helpful to guarantee the accuracy, however if the start point is very far from the optimum, low convergence problems arise, or even worse no convergence is achieved. To this end, the start point is chosen in the failure regions whose probability of failure is close to the target one. The details of the problems or engineering experiences would be useful to choose such a start point.

3. Enhanced convergent condition. Stated again, the sequential formulation is actually an approximation of the original problem. There is a possibility that the optimal designs obtained by the equivalent deterministic optimization might not satisfy the real probabilistic constraints, even if the sub-optimization-procedure is converged. In this sense, it is necessary to execute the reliability analysis after each sub-optimization-procedure to check if the current design is the desired one, although this aggravates somehow the computational expense.

6.1.4 Application of RBRDO on the design optimization of the TMD

The main contribution of this part is to apply RBRDO on passive vibration control, i.e. the design optimization of the TMD. Unlike CSDO, this framework can consider uncertainties in both parameters and excitations. Minimization of the mean square of the response is retained in objective function, which aims to reduce the variability of the random response. Reliability analysis is involved in the probability constraints not only to obtain high reliability but also to control the amplitude of the random response by setting some prescribed threshold. Numerical simulations demonstrate that RBRDO is a powerful tool in the design optimization of the TMD for both deterministic and uncertain structures by studying a SDOF system. This method can be readily extended to MDOF system. Some properties related to the performance f^{opt}, are concluded as follows:

- More variability reduction with respect to the random response will be realized as the mass ratio increases.
- Large damping ratios ζ_T and ζ_S are helpful to reduce f^{opt}.
- To achieve the same target probability of failure $P_{F,t}$, the smaller the associated threshold $x_{S,t}$ is, the larger the structural performance f^{opt} is, and the vise versa.

6.2 Future work

- In this dissertation, the uncertainty is assumed as the aleatory type. In real engineering, probabilistic characteristics of design variables may not be available. In this sense, other theories, such as fuzzy set theory, evidence theory and convex model, can be used. Under these theories, how to apply the concepts of reliability, robustness, or the equivalence is worth to be studied.
- The PCE based MCS method is raised to quantify the uncertainties. Note that this method can deal with high dimensionally dynamic problem induced by the stochastic excitations, provided that the structures are linear. For nonlinear structures however, this method may not be well suited. Although linearization techniques can be used to convert nonlinear problems into linear problems, sometimes strong

nonlinearity cannot be ignored. To this end, extension of this method should be considered in the future.

- In this work, RBRDO is applied on simple structures. It would be interesting to use it to solve more complex systems, such as the buildings with multi-TMD to overcome the mistuned problems, and mechatronic systems, including mechanical as well as electronic hardware and software.

- The current technology for RBRDO has one limitation. That is, current RBRDO just considers component reliability. Even if each component satisfies the reliability target, the whole system may not satisfy the reliability target. Thus, system level RBRDO should be considered in the future.

Bibliography

[1] H. Agarwal. *Reliability based design optimization: Formulations and Methodologies.* PhD thesis, Notre Dame, Indiana, 2004.

[2] A. Chateauneuf. *Principles of reliability-based design optimization.* Taylor & Francis, 2008.

[3] A. Mohsine and A. El Hami. A robust study of reliability-based optimization methods under eigen-frequency. *Computer Methods in Applied Mechanics and Engineering*, 199(17-20):1006–1018, 2010.

[4] G.I. Schuëller and H.A. Jensen. Computational methods in optimization considering uncertainties-An overview. *Computer Methods in Applied Mechanics and Engineering*, 198(1):2–13, 2008.

[5] B.D. Youn. *Advances in reliability-based design optimization and probability analysis.* PhD thesis, The University of Iowa, 2001.

[6] P.W. Christensen and A. Klarbring. *An introduction to structural optimization*, volume 153. Springer Verlag, 2008.

[7] E. Nikolaidis, D.M. Ghiocel, and S. Singhal. *Engineering design reliability applications: for the aerospace, automotive, and ship industries.* CRC, 2007.

[8] Y. Tsompanakis, N.D. Lagaros, and M. Papadrakakis. *Structural design optimization considering uncertainties.* Routledge, 2008.

[9] W.L. Oberkampf, J.C. Helton, C.A. Joslyn, S.F. Wojtkiewicz, and S. Ferson. Challenge problems: uncertainty in system response given uncertain parameters. *Reliability Engineering & System Safety*, 85(1-3):11–19, 2004.

[10] W.L. Ob, S.M. DeLand, B.M. Rutherford, K.V. Diegert, and K.F. Alvin. Estimation of Total Uncertainty in Modeling and Simulation. *Sandia Report SAND2000-0824,Albuquerque, NM*, 2000.

[11] G.J. Klir and T.A. Folger. *Fuzzy sets, uncertainty, and information*, volume 159. Prentice Hall Englewood Cliffs, 1988.

[12] G.J. Klir and B. Yuan. *Fuzzy sets and fuzzy logic: theory and applications*. Prentice Hall PTR Upper Saddle River, NJ, USA, 1995.

[13] K. Sentz, S. Ferson, and Sandia National Laboratories. *Combination of evidence in Dempster-Shafer theory*. Citeseer, 2002.

[14] Y. Ben-Haim and I. Elishakoff. *Convex models of uncertainty in applied mechanics*, volume 112. Elsevier Amsterdam, 1990.

[15] L.P. He, H.Z. Huang, L. Du, X.D. Zhang, and Q. Miao. A review of possibilistic approaches to reliability analysis and optimization in engineering design. *Human-Computer Interaction. HCI Applications and Services*, pages 1075–1084, 2007.

[16] W. Feller. *An introduction to probability theory and its applications*. Wiley-India, 2008.

[17] G.E.P. Box and G.C. Tiao. *Bayesian inference in statistical analysis*. Wiley Online Library, 1973.

[18] J.M. Bernardo, A.F.M. Smith, and M. Berliner. *Bayesian theory*. Wiley New York, New York, USA, 2000.

[19] C. Soize. Random matrix theory and non-parametric model of random uncertainties in vibration analysis. *Journal of sound and vibration*, 263(4):893–916, 2003.

[20] C. Soize. A comprehensive overview of a non-parametric probabilistic approach of model uncertainties for predictive models in structural dynamics. *Journal of Sound and Vibration*, 288(3):623–652, 2005.

[21] Z. Kang. *Robust design optimization of structures under uncertainties*. PhD thesis, Universitat Stuttgart, 2005.

[22] F. Jurecka. *Robust design optimization based on metamodeling techniques*. Shaker Verlag, 2007.

[23] X. Du, A. Sudjianto, and W. Chen. An integrated framework for optimization under uncertainty using inverse reliability strategy. *Journal of Mechanical Design(Transactions of the ASME)*, 126(4):562–570, 2004.

[24] X. Du and W. Chen. Towards a better understanding of modeling feasibility robustness in engineering design. *Transactions-American Society of Mechanical Engineers Journal of Mechanical Design*, 122(4):385–394, 2000.

[25] BF Spencer. State of the art of structural control. *Journal of structural engineering*, 129(7):845–856, 2003.

[26] A. Dasgupta and M. Pecht. Material failure mechanisms and damage models. *Reliability, IEEE Transactions on*, 40(5):531–536, 1991.

[27] W.R. Blischke and D.N.P. Murthy. *Reliability: modeling, prediction, and optimization*. Wiley-Interscience, 2000.

[28] S.H. Crandall and W.D. Mark. *Random vibration in mechanical systems*. Academic Pr, 1963.

[29] P.T. Boggs and J.W. Tolle. Sequential quadratic programming. *Acta numerica*, 4(-1):1–51, 1995.

[30] P.J.M. Van Laarhoven and E.H.L. Aarts. *Simulated annealing: theory and applications*. Kluwer Dordrecht, The Netherlands, 1992.

[31] S.J. Louis and G.J.E. Rawlins. Designer genetic algorithms: Genetic algorithms in structure design. In *Proceedings of the Fourth International Conference on Genetic Algorithms*, pages 53–60. Citeseer, 1991.

[32] C. Prins. A simple and effective evolutionary algorithm for the vehicle routing problem. *Computers & Operations Research*, 31(12):1985–2002, 2004.

[33] W. Stadler. Multicriteria optimization in mechanics(a survey). *Applied mechanics reviews*, 37:277–286, 1984.

[34] R.T. Marler and J.S. Arora. Survey of multi-objective optimization methods for engineering. *Structural and multidisciplinary optimization*, 26(6):369–395, 2004.

[35] A. Osyczka. An approach to multicriterion optimization problems for engineering design. *Computer Methods in Applied Mechanics and Engineering*, 15(3):309–333, 1978.

[36] W. Chen, M.M. Wiecek, and J. Zhang. Quality utility: a compromise programming approach to robust design. *Journal of mechanical design*, 121(2):179–187, 1999.

[37] I. Lee, K.K. Choi, L. Du, and D. Gorsich. Dimension reduction method for reliability-based robust design optimization. *Computers and Structures*, 86(13-14):1550–1562, 2008.

[38] J. Koski. Multicriterion optimization in structural design. *New directions in optimum structural design(A 85-48701 24-39). Chichester, England and New York, Wiley-Interscience, 1984,*, pages 483–503, 1984.

[39] K.A. Proos, G.P. Steven, O.M. Querin, and Y.M. Xie. Multicriterion evolutionary structural optimization using the weighting and the global criterion methods. *AIAA journal*, 39(10):2006–2012, 2001.

[40] A. Messac, C. Puemi-Sukam, and E. Melachrinoudis. Aggregate objective functions and pareto frontiers: Required relationships and practical implications. *Optimization and Engineering*, 1(2):171–188, 2000.

[41] T.W. Athan and P.Y. Papalambros. A note on weighted criteria methods for compromise solutions in multi-objective optimization. *Engineering Optimization*, 27(2):155, 1996.

[42] P.L. Yu and G. Leitmann. Compromise solutions, domination structures, and salukvadze's solution. *Journal of Optimization Theory and Applications*, 13(3):362–378, 1974.

[43] M. Zeleny. *Multiple criteria decision making*, volume 25. McGraw-Hill New York, 1982.

[44] V. Chankong and Y.Y. Haimes. *Multiobjective decision making: theory and methodology*, volume 8. North-Holland New York, 1983.

[45] S. Zionts. Multiple criteria mathematical programming: An updated overview and several approaches. In *Mathematical models for decision support*, pages 135–167. Springer-Verlag New York, Inc., 1988.

[46] Y.Y. Haimes, L.S. Lasdon, and D.A. Wismer. On a bicriterion formulation of the problems of integrated system identification and system optimization. *IEEE Transactions on Systems, Man, and Cybernetics*, 1(3):296–297, 1971.

[47] K. Deb, A. Pratap, S. Agarwal, and T. Meyarivan. A fast and elitist multiobjective genetic algorithm: Nsga-ii. *Evolutionary Computation, IEEE Transactions on*, 6(2):182–197, 2002.

[48] A. Der Kiureghian and P.L. Liu. Structural reliability under incomplete probability information. *Journal of Engineering Mechanics*, 112(1):85–104, 1986.

[49] M. Rosenblatt. Remarks on a multivariate transformation. *The Annals of Mathematical Statistics*, 23(3):470–472, 1952.

[50] B.D. Youn and K.K. Choi. An investigation of nonlinearity of reliability-based design optimization approaches. *Journal of Mechanical Design*, 126(3):403–411, 2004a.

[51] S.S. Isukapalli. *Uncertainty analysis of transport-transformation models*. PhD thesis, Rutgers, The State University of New Jersey, 1999.

[52] H. Contreras. The stochastic finite-element method. *Computers & Structures*, 12(3):341–348, 1980.

[53] D. Ghosh, R. Ghanem, and J. Red-Horse. Analysis of Eigenvalues and Modal Interaction of Stochastic Systems. *AIAA Journal*, 43:2196–2201, 2005.

[54] M. Lou. Modal perturbation method and its applications in structural systems. *Journal of engineering mechanics*, 129:935–943, 2003.

[55] G.B. Beacher and T.S. Ingra. Stochastic fem in settlement predictions. *Journal of the Geotechnical Engineering Division*, 107(4):449–463, 1981.

[56] K.K. Phoon, S.T. Quek, et al. Reliability analysis of pile settlement. *Journal of Geotechnical Engineering*, 116:1717–1735, 1990.

[57] H. Benaroya and M. Rehak. Finite element methods in probabilistic structural analysis: a selective review. *Applied Mechanics Reviews*, 41:201–213, 1988.

[58] P.L. Liu. Finite element reliability of geometrically nonlinear uncertain structures. *Journal of engineering mechanics*, 117:1806–1825, 1991.

[59] B. Sudret and A. Der Kiureghian. *Stochastic finite element methods and reliability: a state-of-the-art report*. Dept. of Civil and Environmental Engineering, University of California, 2000.

[60] I. Elishakoff and Y. Ren. *Finite element methods for structures with large stochastic variations*, volume 7. Oxford University Press, USA, 2003.

[61] G.I. Schuëller and H.J. Pradlwarter. Uncertain linear systems in dynamics: retrospective and recent developments by stochastic approaches. *Engineering Structures*, 31(11):2507–2517, 2009.

[62] N. Wiener. The homogeneous chaos. *American Journal of Mathematics*, 60(4):897–936, 1938.

[63] R.G. Ghanem and P.D. Spanos. *Stochastic finite elements: a spectral approach*. Dover publications, 2003.

[64] C. Soize and R. Ghanem. Physical systems with random uncertainties: chaos representations with arbitrary probability measure. *SIAM Journal on Scientific Computing*, 26:395, 2004.

[65] C. Soize. Generalized probabilistic approach of uncertainties in computational dynamics using random matrices and polynomial chaos decompositions. *International Journal for Numerical Methods in Engineering*, 81(8):939–970, 2010.

[66] S. Sakamoto. Polynomial chaos decomposition for the simulation of non-gaussian nonstationary stochastic processes. *Journal of engineering mechanics*, 128:190, 2002.

[67] R. Ghanem. The nonlinear Gaussian spectrum of log-normal stochastic processes and variables. *Journal of applied mechanics*, 66(4):964–973, 1999.

[68] M. Anders and M. Hori. Stochastic finite element method for elasto-plastic body. *International Journal for Numerical Methods in Engineering*, 46(11):1897–1916, 1999.

[69] R. Field. Numerical methods to estimate the coefficients of the polynomial chaos expansion. In *15th ASCE engineering mechanics conference*, 2002.

[70] S. Acharjee and N. Zabaras. A non-intrusive stochastic galerkin approach for modeling uncertainty propagation in deformation processes. *Computers & structures*, 85(5-6):244–254, 2007.

[71] M. Arnst and R. Ghanem. Probabilistic equivalence and stochastic model reduction in multiscale analysis. *Computer Methods in Applied Mechanics and Engineering*, 197(43-44):3584–3592, 2008.

[72] M. Tootkaboni, L. Graham-Brady, and BW Schafer. Geometrically non-linear behavior of structural systems with random material property: An asymptotic spectral stochastic approach. *Computer Methods in Applied Mechanics and Engineering*, 198(37-40):3173–3185, 2009.

[73] B. Sudret and A. Der Kiureghian. Comparison of finite element reliability methods. *Probabilistic Engineering Mechanics*, 17(4):337–348, 2002.

[74] S.K. Choi, R.V. Grandhi, and R.A. Canfield. Structural reliability under non-gaussian stochastic behavior. *Computers & structures*, 82(13-14):1113–1121, 2004.

[75] R. Ghanem, G. Saad, and A. Doostan. Efficient solution of stochastic systems: application to the embankment dam problem. *Structural safety*, 29(3):238–251, 2007.

[76] B. Sudret. Global sensitivity analysis using polynomial chaos expansions. *Reliability Engineering & System Safety*, 93(7):964–979, 2008.

[77] T. Crestaux, O. Le Maitre, and J.M. Martinez. Polynomial chaos expansion for sensitivity analysis. *Reliability Engineering & System Safety*, 94(7):1161–1172, 2009.

[78] G. Lin and G.E. Karniadakis. Sensitivity analysis and stochastic simulations of non-equilibrium plasma flow. *International Journal for Numerical Methods in Engineering*, 80(6-7):738–766, 2009.

[79] M. Loève. Probability theory, 1977.

[80] C. Hu and B.D. Youn. Adaptive-sparse polynomial chaos expansion for reliability analysis and design of complex engineering systems. *Structural and Multidisciplinary Optimization*, 43:419–442, 2011.

[81] D. Xiu and G.E. Karniadakis. Modeling uncertainty in flow simulations via generalized polynomial chaos. *Journal of Computational Physics*, 187(1):137–167, 2003.

[82] L. Mathelin, M.Y. Hussaini, and T.A. Zang. Stochastic approaches to uncertainty quantification in cfd simulations. *Numerical Algorithms*, 38(1):209–236, 2005.

[83] H.N. Najm. Uncertainty quantification and polynomial chaos techniques in computational fluid dynamics. *Annual Review of Fluid Mechanics*, 41:35–52, 2009.

[84] X. Wan and G.E. Karniadakis. Long-term behavior of polynomial chaos in stochastic flow simulations. *Computer methods in applied mechanics and engineering*, 195(41-43):5582–5596, 2006.

[85] D. Xiu and G.E. Karniadakis. The Wiener–Askey Polynomial Chaos for Stochastic Differential Equations. *SIAM Journal on Scientific Computing*, 24(2):619–644, 2002.

[86] M. Shinozuka and G. Deodatis. Stochastic process models for earthquake ground motion. *Probabilistic engineering mechanics*, 3(3):114–123, 1988.

[87] H.M. Panayirci and G.I. Schuëller. On the Capabilities of the Polynomial Chaos Expansion Method within SFE Analysis - An Overview. *Archives of computational methods in engineering*, 18(1):43–55, 2011.

[88] J.O. Lee, Y.S. Yang, and W.S. Ruy. A comparative study on reliability-index and target-performance-based probabilistic structural design optimization. *Computers & structures*, 80(3-4):257–269, 2002.

[89] J. Tu, K.K. Choi, and Y.H. Park. A new study on reliability-based design optimization. *Journal of mechanical design*, 121(4):557–564, 1999.

[90] C.A. Cornell. A probability-based structural code*. In *ACI Journal Proceedings*, volume 66. ACI, 1969.

[91] H.O. Madsen, S. Krenk, and N.C. Lind. Methods of structural safety. *Englewood Cliffs, NJ*, 1986.

[92] A.M. Hasofer and N.C. Lind. Uncertainties analysis of complex structural systems. *Journal of the Engineering Mechanics Division*, 100(1):111–121, 1974.

[93] R. Rackwitz and B. Flessler. Structural reliability under combined random load sequences. *Computers & Structures*, 9(5):489–494, 1978.

[94] M. Hohenbichler and R. Rackwitz. Non-normal dependent vectors in structural safety. *Journal of the Engineering Mechanics Division*, 107(6):1227–1238, 1981.

[95] Y.T. Wu, H.R. Millwater, and T.A. Cruse. Advanced probabilistic structural analysis method for implicit performance functions. *AIAA journal*, 28(9):1663–1669, 1990.

[96] K.K. Choi and B.D. Youn. Hybrid analysis method for reliability-based design optimization. In *2001 ASME Design Engineering Technical Conference and Computers and Information in Engineering Conference, Sep 9-12 2001*, pages 339–348, 2001.

[97] R. Rackwitz. Reliability analysis–a review and some perspectives. *Structural Safety*, 23(4):365–395, 2001.

[98] G.I. Schuëller, H.J. Pradlwarter, and P.S. Koutsourelakis. A critical appraisal of reliability estimation procedures for high dimensions. *Probabilistic Engineering Mechanics*, 19(4):463–474, 2004.

[99] K. Breitung. Asymptotic approximations for multinormal integrals. *Journal of Engineering Mechanics*, 110:357, 1984.

[100] A. Der Kiureghian and M. De Stefano. Efficient algorithm for second-order reliability analysis. *Journal of engineering mechanics*, 117:2904, 1991.

[101] Y. Zheng and PK Das. Improved response surface method and its application to stiffened plate reliability analysis. *Engineering structures*, 22(5):544–551, 2000.

[102] B.D. Youn and K.K. Choi. A new response surface methodology for reliability-based design optimization. *Computers & structures*, 82(2-3):241–256, 2004.

[103] S.M. Wong, R.E. Hobbs, and C. Onof. An adaptive response surface method for reliability analysis of structures with multiple loading sequences. *Structural safety*, 27(4):287–308, 2005.

[104] M. Lemaire. Finite element and reliability- combined methods by response surface. *PROBAMAT-21 st century: Probabilities and materials- Tests, models and applications for the 21 st century*, pages 317–331, 1998.

[105] R. Jin, W. Chen, and T.W. Simpson. Comparative studies of metamodelling techniques under multiple modelling criteria. *Structural and Multidisciplinary Optimization*, 23(1):1–13, 2001.

[106] N. Meteopolis and S. Ulam. The monte carlo method. *Journal of the American Statistical Association*, 44(247):335–341, 1949.

[107] J.M. Hammersley and D.C. Handscomb. *Monte carlo methods*. Taylor & Francis, 1975.

[108] R.Y. Rubinstein and D.P. Kroese. *Simulation and the Monte Carlo method*. Wiley-interscience, 2008.

[109] P. Glasserman. *Monte Carlo methods in financial engineering*. Springer Verlag, 2004.

[110] B.F.J. Manly. *Randomization, bootstrap and Monte Carlo methods in biology*. Chapman & Hall/CRC, 2007.

[111] George S. Fishman. *Monte Carlo: concepts, algorithms, and applications*. Springer, 1996.

[112] S.K. Au. *On the solution of first excursion problems by simulation with applications to probabilistic seismic performance assessment*. PhD thesis, California Institute of Technology, 2001.

[113] R.E. Melchers. Importance sampling in structural systems. *Structural safety*, 6(1):3–10, 1989.

[114] A. Der Kiureghian and T. Dakessian. Multiple design points in first and second-order reliability. *Structural Safety*, 20(1):37–49, 1998.

[115] G.L. Ang, A.H.S Ang, and W.H. Tang. Optimal importance-sampling density estimator. *Journal of engineering mechanics*, 118(6):1146–1163, 1992.

[116] S.K. Au and J.L. Beck. First excursion probabilities for linear systems by very efficient importance sampling. *Probabilistic Engineering Mechanics*, 16(3):193–207, 2001.

[117] S.K. Au and J.L. Beck. Estimation of small failure probabilities in high dimensions by subset simulation. *Probabilistic Engineering Mechanics*, 16(4):263–277, 2001.

[118] J. Ching, S.K. Au, and J.L. Beck. Reliability estimation for dynamical systems subject to stochastic excitation using subset simulation with splitting. *Computer methods in applied mechanics and engineering*, 194(12-16):1557–1579, 2005.

[119] J. Ching, J.L. Beck, and S.K. Au. Hybrid subset simulation method for reliability estimation of dynamical systems subject to stochastic excitation. *Probabilistic engineering mechanics*, 20(3):199–214, 2005.

[120] G.I. Schuëller and H.J. Pradlwarter. Benchmark study on reliability estimation in higher dimensions of structural systems-an overview. *Structural Safety*, 29(3):167–182, 2007.

[121] P.S. Koutsourelakis, H.J. Pradlwarter, and G.I. Schuëller. Reliability of structures in high dimensions, part I: algorithms and applications. *Probabilistic Engineering Mechanics*, 19(4):409–417, 2004.

[122] H.A. Jensen and M.A. Valdebenito. Reliability analysis of linear dynamical systems using approximate representations of performance functions. *Structural Safety*, 29(3):222–237, 2007.

[123] N. Kuschel and R. Rackwitz. Two basic problems in reliability-based structural optimization. *Mathematical Methods of Operations Research*, 46(3):309–333, 1997.

[124] D.M. Frangopol and K. Maute. Life-cycle reliability-based optimization of civil and aerospace structures. *Computers & structures*, 81(7):397–410, 2003.

[125] C. Papadimitriou, L.S. Katafygiotis, and S.K. Au. Effects of structural uncertainties on tmd design: A reliability-based approach. *Journal of structural control*, 4(1):65–88, 1997.

[126] S. Chakraborty and B.K. Roy. Reliability based optimum design of tuned mass damper in seismic vibration control of structures with bounded uncertain parameters. *Probabilistic Engineering Mechanics*, 26(2):215–221, 2011.

[127] B.D. Youn and K.K. Choi. An investigation of nonlinearity of reliability-based design optimization approaches. *Journal of mechanical design*, 126(3):403–411, 2004.

[128] B.D. Youn, K.K. Choi, and L. Du. Enriched performance measure approach for reliability-based design optimization. *AIAA journal*, 43(4):874–884, 2005.

[129] M. Papadrakakis and N.D. Lagaros. Reliability-based structural optimization using neural networks and monte carlo simulation. *Computer methods in applied mechanics and engineering*, 191(32):3491–3507, 2002.

[130] X. Du and W. Chen. Sequential optimization and reliability assessment method for efficient probabilistic design. *Transactions-American Society of Mechanical Engineers Journal of Mechanical Design*, pages 225–233, 2004.

[131] Y.T. Wu, Y. Shin, R. Sues, and M. Cesare. Safety-factor based approach for probability-based design optimization. In *Proceedings of the 42rd AIAA/ASME/ASCE/AHS/ASC Structures, Structural Dynamics, and Materials Conference, number AIAA-2001-1522, Seattle, WA*, 2001.

[132] T. Zou and S. Mahadevan. A direct decoupling approach for efficient reliability-based design optimization. *Structural and Multidisciplinary Optimization*, 31(3):190–200, 2006.

[133] H. Agarwal, C.K. Mozumder, J.E. Renaud, and L.T. Watson. An inverse-measure-based unilevel architecture for reliability-based design optimization. *Structural and Multidisciplinary Optimization*, 33(3):217–227, 2007.

[134] A. Mohsine, G. Kharmanda, and A. El-Hami. Improved hybrid method as a robust tool for reliability-based design optimization. *Structural and Multidisciplinary Optimization*, 32(3):203–213, 2006.

[135] W. Chen, J.K. Allen, K.L. Tsut, and F. Mistree. A procedure for robust design: Minimizing variations caused by noise factors and control factors. *Journal of mechanical design*, 118(4):478–485, 1996.

[136] G. Taguchi. Taguchi on robust technology development: Bringing quality engineering upstream. *ASME Press, New York*, 1993.

[137] A. Parkinson, C. Sorensen, and N. Pourhassan. A general approach for robust optimal design. *Journal of mechanical design*, 115(1):74–80, 1993.

[138] S. Sundaresan, K. Ishii, and D.R. Houser. A robust optimization procedure with variations on design variables and constraints. *Engineering Optimization*, 24(2):101–117, 1995.

[139] M.F. Pellissetti and G.I. Schuëller. The effects of uncertainties in structural analysis. *Structural Engineering and Mechanics*, 25(3):311–330, 2007.

[140] M.T. Yang and J.H. Griffin. A normalized modal eigenvalue approach for resolving modal interaction. *Journal of engineering for gas turbines and power*, 119:647–650, 1997.

[141] M.A. Gutiérrez and S. Krenk. *Stochastic finite element methods*. Wiley Online Library, 2004.

[142] R.H. Cameron and W.T. Martin. The orthogonal development of non-linear functionals in series of Fourier-Hermite functionals. *The Annals of Mathematics*, 48(2):385–392, 1947.

[143] M. Abramowitz and I.A. Stegun. Handbook of mathematical functions, with formulas, graphs, and mathematical tables. *Dover books on advanced mathematics.*, 1972.

[144] M. Berveiller. *Stochastic finite elements: intrusive and non intrusive methods for reliability analysis*. PhD thesis, Université Blaise Pascal, Clermont-Ferrand, 2005.

[145] L. Meirovitch. *Fundamentals of vibrations*. Mechanical engineering series. McGraw-Hill, 2001.

[146] D.E. Newland. *An introduction to random vibrations, spectral and wavelet analysis*. Longman Scientific & Technical, 1993.

[147] H.A. Jensen. Design and sensitivity analysis of dynamical systems subjected to stochastic loading. *Computers & structures*, 83(14):1062–1075, 2005.

[148] R. Ghanem and D. Ghosh. Efficient characterization of the random eigenvalue problem in a polynomial chaos decomposition. *International Journal for Numerical Methods in Engineering*, 72(4):486–504, 2007.

[149] B.J. Debusschere, H.N. Najm, P.P. Pébay, O.M. Knio, R.G. Ghanem, and O.P. Le Maitre. Numerical challenges in the use of polynomial chaos representations for stochastic processes. *SIAM journal on scientific computing*, 26(2):698–719, 2005.

[150] L. Pichler, H.J. Pradlwarter, and G.I. Schuëller. A mode-based meta-model for the frequency response functions of uncertain structural systems. *Computers & Structures*, 87(5-6):332–341, 2009.

[151] R.J. Allemang. The modal assurance criterion–twenty years of use and abuse. *Sound and Vibration*, 37(8):14–23, 2003.

[152] J. Kanda and B. Ellingwood. Formulation of load factors based on optimum reliability. *Structural Safety*, 9(3):197–210, 1991.

[153] H.A. Jensen. Structural optimization of linear dynamical systems under stochastic excitation: a moving reliability database approach. *Computer methods in applied mechanics and engineering*, 194(12-16):1757–1778, 2005.

[154] M.A. Valdebenito and G.I. Schuëller. Efficient strategies for reliability-based optimization involving non-linear, dynamical structures. *Computers & Structures*, 2010.

[155] S.K. Au. Reliability-based design sensitivity by efficient simulation. *Computers & structures*, 83(14):1048–1061, 2005.

[156] Y.T. Wu. Computational methods for efficient structural reliability and reliability sensitivity analysis. *AIAA journal*, 32(8):1717–1723, 1994.

[157] Y.T. Wu and S. Mohanty. Variable screening and ranking using sampling-based sensitivity measures. *Reliability Engineering & System Safety*, 91(6):634–647, 2006.

[158] D. Padmanabhan, H. Agarwal, J.E. Renaud, and S.M. Batill. A study using monte carlo simulation for failure probability calculation in reliability-based optimization. *Optimization and Engineering*, 7(3):297–316, 2006.

[159] R.J. McNamara. Tuned mass dampers for buildings. *Journal of the Structural Division*, 103(9):1785–1798, 1977.

[160] K. Kwok. Damping increase in building with tuned mass damper. *Journal of Engineering Mechanics*, 110(11):1645–1649, 1984.

[161] M.P. Singh, S. Singh, and L.M. Moreschi. Tuned mass dampers for response control of torsional buildings. *Earthquake engineering & structural dynamics*, 31(4):749–769, 2002.

[162] J.M. Ueng, C.C. Lin, and J.F. Wang. Practical design issues of tuned mass dampers for torsionally coupled buildings under earthquake loadings. *The Structural Design of Tall and Special Buildings*, 17(1):133–165, 2008.

[163] J.P. den Hartog. *Mechanical vibrations.* London: MacGraw-Hill Publishing Company, Ltd, 1956.

[164] G.B. Warburton and E.O. Ayorinde. Optimum absorber parameters for simple systems. *Earthquake Engineering & Structural Dynamics*, 8(3):197–217, 1980.

[165] G.B. Warburton. Optimum absorber parameters for various combinations of response and excitation parameters. *Earthquake Engineering & Structural Dynamics*, 10(3):381–401, 1982.

[166] Y. Fujino and M. Abe. Design formulas for tuned mass dampers based on a perturbation technique. *Earthquake engineering & structural dynamics*, 22(10):833–854, 1993.

[167] C. Li and Y. Liu. Optimum multiple tuned mass dampers for structures under the ground acceleration based on the uniform distribution of system parameters. *Earthquake engineering & structural dynamics*, 32(5):671–690, 2003.

[168] A.Y.T. Leung, H. Zhang, C.C. Cheng, and Y.Y. Lee. Particle swarm optimization of tmd by non-stationary base excitation during earthquake. *Earthquake Engineering & Structural Dynamics*, 37(9):1223–1246, 2008.

[169] G.C. Marano, R. Greco, and S. Sgobba. A comparison between different robust optimum design approaches: Application to tuned mass dampers. *Probabilistic Engineering Mechanics*, 25(1):108–118, 2010.

[170] T. Igusa and AD Kiureghian. Response of uncertain systems to stochastic excitation. *Journal of engineering mechanics*, 114(5):812–832, 1988.

[171] H. Jensen, M. Setareh, and R. Peek. Tmds for vibration control of systems with uncertain properties. *Journal of Structural Engineering*, 118(12):3285–3296, 1992.

[172] G.C. Marano, S. Sgobba, R. Greco, and M. Mezzina. Robust optimum design of tuned mass dampers devices in random vibrations mitigation. *Journal of Sound and Vibration*, 313(3-5):472–492, 2008.

[173] H. Tajimi. A statistical method of determining the maximum response of a building structure during an earthquake. In *Proc. 2d World Conf. Earthquake Eng. Tokyo and Kyoto*, volume 2, pages 781–798, 1960.

[174] L.D. Lutes and S. Sarkani. *Stochastic analysis of structural and mechanical vibrations*. Prentice Hall, 1997.

Appendix A

Publications of this Ph.D work

---

[1]. H. Yu, F. Gillot and M. Ichchou. A polynomial chaos expansion based reliability method for linear random structures. To Advances in Structural Engineering, ***under review***.

[2]. H. Yu, F. Gillot and M. Ichchou. Reliability based robust design optimization for tuned mass damper in passive vibration control of deterministic/uncertain structures. To Journal of Sound and Vibration, ***under review***.

[3]. H. Yu, F. Gillot, A. Moshine, and M. Ichchou. A simple method able to deal with time-dependent reliability problems in dynamic systems. IV European Congress on Computational Mechanics: Solids, Structures and Coupled Problems in Engineering, Paris, France, 16-21 May, 2010, Palais des Congrès.

[4]. H. Yu, F. Gillot and M. Ichchou. Hermite polynomial chaos expansion method for stochastic frequency response estimation considering modal intermixing. 3rd International Conference Methods in Structural Dynamical & Earthquake Engineering, Corfu, Greece, 26-28 May 2011.

[5]. A. Mohsine, F. Gillot, H. Yu, M. Ichchou. Optimisation fiabiliste: État limite dépendant du temps. First International Conference IMPACT, Djerba, Tunisia, March 22-24, 2010.

dernière page de la thèse

AUTORISATION DE SOUTENANCE

Vu les dispositions de l'arrêté du 7 août 2006,

Vu la demande du Directeur de Thèse

Monsieur M. ICHCHOU

et les rapports de

Monsieur A. EL HAMI
Professeur - INSA de Rouen - Dépt. Mécanique - Campus du Madrillet - BP 08 - 76801 Saint-Etienne-du-Rouvray cedex

Et de

Monsieur M. COLLET
Chargé de Recherche HDR - FEMTO ST - Université de Franche-Comté - Département de Mécanique Appliquée - 24 chemin de l'épitaphe - 25000 Besançon

Mademoiselle YU Hang

est autorisé à soutenir une thèse pour l'obtention du grade de **DOCTEUR**

Ecole doctorale MECANIQUE, ENERGETIQUE, GENIE CIVIL ET ACOUSTIQUE

Fait à Ecully, le 10 novembre 2011

P/Le Directeur de l'E.C.L.
La Directrice des Etudes

ECOLE CENTRALE DE LYON
SCOLARITE
3ème Cycle

M-A. GALLAND